Metals and Ceramics Division

Heavy Vehicle Propulsion Materials Program
Quarterly Progress Report for
October through December 2003

D. R. Johnson
Technical Project Manager

Prepared for
U.S. Department of Energy
Assistant Secretary for Energy Efficiency and Renewable Energy
Office of FreedomCAR and Vehicle Technologies Program
VT 05 01 020

Prepared by the
OAK RIDGE NATIONAL LABORATORY
Oak Ridge, Tennessee 37831-6066
Managed by
UT-Battelle, LLC
for the Department of Energy
Under contract DE-AC05-00OR22725

CONTENTS

Materials for Fuel Systems

Manufacturing Technology for Cermet Components (SIU-C)

High Toughness Materials (ORNL)

Materials for Exhaust Aftertreatment

Materials for Exhaust Aftertreatment (Caterpillar Inc.)

Catalyst Characterization (ORNL and Cummins Inc.)

Development of NO_x Sensors for Heavy Vehicle Applications (ORNL and Ford Motor Company)

Ultra-High Resolution Electron Microscopy for Characterization of Catalyst Microstructures and De-activation Mechanisms (ORNL)

Microstructural Changes in NO_x Trap Materials under Lean and Rich Conditions at High Temperatures (ORNL)

Materials for Air Handling, Hot Section, and Structural Components

Lightweight Valve Train Materials (Caterpillar Inc.)

Engineered Surfaces for Diesel Engine Components (Caterpillar Inc.)

Cermet Materials for Diesel Engine Wear Applications (Cummins Inc.)

Nanoengineered Materials (North Carolina A&T State University)

NDE of Diesel Engine Components (Argonne National Laboratory)

Durability of Diesel Engine Component Materials (ORNL)

Life Prediction of Diesel Engine Components (ORNL and Caterpillar)

Low-Cost Manufacturing of Precision Diesel Engine Components (ORNL)

Advanced Machining and Sensor Concepts (University of Michigan)

Advanced Cast Austenitic Stainless Steels for High-Temperature Components (ORNL and Caterpillar Inc.)

Laser Surface Texturing of Lubricated Ceramics (ORNL)

High-Density Infrared Surface Treatment of Materials for Heavy-Duty Vehicles (ORNL)

Titanium Alloys for Heavy-Duty Vehicles (ORNL)

Mechanical Behavior of Ceramic Materials for Heavy Duty Diesel Engines (ORNL)

Deformation Processes for the Next Generation Ceramics (ORNL)

Development of Titanium Components for a Heavy-Duty Diesel Engine Turbocharger (Caterpillar Inc.)

Test and Materials Standards

Surface Modification of Engineering Materials for Heavy Vehicle Applications (NIST)

IEA Implementing Agreement for a Programme of Research and Development on Advanced Materials for Transportation Applications (ORNL)

Testing Standards (NIST)

IEA – Rolling Contact Fatigue (ORNL)

Manufacturing Technology for Cermet Components

D. E. Wittmer
Southern Illinois University

Objective/Scope

The purpose of this work is to investigate the potential of low-cost manufacturing processes for ceramic and cermet diesel engine components. The primary task is to develop cost effective processing, forming and sintering methodologies for cermet and ceramic formulations, used by industrial diesel engine manufacturers.

Technical Highlights

Task 1. Collaboration with industrial partner(s).

This task involves the collaboration with industrial partners to assist them in processing and sintering of their diesel engine components. Our goal is provide assistance in processing and sintering which may result in a reduction in surface reactions and part warping. Moreover, this may also provide an alternative sintering process that will allow improved throughput efficiency and manufacturing economy. Due to the proprietary nature of this task, any research data generated from this task is normally controlled by the terms of each specific confidentiality agreement. The reporting of this data and any results are the responsibility of the industrial partner(s).

During this reporting period a die with the capability of producing a prototype plunger of complex geometry by low-pressure injection molding was completed and tested. Figure 1 is the aluminum die opened; exposing the near-net shape plunger. Figure 2 shows the plunger prototype as it was removed from the die and with the sprew removed. The cermet composition used was the reaction sintered Ni3Al-TiC (50/50) formulation which has been discussed in previous reports. The binder is presently being removed from a batch of these prototypes and they will be sintered during the next reporting period.

Also during this reporting period, 4 test bars were received from Jim Stephen at CoorsTek for sintering in the belt furnace. These bars will be sintered during the next sintering run and returned to him for evaluation.

Task 2. Cost Effective Processing and Sintering

This task was completed and reported in previous quarterly report.

Task 3. Economic Comparison of Materials and Processing of Cermets for Use as Diesel Engine Components

This task was completed as reported previously.

Task 4. Effect of High Heating Rates on Sintering of Cermets

The goal of this is to evaluate the use of very high heating rates on the densification of selected intermetallic bonded-TiC cermets. If extremely high heating rates can be used to sinter these cermets, it offers the opportunity to even further reduce the manufacturing cost. Previously reaction sintered 50% Ni3Al-50% TiC was injection molded into test rods for the sintering trials. During this reporting period, sintering rates of up to 750°C/min were investigated, but problems with the furnace caused the termination of the testing. The high heating rates adversely affected the take up gear, which is made from UHMW-PE. The SiC belt in contact with the gear was transferring too much heat to the gear, causing the gear to warp. The UHMW-PE gear which is OEM is shown in Figure 3. This figure shows the discoloration of the gear from the high temperatures. An aluminum gear was designed and machined at SIUC, thanks to our technician Gerald Fink, and was recently installed on the belt furnace. Figure 4 shows the new aluminum gear installed on the furnace. Following the installation of the new gear a successful test run was accomplished. Some of the prototypes from Task 1 will be used in this task during the next reporting period.

Status of Milestones

1.	Collaboration with Industrial Partners	On Schedule
2.	Cost Effective Processing and Sintering of Diesel Engine Components	Completed
3.	Economic Comparison	Completed
4.	Effect of high heating rates	On Schedule

Communications/Visits/Travel

D. E. Wittmer spoke with D. Ray Johnson and Terry Tiegs about the technical progress and future of program.

D. E. Wittmer spoke with Jim Stephen from CoorsTek about samples of cermets and also received some test bars from him for sintering.

Problems Encountered

Overheating of take up gear in belt furnace delayed sintering trials. Solution was replacement of polymer gear with metal gear and problem has been solved.

Publications and Presentations

None

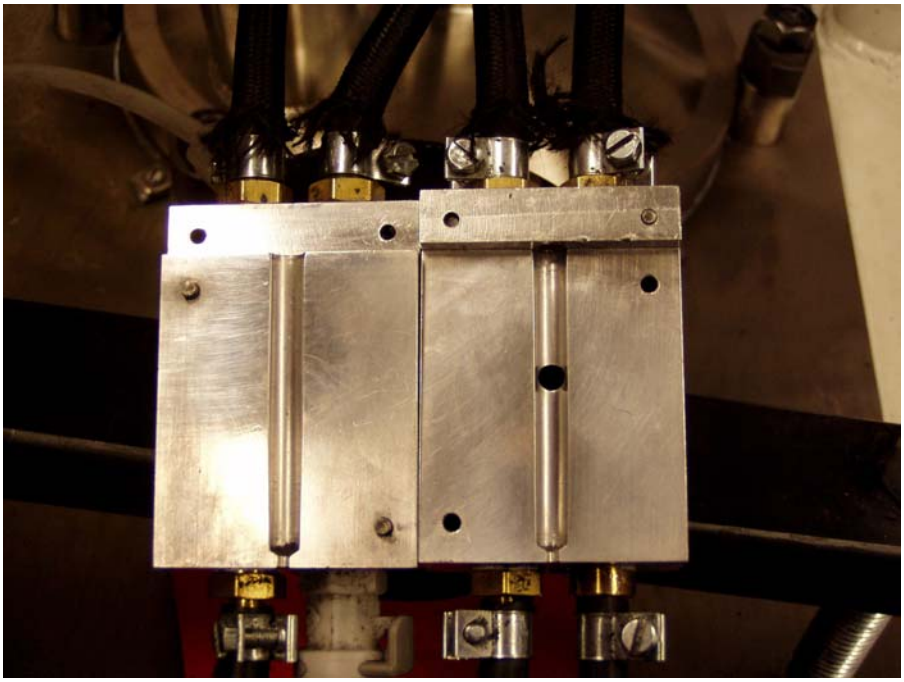

Figure 1. Injection molding die for prototype plunger.

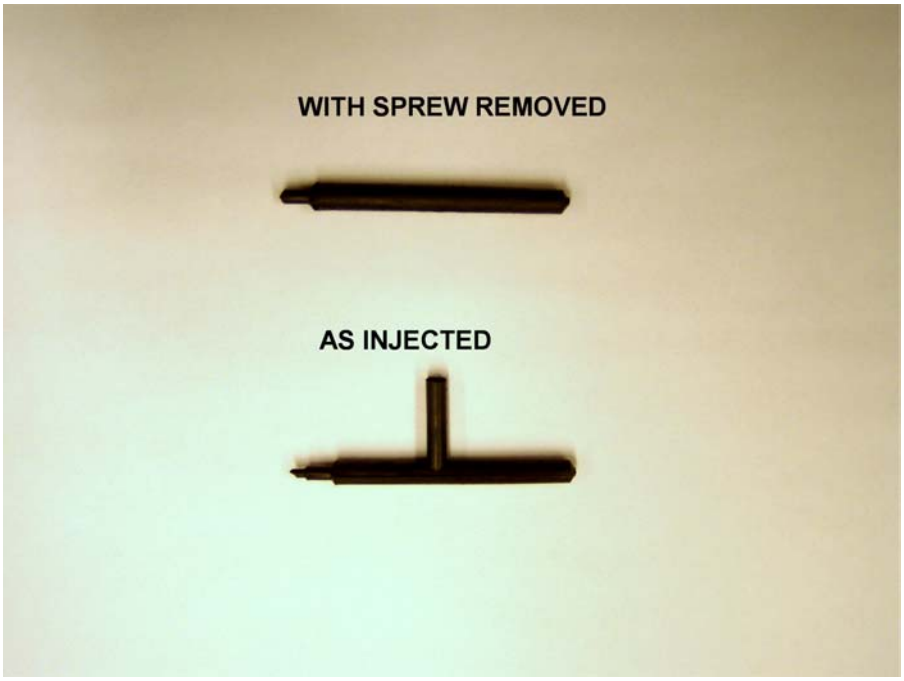

Figure 2. Prototype injection molded fuel injector plungers.

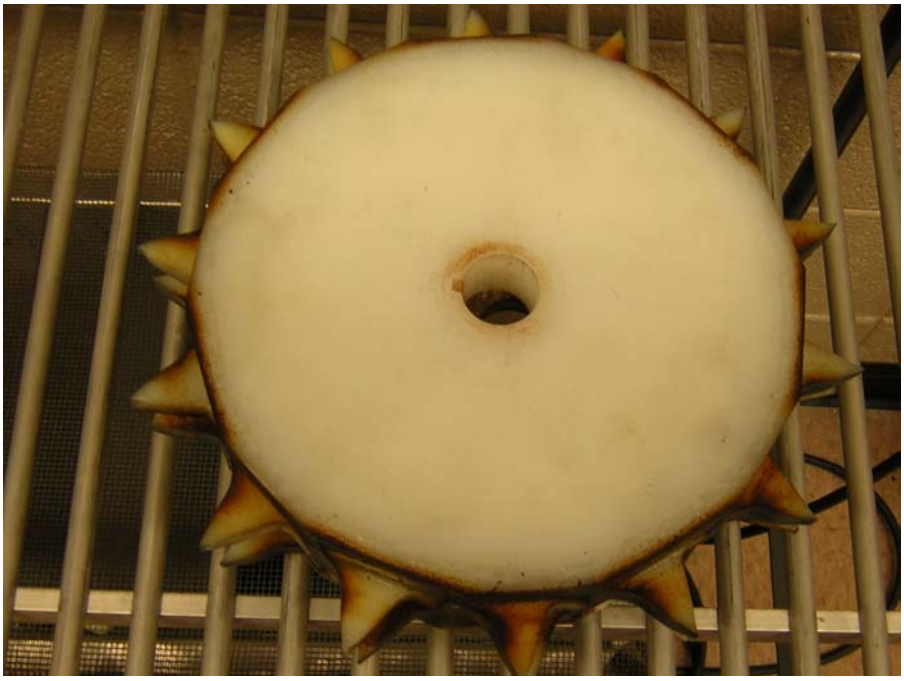

Figure 3. UHMW-PE gear on belt furnace.

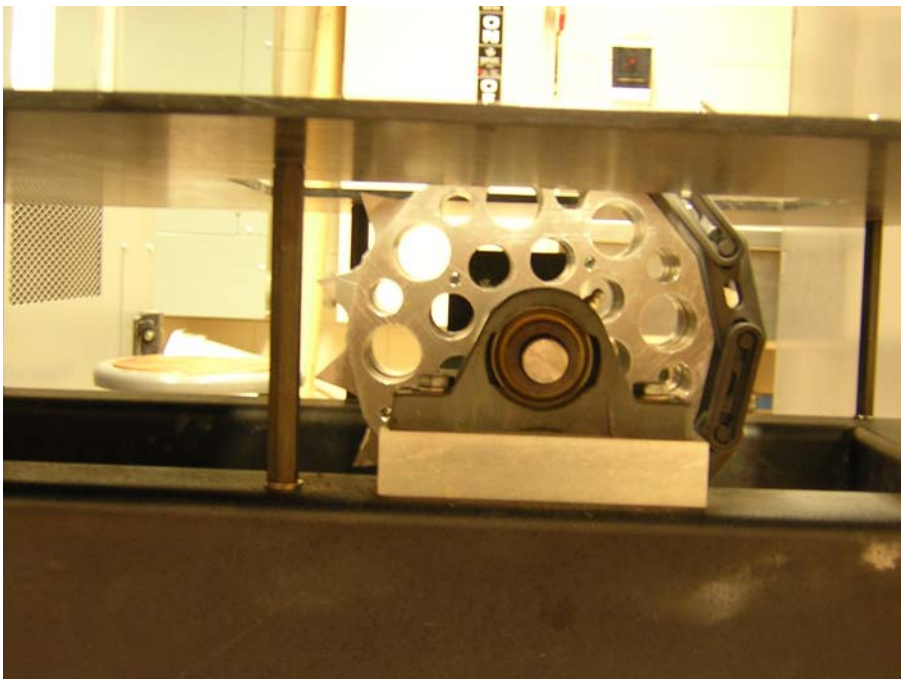

Figure 4. Aluminum gear installed on belt furnace.

High Toughness Materials

T. N. Tiegs, F. C. Montgomery, and P. A. Menchhofer
Oak Ridge National Laboratory

Objective/Scope

Significant improvement in the reliability of structural ceramics for advanced diesel engine applications could be attained if the critical fracture toughness (K_{Ic}) were increased without strength degradation. Currently, the project is examining toughening of ceramics by incorporation of ductile intermetallic phases.

Technical Highlights

Previous studies have shown that the properties of the aluminide-bonded ceramics are attractive for diesel engine applications and consequently, development of these materials was started. At the present time, TiC-based composites with 40-60 vol % Ni_3Al are being developed because they have expansion characteristics very close to those for steel. Previously, the general property envelope has been studied and the compositions refined. Further processing studies are needed to examine lot-to-lot variation using statistically designed experiments, determine compaction behavior, assess dimensional control during sintering, identify suitable binders which will not add carbon ash during sintering, and develop a viable and cost-effective source of NiAl powder. The development effort is being done in collaboration with CoorsTek, Inc.

Large Batch Processing of TiC-Ni_3Al Composites – Several large batches (>3 kg) of a 50% TiC-Ni_3Al (with 2% Mo) composition have been milled and blended together to produce ~13 kg of powder. Approximately 10 kg were sent to CoorsTek for injection molding testing. A large batch (>3 kg) was also produced that used a cheaper NiAl powder that was coarser than previously used. Much of the earlier work used powder that had particle sizes ≤20 µm. The batch produced recently used NiAl powder with particle sizes ≤150 µm (-100 mesh).

Alternate Precursors for Ni_3Al Formation - All previous work used a combination of Ni and NiAl for an in-situ reaction to form the Ni_3Al. Because the costs of the starting raw materials can be a significant fraction of the total cost of a component, alternative materials for fabricating the cermets are of interest. Several new batches were milled and pressed into discs and billets. The compositions are described in Table 1. The samples are currently awaiting the repair of the sintering furnace, which has been out of service for two months.

As shown, several different compositions are being examined. The new batch of Al-30 Ni from the catalyst manufacturer will determine if these materials can be made without the impurities as observed previously. Earlier work demonstrated that these precursors produced high density parts, but had low strengths because of impurity contamination. One of the other samples will reexamine the use of prealloyed Ni_3Al (made by gas atomization). Earlier work at high TiC contents (70-90 vol %) showed these Ni_3Al powders produced non-homogeneous microstructures with large 'pools' of Ni_3Al surrounded by the finer TiC grains. However, with the TiC content of interest now at 50 vol %, the presence of the Ni_3Al 'pools' may not be significant to the performance of the cermets. Samples were also fabricated using a commercial Hastelloy X powder. This is a Ni-Cr-Fe-Mo alloy with good oxidation and corrosion resistance.

An attempt was made to make a prereacted Al-Ni precursor that could be milled to fine sizes during the normal processing of the cermets. Thermodynamic calculations indicated that the lowest heat of formation per gram was associated with making Al_3Ni. Appropriate amounts of Al and Ni were dry milled and then fired (at slow heating rate) to 700°C, which is sufficient to melt the Al. The resulting reacted product was very hard and non-friable. Consequently, this route to producing an Al-Ni precursor did not appear to be one with significant potential.

Table 1. Summary of TiC-Ni_3Al compositions fabricated.

Batch No.	TiC Content (vol %)	Ni_3Al source
DC-3-7	50	NiAl + Ni (Milling done with larger WC media)
DC-3-8	50	Al-30 Ni Catalyst (New batch from manufacturer)
DC-3-9	50	Prealloyed Ni_3Al (-325 mesh)
DC-3-10	50	Reacted Al_3Ni
DC-3-11	50	Hastelloy X

Status of Milestones
On schedule.

Communications/Visits/Travel
Travel by T. N. Tiegs to Chicago, IL, on Dec. 9-10 to attend the 2004 Powder Metallurgy Conference planning meeting.

Problems Encountered
The sintering furnace used for processing studies has been out of service for two months because of a bad controller. Several runs were made before the controller problem was identified and consequently a number of samples were ruined.

Publications
None.

Materials for Exhaust Aftertreatment

Paul W. Park, Alexander G. Panov, Svetlana Zemskova, and Craig F. Habeger
Caterpillar Inc.

Objective/Scope

The objective of this effort is to develop and evaluate materials that will be utilized in aftertreatment systems for diesel engines. These materials include catalysts for NOx abatement, filtration media for particulate abatement, and materials to improve NO_x sensing capabilities in the exhaust system. This project is part of a Caterpillar strategy to meet EPA requirements for regulated emissions in 2007 and beyond. This year's focus is on the durability of NO_x catalysts developed for lean burn applications in the presence of sulfur, evaluation of filtration properties of sintered metal media for application in diesel particulate filters (DPF), and evaluation of current NO_x sensor technologies while developing materials to improve sensing capabilities.

Technical Highlights

Lean- NO_x. The screening tests to identify the best reductant for the selected lean- NO_x catalyst were completed. Dodecane (C12 straight chain hydrocarbon) was the best reductant in terms of NO_x reduction performance as well as feasibility for real application among various hydrocarbons tested in the study including ethanol, propanol, butanol, hexanol, octanol, octane, and hexadecane, 2 ppm sulfur diesel, 8 ppm sulfur diesel, 500 ppm sulfur diesel, gasoline and kerosene. The results showed that 70% and 90% NO_x reduction were achieved using dodecane of 3:1 and 6:1 C1/ NO_x ratio, respectively with 0.1% NO, 9% O_2 and 7% H_2O in the temperature range of 350-400°C at 30,000h^{-1}.

A series of catalyst samples prepared with various silver loadings and preparation techniques were also evaluated in order to optimize catalyst formulation for dodecane reductant. Using the single step sol-gel method more silver was able to be loaded on the catalyst to promote lean-NOx performance. Transferring the preparation technique to washcoated bricks is in progress.

The study of H_2 effect on the lean- NO_x performance began with using a bench test system. The study will help to understand the impact of a reformer, which produces H_2, on lean- NO_x performance of a selected catalyst.

PM Trap. First generation of the test protocol for soot oxidation studies on the catalyzed diesel particulate filters was developed during this quarter. The test procedure utilizes a flow reactor system equipped with differential pressure transducer that allows monitoring backpressure change during the regeneration. The reaction mixture contains NO or NO_2, oxygen and nitrogen and the soot oxidation is monitored by CO_2 production.

The sensitivity of the analytical instruments and the robustness of the reaction system were found to be appropriate to perform the studies. Effects of temperature, space velocity, and gas composition on the soot oxidation rates are being investigated.

Two catalyzed SiC filters were prepared in house. Both are using the same Pt based formulation. One filter is utilizing deep-bed filtration, while the other surface filtration. Study of the soot

oxidation rates on these filters will reveal if utilization of the catalyzed deep-bed filter increased soot oxidation rates.

NOx Sensor. Evaluation of a developer's NO_x sensor has been completed. The sensor has a good response to NO concentrations between 0-130ppm (10% oxygen : 90% nitrogen as carrier gas mixture). Reproducibility test showed that for NO_x range of 10-130ppm the developer's sensor response can vary up 4.5%, but for lower NO_x range of 0-10ppm variations go up to 23%. The sensor does not respond if nitrogen only was used as a carrier gas. Therefore, there is a concern over the performance during rich exhaust conditions. In addition, the sensor response is not linear if the gas flow pressure in the system goes above 1.5 psi.

Evaluation of oxygen pumping electrodes for amperometric NO_x sensors continued. The first two compositions did not perform as well as expected; however four more compositions exist and will be evaluated during the second quarter. The first two compositions did not distinguish between NO and oxygen and were therefore not selective.

Future Plans

(1) Scale-up catalyst to conduct engine tests
(2) Assess various reformer technologies to provide ideal reductants to the catalysts
(3) Evaluate NO_x sensors.
(4) Continue the interaction with sensor developers to meet heavy-duty diesel needs.

Travel

Svetlana Zemskova, the 4th DOE National Laboratory Catalysis Conference (NL Cat 2003), Oak Ridge, TN, October 22-24, 2003.

Status of FY 2003 Milestones

1) *Catalyst Durability:* Improve catalyst durability for sulfur poisoning (in progress)
2) *Washcoat Technology:* Develop a controlled catalyst coating technique in order to fully demonstrate selected catalyst chemistries on a full size honeycomb monolith (in progress)

Publications

Carrie L. Boyer, Paul W. Park, "Effect of SO_2 on the Activity over Ag/γ-Al_2O_3 Catalysts for the Reduction of NO_x in Lean Conditions" was submitted for publication in J. Catal.

Conferences/Seminars/Presentations

Svetlana Zemskova, Paul Park (CAT AMT), J. S. Lin (Solid State Division of Oak Ridge National Laboratory, Oak Ridge, TN), J. Wen, I. Petrov (Center for Microanalysis of Materials, University of Illinois at Urbana- Champaign, Urbana-Champaign, IL) "Synthesis and Characterization of High Surface Area Mesoporous Alumina for Catalyst Support Application" was presented at the 4th DOE National Laboratory Catalysis Conference (NL Cat 2003), Oak Ridge, TN, October 22-24, 2003.

Catalyst Characterization

Thomas Yonushonis and Roger England
Cummins Inc.
and Thomas Watkins
Oak Ridge National Laboratory

Objective

The objective of this effort is to produce a quantitative understanding of the processing and in-service effects on NOx adsorber catalyst technology leading to an exhaust aftertreatment system with improved catalyst performance capable of meeting the 2007 emission requirements.

Samples and Approach

A Cummins catalyst supplier provided new catalyst materials, which are being examined with diagnostic tools developed under the CRADA. Investigations of these candidate-production materials are being implemented on both the bench and engine research scale. These investigations include the examination of unused and engine-aged catalyst samples. Investigative tools included transmission electron microscopy (TEM), X-ray diffraction (XRD), Raman Spectroscopy and infrared spectroscopy (IR).

Technical Highlights

A new capability to collect drift-compensated spectral image datasets using a Hitachi HD-2000 Scanning Transmission Electron Microscope (STEM) and Noran System Six microanalysis system was applied to the catalyst samples from this CRADA. Traditional microanalysis in a Transmission electron microscope (TEM) or STEM consists of collecting the X-rays which are generated by the high energy electrons passing through the sample and analyzing the energy of the x-rays to understand the elemental composition of the sample. In this way, a few spectra can be acquired to probe the elemental spatial distribution. In a STEM, the additional technique of X-ray mapping is possible in which the analyst defines a few elements which are expected and records the location of the electron beam from which X-rays of limited energy are emitted. Using spectral imaging techniques, rather than looking at only a small range of X-ray energies, a full 1024 or 2048 energy channel spectrum is saved for each electron probe position. As an example a 512 X 384 pixel image (over 190,000 spectra) is shown in Figure 1. In Figure 1A, a Z-contrast image from a sample prior to engine testing (0 desulfation time) shown bright spots indicating areas of high atomic number. In Figure 1B, the distribution of one of the elements scanned, Pt, in the same region is shown. Figure 2 demonstrates some of the statistical analysis that can now be applied to this collection of data in order to visualize the data more clearly and understand complex chemical and spatial trends. Only with long time acquisition can adequate counting statistics be achieved. Thus, compensation for the inherent drift in any (S)TEM system is required to maintain the high spatial resolution of (S)TEM in the analytical dataset, particularly where the samples are thin and the achievable X-ray counts rates are modest at best.

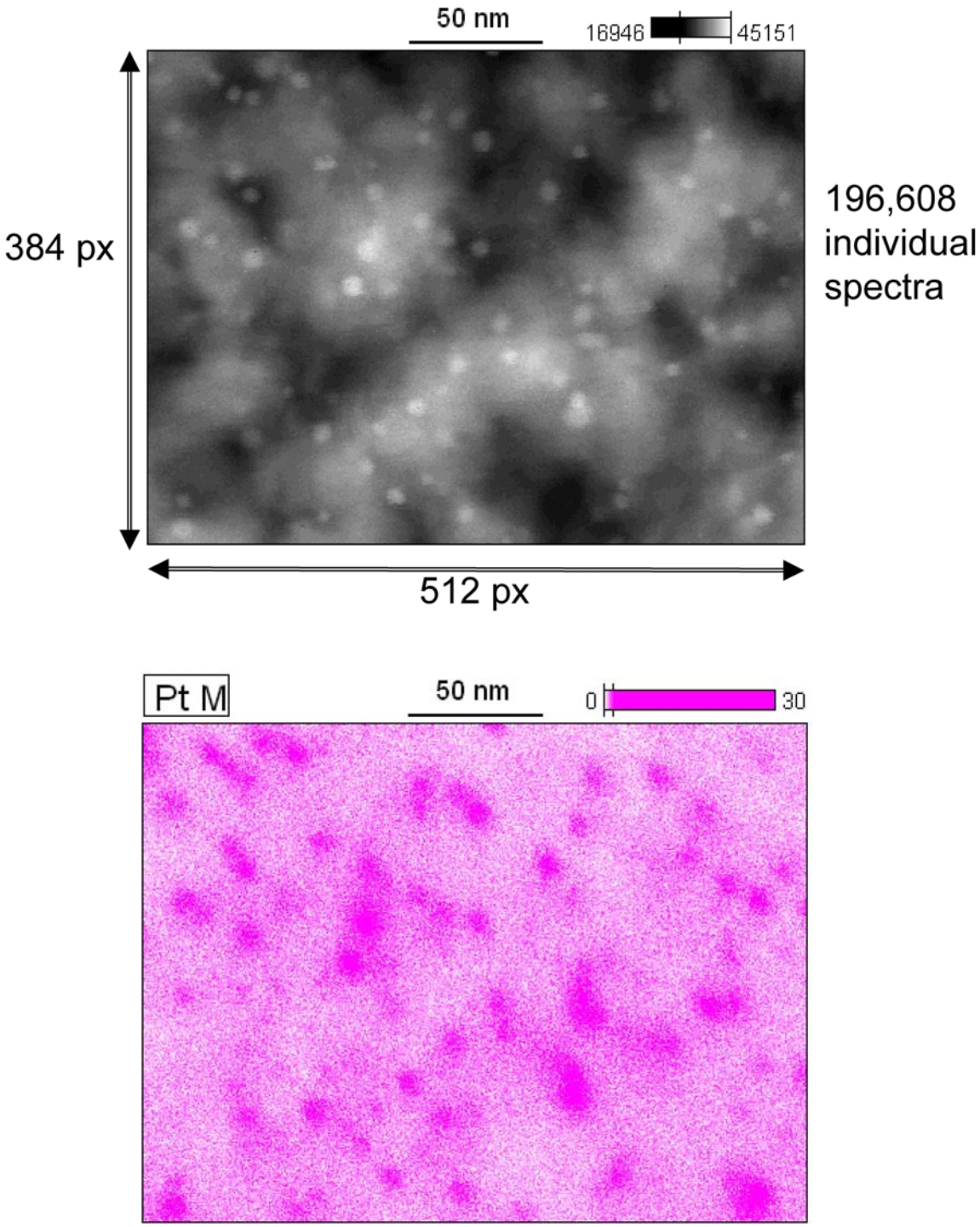

Figure 1A, Z-contrast image of a catalyst sample via STEM with a corresponding X-ray Spectra image, B, of locations where Pt was detected.

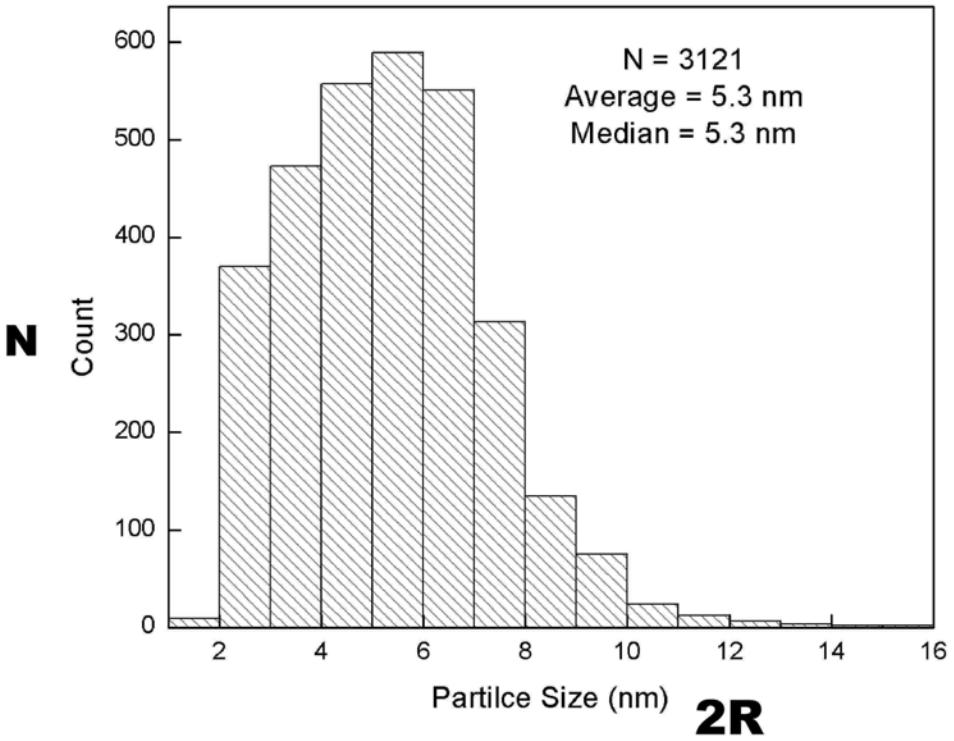

Figure 2. A histogram of number of Pt particles, N, as a function of particle size range for the above data.

Development of NO_x Sensors for Heavy Vehicle Applications

Timothy R. Armstrong, David L. West, Fred C. Montgomery
Oak Ridge National Laboratory
CRADA No. ORNL 01-0627
with Ford Motor Company

Objective

The proposed project seeks to develop technologies and materials that will facilitate the development of NO_x and ammonia sensors. The development of low-cost, simple NO_x will facilitate the development of ultra-low NO_x emission engines, directly supporting the OHVT goals.

Technical Highlights

Two material sensor configuration (oxide on Pt)

1. "NO-selective" behavior achieved with multilayer (oxide on Pt) sensing element using Cr_2O_3/Pt, $CuWO_4$/Pt).
2. NO selective behavior appears to be related to the relative efficacy of Pt for the reduction/oxidation of O_2.
3. Little O_2 sensitivity is observed in these sensors.

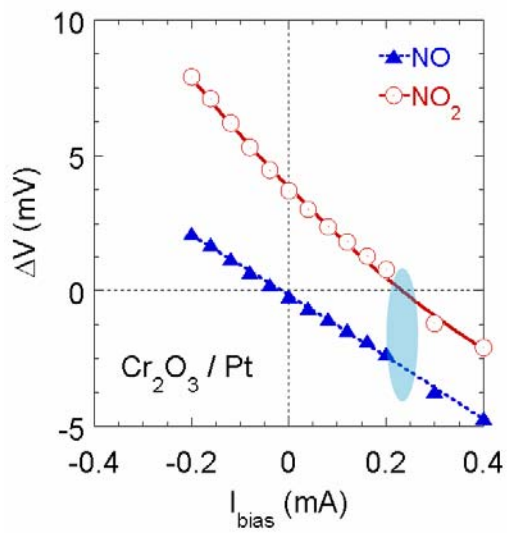

Figure 1. I-V curve for multilayer sensor. Highlighted region indicates that a bias current of 0. 22 mA will reduce the NO_2 signal to zero resulting in a sensor that measures only NO.

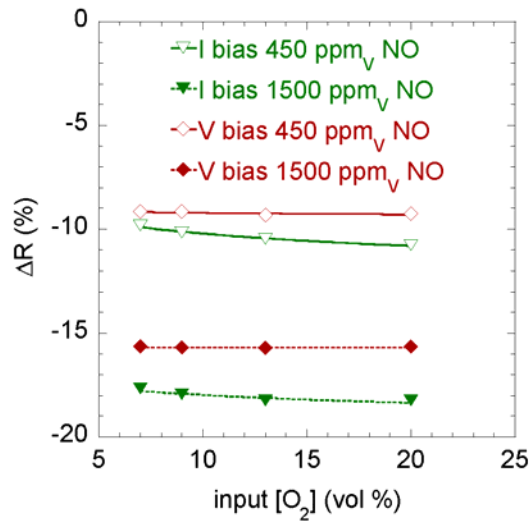

Figure 2. Plot showing oxygen insensitivity of multilayer NO sensor.

4. This is the only sensor configuration developed to date that results in a pure NO or NO_2 sensor. Single material sensor configuration (oxide only).

5. Single material sensing element gives "total NO_x" behavior over a narrow biasing range.
6. We have explored interdigitated designs with these sensing elements
    a. Irrespective of geometry, the single material design has a large O_2 sensitivity, increasing as the NO_x concentration decreases
    b. The interdigitated: designs give much larger signals (in terms of percent change in resistance) than the "original" design.
7. Non interdigitated designs show a small O_2 sensitivity.

Status of FY 2003 Milestones

Although this project had a late kick-off, we are ahead of schedule of most of the milestones:

1. Modify current sensor test stand for operation at 800°C (delayed at request of Ford)
2. Test NGK sensor in modified test stand (delayed at request of Ford)
3. Deliver NO_x catalyst assessment and program plan to Ford (completed 6/2002)
4. Construct NO_x electrode test stand. (Completed 12/2003)
5. Deliver report on initial rest results (Completed 2/2003)
6. Design and procure screens for simplified NO_x sensor design. (Completed 12/2003)
7. Produce first simplified NO_x sensors for testing (Completed September 2003).

FY 2004 Milestones on target

Communications/Visits/Travel

1. A quarterly report will be delivered to Ford in January 2004.
2. Communications with LLNL and DOE HQ (R. Sullivan) have been initiated at the request of Ford to coordinate the ORNL and LLNL efforts to accelerate sensor development.

Problems Encountered

None to date.

Publications

None this quarter.

Intellectual Property Filed

None this quarter.

Ultra-High Resolution Electron Microscopy for Characterization of Catalyst Microstructures and De-activation Mechanisms

L. F. Allard, D. A. Blom, K. K. Lester, C.K. Narula and M. A. O'Keefe
Oak Ridge National Laboratory

Objective/Scope

The objective of the research is to characterize the microstructures of catalyst materials of interest for the treatment of NO_x emissions in diesel and lean-burn gasoline engine exhaust systems. The research heavily utilizes new capabilities and techniques for ultra-high resolution transmission electron microscopy (UHR-TEM). The research is focused on understanding the effects of reaction conditions on the changes in morphology of heavy metal species on "real" catalyst support materials (typically oxides). These changes are being studied utilizing samples treated in both steady-state bench reactors and a special *ex-situ* catalyst reactor system especially constructed to allow appropriate control of the reaction.

Technical Progress

Studies of a model NO_x trap catalyst composed of 2% by weight Pt on a mixed CeO_2-ZrO_2-La_2O_3-BaO-Al_2O_3 support material (or more formally, 2%Pt-98%[10%CeO_2-ZrO_2-90%(2%La_2O_3-98%BaO.6Al_2O_3)]) are continuing, with a series of reaction treatments that are revealing the behavior of the Pt species with treatment condition. Specifically, the thermal durability/stability, and catalyst restructuring behavior under exposure to diesel/gasoline-lean/rich simulated exhaust are being studied. In companion work, it has been observed that nearly atomically dispersed Pt species on the surface of some of the oxide phases in the Fresh sample undergo agglomeration into discrete crystallites 20 nm or more in size after thermal aging at 500°C in air, and then re-disperse into particles 1-2 nm in size after lean NO_x treatment for 4 h at 500°C. In order to fully understand the mechanisms that produce this unexpected result, the resultant catalyst particle structure and distribution is being characterized using high-resolution microscopy techniques. We are presently utilizing a JEOL 2010F STEM/TEM instrument with resolution of 0.14 nm in annular dark-field images, and 0.19 nm in bright-field TEM images, to characterize the dispersion morphologies of the Pt species.

In order to fully understand changes in Pt morphology as a result of reaction treatment, and specifically the influence of support structures on Pt morphology, the dispersion of Pt on the various oxide phase components of the Fresh (as-prepared) sample, have been characterized. This information may ultimately prove useful to help characterize the relationship between Pt dispersions on Fresh material with the Pt particle distribution on the as-reacted samples, leading to an understanding of reaction kinetics and the important microstructural features that control Pt particle growth under reaction conditions.

Examples of typical Pt dispersions on the alumina and ceria-zirconia phases in the Fresh preparation are given in Fig. 1a and b, respectively. These bright-field high resolution TEM images show the presence of Pt clusters which we now believe to be "rafts" of Pt atoms that are

1, 2 or perhaps 3 atomic layers thick. Typical Pt rafts on the alumina phase are 0.5 to 2nm in diameter. The 2nm diameter rafts, if they were actually discrete crystalline particles, would show lattice structure at the resolution provided in these images. The fact that no such lattice structure has been identified in any images to date supports the suggestion that the Pt species are in essentially 2-dimensional configurations on the support surface. The Pt rafts on the crystalline Ce-Zr phase, Fig. 1b, are 0.5 to 1nm in size (arrows). Because such small amounts of Pt are difficult to unambiguously identify in bright-field images, it is useful to have correlating dark-field images from the same sample area. Figure 2a and 2b show higher magnification images of the alumina phase from Fig. 1a. The dark-field image of Fig. 2b shows bright contrast for the high atomic number Pt species, and reveals the presence of Pt in areas where the contrast in the bright-field image is obscured by the high phase contrast of the support material. It is likely that Pt is dispersed on the surface nearly at the atomic level (single atoms or clusters of just a few atoms) in addition to the more visible, larger structures seen in the image. Credence to the raft hypothesis is further strengthened by the observation of the Pt rafts marked A and B in Fig. 2a. Although both rafts have similar diameters, raft A shows brighter contrast than raft B, consistent with the premise that it contains an extra layer of atoms. The sub-Ångstrom resolution that will be provided by the ACEM when it is operational should allow the individual atoms to be imaged, so that the number of layers in a particular raft can be more easily identified.

It might be expected that the Pt rafts would also be seen in profile at the edge-on surface of the support material. In the case of the images of the alumina support phase taken to date, no edge-on Pt species have been seen, likely because of the buildup of a contamination layer under observation in the microscope that obscures the original surface. The Ce-Zr particle in Fig. 2b, however, may show Pt rafts edge-on (as labeled), since the crystalline structure of the Ce-Zr phase extends to the surface of the particle. Again, more complete information gained from the higher resolution expected from the ACEM should allow these structures to be unambiguously clarified.

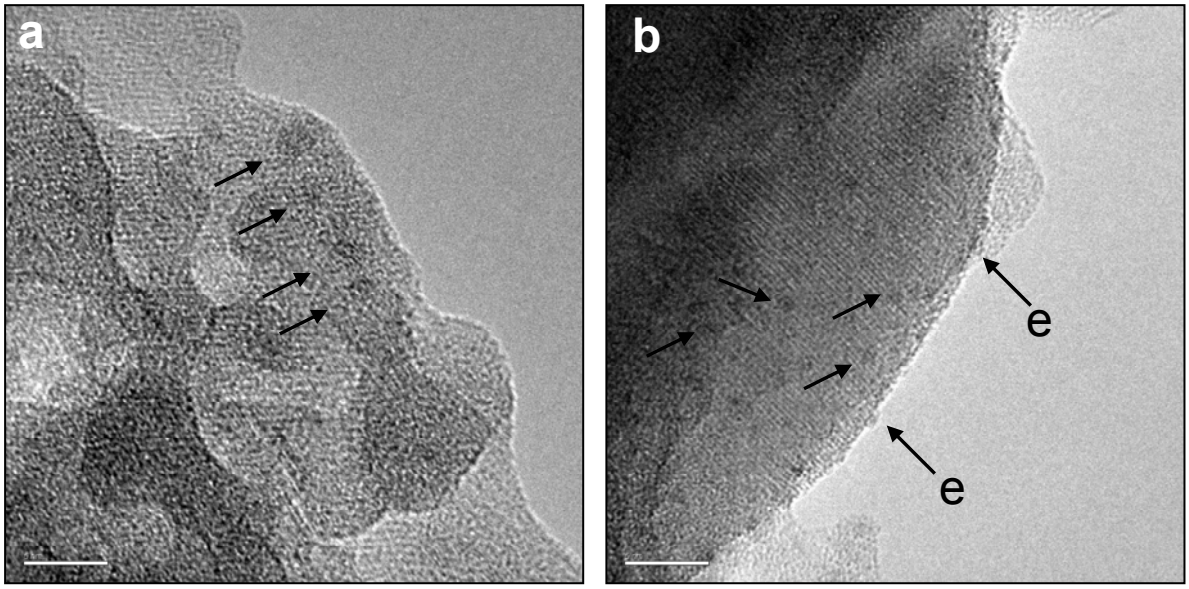

Fig. 1 a) Alumina phase with Pt rafts (arrows); b) Ce-Zr phase with Pt rafts (arrows). Possible edge-on rafts shown also (arrows e). Scale = 5 nm.

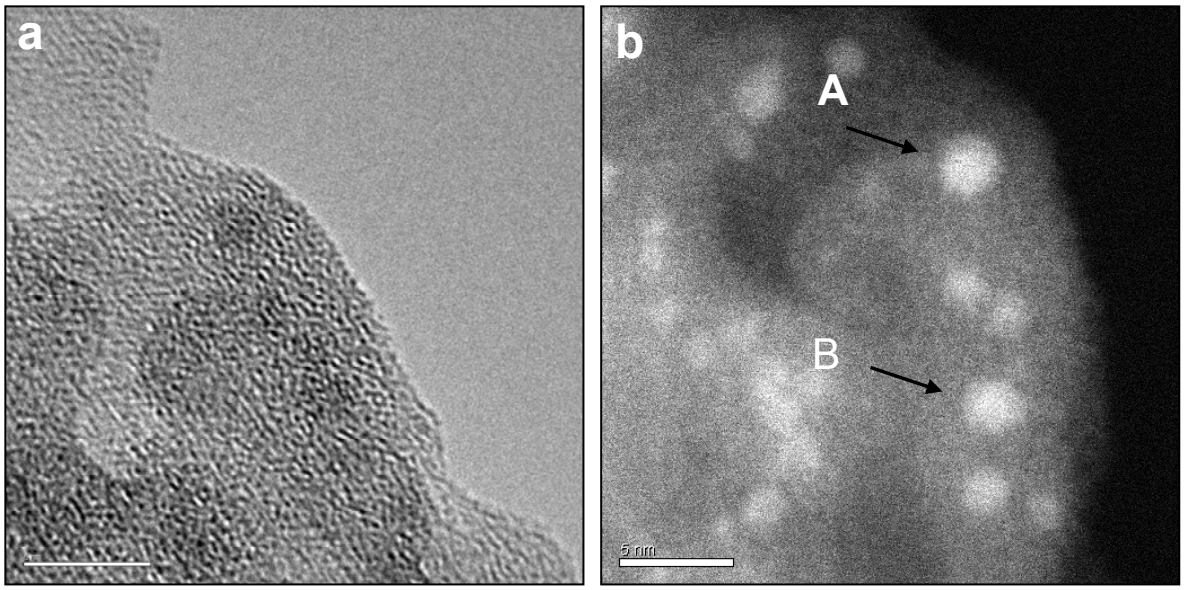

Fig. 2 a) Higher magnification bright-field image of Pt rafts on alumina. Some rafts easily visible, but other Pt species not as readily evident in the BF image as in the corresponding annular dark-field image of 2b (note small clockwise rotation of 2b vs 2a). Scale = 5 nm.

Characterization of Nano-Particle Shapes via Ultra-High-Resolution Imaging

The ability to precisely determine the morphology of nanoparticles is a goal of catalyst research, since the important reaction mechanisms that are controlled by the catalyst species depend on the interaction of impinging gaseous species with the exposed crystal planes on the particle surfaces. The HTML's new ACEM, with better than 0.1 nm ultimate resolution in dark-field imaging mode, is expected to provide images that will be directly interpretable in terms of the number of atoms in each resolved atomic column in the imaged particle. A complementary technique that will be available also on the new microscope takes advantage of the superior stability of the high voltage and objective lens current power supplies that have been specified, and the ultra-high-resolution objective lens pole piece on the instrument. This combination of features will allow standard bright-field images to be obtained which, after suitable processing, will give an ultimate resolution also in the sub-Ångstrom range. The processing technique is called "focal series reconstruction," (FSR)[1], and it involves acquisition of a series of images at known focus levels, and subsequent processing of those images to eliminate the effects of spherical aberration so a true representation of the structure can be obtained. We have implemented software to allow this FSR technique to be practiced on our JEOL 2010F TEM, which has optical characteristics similar to those of the new ACEM, but without the power supply stability that allows resolution to about 1.3Ångstroms. However, in collaboration with colleague Dr. Michael O'Keefe at Lawrence Berkeley National Laboratory, we have a demonstration of the potential for the technique to produce information at the 1Å or better level, which will allow the goal of particle morphology determination to be achieved. As an example, Figure 3a shows a model of a cube-

octahedral particle of palladium (structure similar to platinum and gold), which has 6 atoms in edge columns, and 11 atoms in the central column. The computed exit surface wave intensity is shown in Figure 3b; this is the image that would be revealed by FSR processing. A line scan of the intensity taken across the plane **a-b** as shown, illustrates the discrete intensity jumps associated with successive columns containing 1,3,5,7,9 and 11 atoms. Other line traces (such as **c-d**) show similar discrete jumps, so that by one appropriate image reconstruction, and several appropriate line traces, an initial measure of the full structure of the particle can be obtained. Images of real particles processed similarly (such as shown in the 2003 annual report), coupled with sub-Ångstrom resolution dark-field images, should allow us for the first time to provide information on the true morphologies of catalyst nanoparticles on our emission catalyst materials.

Status of Milestones

On schedule.

Communications/Visits/Travel

Two visits for one week each from Dr. M. A. O'Keefe, Lawrence Berkeley National Laboratory, to implement the capability to do Focal Series Reconstruction for high resolution imaging on the JEOL 2010F TEM.

Publications

Abstract submitted to the Instrumentation and Metrology for Nanotechnology Grand Challenge Workshop at the National Institute for Standards and Technology, Jan. 2004: "Sub-Ångstrom Electron Microscopy for Materials Science," M. A. O'Keefe and L. F. Allard.

References

1. M.A. O'Keefe, E.C. Nelson and **L.F. Allard**, "Focal-Series Reconstruction of Nanoparticle Exit-Surface Electron Wave," *Microscopy and Microanalysis 2003*.

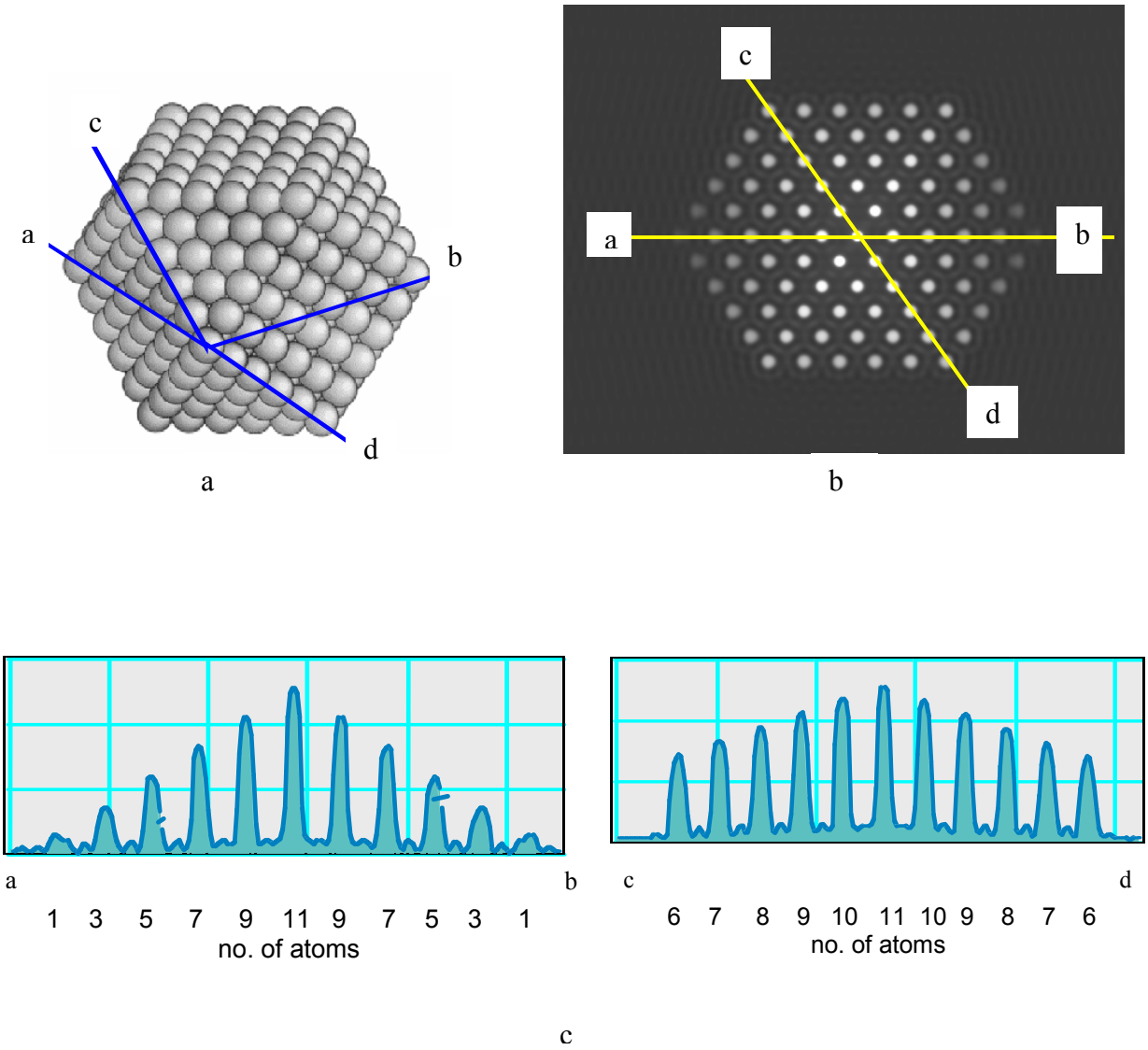

Fig. 3 a) Model of cube-octahedral particle, with 6 atoms in edge columns, and 11 atoms in the central column; b) image calculated from a focal-series reconstruction, viewed along the central column direction, with atom columns shown in white; c) intensity profiles along the traces a-b and c-d, showing the discrete intensity associated with the precise number of atoms in each successive column.

Microstructural Changes in NO_x Trap Materials under Lean and Rich Conditions at High Temperatures

C.K. Narula, K. K. Lester, H. M. Meyer III, and L.F. Allard
Oak Ridge National Laboratory

Objective/Scope

The introduction of diesel-engine-based heavy-duty trucks and passenger vehicles depends on the successful development of a strategy to treat nitrogen oxides (NO_x) emissions. A catalyst or a combination of catalysts that can convert NO_x into inert gases under oxidizing conditions over a complete range of exhaust temperatures does not presently exist. Among NO_x treatment strategies, lean NO_x traps (LNT) are the most likely candidates for early deployment because they are consumer transparent (no action needed on the part of consumers) and can be system-integrated into current vehicle control strategies [1].

NO_x traps collect engine out NO_x during lean operation and treat it during short rich operation cycles [2]. The NO_x traps can be considered to be derived from commercial three-way catalysts (TWC) installed to treat stoichiometric emissions from engines operating at air-fuel ratios of ~14. As such, the basic components of NO_x traps are identical to three-way catalysts. The advance version of three-way catalyst is a two layer system on a honeycomb substrate with the inner layer based on platinum-alumina and the outer layer on rhodium-ceria-zirconia. The NO_x traps derived from advanced three-way catalysts are identical to these with the exception of high baria content (the upper limit being close to 20%) in the alumina layer.

Fresh NO_x traps work very well but cannot sustain their high efficiency over the life-time of vehicles. The gradual and persistent deterioration in the performance of commercial TWC is quite well known [3]. The performance deterioration in NO_x traps is believed to be caused by aging due to high-temperature operation and sulfation-desulfation cycles necessitated by the sulfur oxides in the emissions from the oxidation of sulfur in fuel. The formation of barium aluminate is also considered to be a cause of performance deterioration since barium aluminate forms on thermal aging and is an inefficient NO_x adsorber. Until last year, the aging related microstructural changes in precious metals component were not available in open literature. In our previous reports, we summarized our studies of fresh and aged supplier samples that clearly show changes that occur on aging under various operating conditions. The prominent changes are sintering and migration of precious metals and migration of barium leading to reduced precious metal-adsorber surface area available for NO_x adsorption in lean cycles.

In order to design a thermally durable NO_x trap, there is a need to understand the changes in the microstructure of materials that occur during various modes of operation (lean, rich, and lean-rich cycles). This information can form the basis for selection and design of new NO_x trap materials that can resist the deterioration under normal operation. The first goal of the project is to determine if one or all of the microstructural changes take place during lean, rich, or lean-rich cycles.

The tasks to achieve this goal are as follows:

- Complete microstructural characterization of fresh and thermally aged NO_x trap materials to determine the species formed as a result of aging.
- Complete microstructural characterization of fresh NO_x trap materials after exposure to lean conditions to determine the species formed during lean cycles.
- Complete microstructural characterization of fresh NO_x trap materials after exposure to rich conditions to determine the species formed during rich cycles.

The second goal of the project is to investigate and design new materials that can withstand NO_x trap operating conditions without undergoing detrimental structural changes. The results from first goal will provide insights into changes that occur in NO_x trap materials at a microstructural level upon extended exposure to NO_x trap operating conditions enabling selection and design of materials for the second goal.

In order to carry out a detailed study of role of operating condition in inducing these changes, we synthesized a model NO_x trap catalyst 2%Pt-98%[10%CeO_2-ZrO_2-90%(2%La_2O_3-98%BaO.6Al_2O_3)]. The structural characterization of this catalyst was also summarized in the previous reports.

In this report, we summarize our study of thermal aging of 2%Pt-98%[10%CeO_2-ZrO_2-90%(2%La_2O_3-98%BaO.6Al_2O_3)] and compare it to lean NO_x aging carried out in the updated ex-situ reactor (described previously). Our previous studies have shown that the model catalyst substrate 98%[10%CeO_2-ZrO_2-90%(2%La_2O_3-98%BaO.6Al_2O_3)] (excluding noble metals) retains its beneficial surface properties even after thermal aging at 1050°C. In the following sections, we describe our results on the aging of the NO_x trap materials.

A. Thermal Aging of Model NO_x Trap Catalyst

We completed the thermal aging and microstructural characterization of the model NO_x trap catalyst 2%Pt-98%[10%CeO_2-ZrO_2-90%(2%La_2O_3-98%BaO.6Al_2O_3)]. A comparison of these results with those obtained on microstructral analysis of aged supplier samples (previous report) clearly shows that the aging of various components of NOx trap systems do not result from thermal aging only.

The TEM studies of the freshly prepared model catalyst 2%Pt-98%[10%CeO_2-ZrO_2-90%(2%La_2O_3-98%BaO.6Al_2O_3)] show the substrate to be primarily amorphous. The precious metal particles (Pt particles) are generally ~1nm in diameter.

We carried out the thermal aging of the 2%Pt-98%[10%CeO_2-ZrO_2-90%(2%La_2O_3-98%BaO.6Al_2O_3)] at 500, 600, 700, 800, and 900°C for 4 hours in air. The substrate does not show significant difference except the XRD peaks for the barium aluminate component gradually increases with increased sintering temperature (previous report). The TEMs of fresh and thermally aged samples at 500ºC are shown in Figures 1 and 2 respectively. The sintering of Pt can be observed even at 500ºC as an increase in particle size to ~30-40 nm.

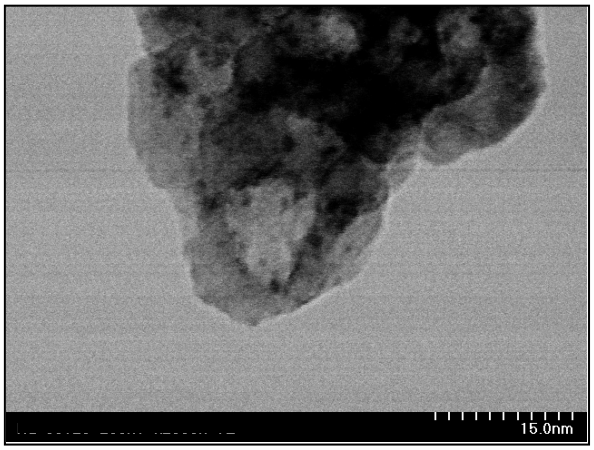

Fig. 1: Transmission electron image of fresh Pt/[10%CeO_2-ZrO_2-90%(3%La_2O_3-97%BaO.6Al_2O_3)] Pt particles are ~1nm in diameter.

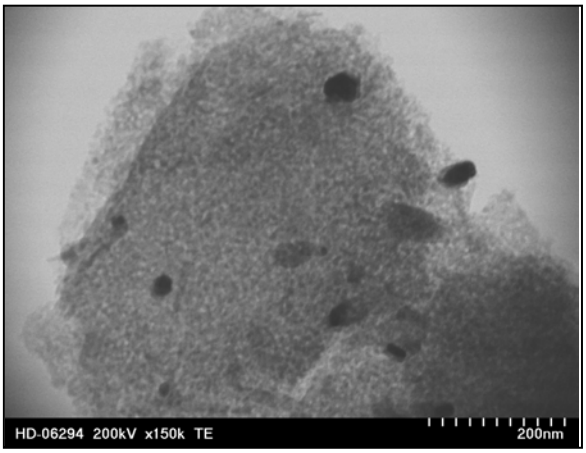

Fig. 2: Transmission electron image of thermally aged Pt/[10%CeO_2-ZrO_2-90%(3%La_2O_3-97%BaO.6Al_2O_3)]. Pt particles are ~30-40 nm in diameter.

Sintering of Pt increases with an increase in the thermal aging temperature. After aging at 900ºC, the Pt particle size increases to 70-80nm (with an occasional very large particle ~150 nm).

While diesel exhaust treatment systems do not see temperatures above 500ºC, our incentive for high temperature studies comes from high-temperature applications of NO_x traps. For example, the temperature of the exhaust from lean gasoline engines utilizing almost identical NO_x traps can easily reach 800-900ºC.

B. Aging of Model Catalyst under Simulated Lean Diesel Exhaust

We placed a fresh sample of the model catalyst, 2%Pt-98%[10%CeO_2-ZrO_2-90%(2%La_2O_3-98% BaO.6Al_2O_3)], in the ex-situ reactor system (described previously) and exposed it to lean diesel exhaust conditions at 500°C for 4 hours [CO, CO_2, H_2, HC, NO_x, H_2O, flow rate 100cc/min]. As noted in section A, the Pt particle size is less than 1nm in the fresh sample. Some sintering of Pt particles is observed under these conditions and the size grows to ~2.5nm, see Figure 3. However, the sintering is significantly less than that observed on thermal aging (~30-40 nm) at 500°C in air.

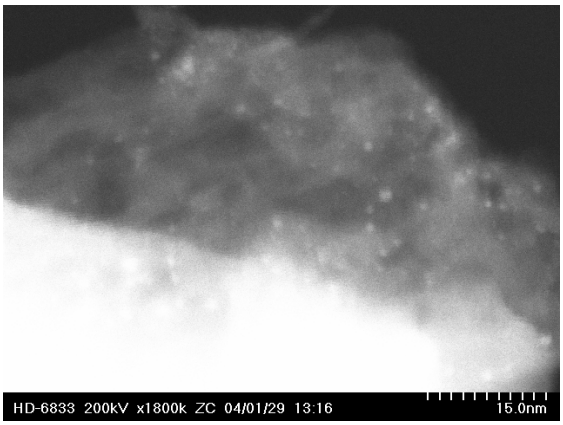

Fig. 3: Transmission electron image of fresh Pt/[10%CeO_2-ZrO_2-90%(3%La_2O_3-97%BaO.6Al_2O_3)] after exposure to simulated lean diesel exhaust. Pt particles are ~2.5nm in diameter.

Interestingly, the sample exposed to lean diesel exhaust conditions at 500°C after thermal aging shows partial redispersion of Pt particles. We placed a sample of the thermally aged (500°C, air, 4h) model catalyst, 2%Pt-98%[10%CeO_2-ZrO_2-90%(2%La_2O_3-98%BaO.6Al_2O_3)], in the ex-situ reactor system and exposed it to lean diesel exhaust conditions at 500°C for 4 hours. As mentioned previously, this reactor system permits monitoring of microstructural changes of the same areas in the TEM before and after exposure to various reaction conditions. Figure 4 shows the dark field image of the thermally aged 2%Pt-98%[10%CeO_2-ZrO_2-90%(2%La_2O_3-98%BaO.6Al_2O_3)] catalyst to accentuate the metal particles. Figure 5 shows the dark-field image of same area after 4h exposure to the simulated exhaust at 500°C. A redistribution of the Pt particles occurs and the particle size decreases from 30-40nm to 5-10nm. EDS confirmed that the particles shown are indeed Pt and are not other metals coming from another source, such as the support grid or ex-situ reactor. Increasing the simulated exhaust temperature to 600°C did not lead to sintering, but the redispersion of Pt particles was observed again.

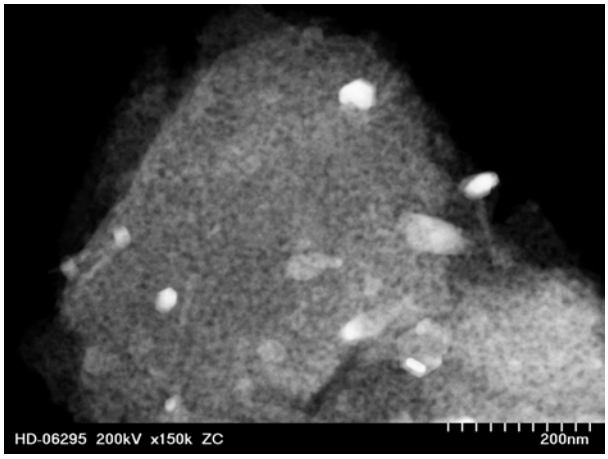

Fig. 4: Dark-field Z-contrast image of thermally aged Pt/[10%CeO_2-ZrO_2-90%(3%La_2O_3-97%BaO.6Al_2O_3)]. Pt particles are ~30-40 nm in diameter.

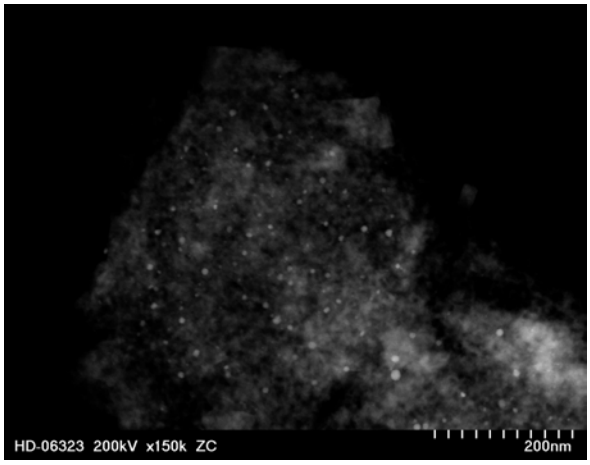

Fig. 5: Dark-field Z-contrast image of the exact same area as Figure 3 after exposure to simulated lean diesel exhaust. Pt particles are ~5-10 nm in diameter.

In general, the particle size of precious metal component of the catalysts increases upon extended exposure to automotive operating conditions [3]. The redispersion of Pt particles under simulated diesel exhaust is quite unexpected because these conditions do not match the conditions under which redispersion has previously been observed. Chu and Ruckenstein found that after a number of heating cycles, in H_2 or O_2, Pt particles redisperse upon a final heating in O_2 and sinter upon a final heating in H_2 [4]. Johnson and Keith found that thermal aging of Pt/alumina under oxidizing conditions and subsequent heat treatment in H_2 leads to Pt redispersion [5]. Weller and Montagna also found the redipersion of Pt in Pt-Al_2O_3 on cyclic exposure to O_2 and H_2 during reduction step [6]. They also noted that the redispersed Pt is resistant to sintering [6]. The redispersion is not limited to Pt-Al_2O_3 systems but has also been observed in Ni-Al_2O_3 and Ni-SiO_2 systems when oxidation was carried out at 600ºC and reduction at 400ºC [7]. In our system, the samples were thermally aged in air, then exposed to lean exhaust conditions, and finally cooled under lean conditions. The results have been found to be reproducible.

It is important to note that the experiments in the ex-situ reactor system do not precisely duplicate the aging of NO_x traps during normal operation. The alternating lean/rich conditions are not present in our experiments; instead, our samples are exposed to lean conditions, and lack of control on space velocity due to very small amount of catalyst leads to NO_x absorber saturation conditions. The saturation condition persists throughout our treatment.

Although the mechanism of redispersion under simulated lean NO_x diesel conditions remains to be determined, these results seem to suggest that the Pt particles only grow to 5-10 nm in size after sintering in a lean diesel exhaust at 500ºC (as opposed to 30-40nm after exposure to air at 500ºC) because the concurrent redispersion prevents further increase in particle size.

Our studies in the next quarter will be focus on following experiments:

- Reproduce results in a bench top flow reactor where we can control the flow rate of simulated exhaust.
- The lower and upper limit temperatures of thermal treatment under lean diesel conditions that facilitate redispersion of platinum.
- The time needed to achieve redispersion.

If the time, temperature, and exhaust flow rate required for redispersion can be built into vehicle strategy, our results will facilitate NO_x trap deployment.

C. Surface Studies of Fresh and Aged Model NO_x Trap Catalyst:

The results of X-ray photoelectron spectroscopy analysis (XPS) of 2%Pt-98%[10%CeO_2-ZrO_2-90%(2%La_2O_3-98%BaO.6Al_2O_3)] are presented in Table I. Powder samples of the fresh, thermally aged (500ºC in air for 4h), and lean simulated exhaust-exposed (after thermal aging) catalysts were pressed onto an indium foil then analyzed.

Table I: XPS Analysis of 2%Pt-98%[10%CeO_2-ZrO_2-90%(2%La_2O_3-98%BaO.6Al_2O_3)].

Element	Fresh		Thermally Aged at 500ºC in Air for 4 hours		Aging under simulated lean diesel exhaust at 500ºC for 4 hours	
	Atomic%	Wt%	Atomic %	Wt %	Atomic%	Wt%
O	57.8	33.5	59.3	34.9	61.7	37.7
Al	26.6	26.0	27.6	27.4	26	26.8
C	6.3	2.7	3.7	1.6	4.1	1.9
Ba	3.9	19.4	5.9	29.8	5.1	26.7
La	2.2	11.0	0.5	2.5	0.6	3.2
N	0.3	0.2	0.2	0.1	0	0
Pt	1	7.1	0.5	3.6	0.5	3.7

The high concentration of Pt and La in fresh samples is due to the migration of these elements to the surface. Thermally aged samples probably achieve a redistribution of elements leading to reduced concentration of these elements on the surface. When a thermally aged sample is exposed to simulated lean NO_x conditions for about 4 h at 500ºC, the surface composition does not change significantly. The lack of a significant increase in nitrogen or carbon after extended exposure to lean diesel exhaust is puzzling. Further experiments are in progress to determine if it is just a surface phenomenon, or if the bulk material loses nitrate during our cooling protocol.

Other activities

Gas flow controllers, water pump, and gas analyzers have been received and we initiate assembly of a bench-top flow reactor in a laboratory at National Transportation Research Center (NTRC). Other items will be added to the flow reactor upon receipt.

References

1. Miyoshi, N.; Matsumoto, S.; Katoh, K.; Tanaka, T.; Harada, J.; Takahashi, N.; Yokota, K.; Sigiura M., and Kasahra, K.; "Development of New Concept Three-Way Catalyst for Automotive Lena-Burn Engines", SAE paper 95-0809.
2. Takahashi, N.; Shinjoh, H.; Iijima, T.; Suzuki, T.; Yamazaki, K.; Yokota, K.; Suzuki, H.; Miyoshi, N.; Matsumoto, S.; Tanizawa, T.; Tateishi, S.; and Kasahara, K.; "The New Concept 3-Way Catalyst for Automotive Lean-Burn Engine: NO_x Storage and Reduction Catalyst", Catalysis Today, 1996, **27**, 63-69.
3. Gandhi, H.S., Graham, G.W., and McCabe, R.W., "Automotive Exhaust Catalysis", J. Cat., 2003, **216**, 433-442.
4. Chu, Y.F.; Ruckenstein, E.; "On the Sintering of Platinum on Alumina Model Catalyst", Journal of Catalysis, 1978, 55, 281-298.
5. Johnson, M.F.L.; Keith, C.D.; "The State of Platinum in Re-Forming Catalysis", 1963, **67**, 201.
6. Weller, S.W., Montagna, A.A.; "O_2 Chemisorption at High Temperatures on Platinum-Alumina and Platinum-Zeolite", J. Catal., 1971, **20**, 394.
7. Nakayama, T.; Arai, M.; Nishiyama, Y.; "Dispersion of Nickel Particles Supported on Alumina and Silica in Oxygen and Hydrogen", J. Cat., 1984, **87**, 108.

Lightweight Valve Train Materials

Mark J. Andrews
Caterpillar Inc.

Introduction

Valve train components in heavy-duty engines operate under high stresses and temperatures, and in severe corrosive environments. In contrast, the valve train components in the light-duty engine market requires cost-effective reliable materials that are wear resistant and lightweight in order to achieve high power density. For both engine classes, better valve train materials need to be identified to meet market demand for high reliability and improved performance while providing the consumer lower operating costs.

Advanced ceramics and emerging intermetallic materials are highly corrosion and oxidation resistant, and possess high strength and hardness at elevated temperatures. These properties are expected to allow higher engine operating temperatures, lower wear, and enhanced reliability. In addition, the lighter weight of these materials (about 1/3 of production alloys) will lead to lower reciprocating valve train mass that could improve fuel efficiency. This research and development program is an in-depth investigation of the potential for use of these materials in heavy-duty engine environments.

The overall valve train effort will provide the materials, design, manufacturing, and economic information necessary to bring these new materials and technologies to commercial realization. With this information, component designs will be optimized using computer-based lifetime prediction models, and validated in rig bench tests and short-and long-term engine tests.

Program Overview

Information presented in this report is based on previous proprietary research conducted under Cooperative Agreement DE-FC05-97OR22579.

Ceramic Materials

Silicon nitride materials have been targeted for valve train materials in automotive and diesel industries since early 1980's. Some silicon nitride material grades have reached a mature level of materials processing, capable of implementing into production. Commercial realizations have been reported in both automotive and diesel valve trains, with large-scale production underway. The silicon nitride valve train components in production are used in high rolling contact stress applications and have exhibited superior wear resistance, and longevity.

Intermetallic Materials

Titanium aluminide based intermetallics retain their strength to elevated temperature and are highly corrosion-resistant. They are lightweight, and posses high fracture toughness. These alloys are actively being investigated for several aerospace and automotive applications.

Summary

Valve Test Rig

The valve bench rig added an additional 400 hours of rig time to a set of NT551 silicon nitride valves that have already accumulated 100 hours of test time. These valves will be examined by

ANL using optical and NDE techniques to assess the accumulation of cyclic damage. Table I shows the test parameters for the 500-hour test time. Note that an additional test parameter of using an out-of-alignment valve guide was unsuccessful. Altering the alignment of the valve guide in the engine head resulted also in distorting the inside diameter of the guide. This made the valve insertion into the guide very difficult and the motion of the valve was with great resistance.

Advanced Materials Technology is considering the acquisition of a second valve test rig located in TC-L at the Tech Center. This test rig can accommodate 3400 and 3500 series engine valves and applies a hydraulic load to the valve face, simulating the combustion pressure load. The rig applies the simulated combustion load cyclically and uses standard Caterpillar seat insert components. The rig can also apply a cyclic thermal load through induction heating.

Machining Study

The cylindrical test specimens having a nominal diameter of 8 mm and a length of 75 mm have completed the application of three different super-finishing machining steps. The finishing steps remove approximately 15-20 μm of the surface as a means to remove machining damage. Samples of each test conditions were sent to ANL for nondestructive evaluation and the remaining specimens were shipped to ORNL for strength tests. Additional test specimens will be sent to ANL for NDE and then returned for strength tests at ORNL. NDE images detecting defects or surface flaws generated by ANL will be compared to the fractured specimens in order to assess the predictive capability of the NDE.

Silicon Nitride Valve Blanks

Fifty silicon nitride engine valve blanks fabricated from silicon nitride ceramics were finished machined at Junker Machining in Norarch, Germany. Probabilistic designs for the ceramic valves were generated prior to machining that combined finite element modeling with brittle materials life prediction codes. Four different valve designs were machined in order to accommodate both diesel and natural gas Caterpillar engine platforms.

Junker Machining exceeded all of the machining tolerances of the ceramic valves with the exception of the fillet radius region. An error by Junker was made in reading the valve print specifications, resulting in the absence of a specialized grinding wheel. The surface Ra in the fillet radius region is approximately 3 times rougher than specified by the prints. The decision to machine the valves was made leaving the fillet region with a rougher surface. Strength results obtained from the super-finishing machining study will determine if the fillet radius region will undergo this process to improve the surface roughness. The surface/subsurface of the machined ceramic valves are presently being examined using nondestructive methods developed at Argonne National Laboratory (ANL). Bench tests will be performed after the ceramic valves return from ANL that will then be followed by engine tests.

Life Prediction of Ceramic Engine Valves

Efforts to upgrade the CERAMIC and ERICA computer codes were successful. ERICA now accepts new versions of ANSYS finite element software and the CERAMIC has a bootstrapping technique to assess confidence intervals. However additional software errors have been detected, making CERAMIC unable to life predictions of finite element components.

Intermetallic Materials Research
Ten γ-TiAl valve head blanks were shipped to Junker Machining in Norarch Germany for rough machining the heads for the 3401 diesel inlet valve. The valve heads will be returned to Caterpillar where valve stems will be attached to the heads through friction welding. With the stems attached to the heads, the valves will be sent to Junker Machining for final dimensional machining.

ANL
Shipments of cylindrical test specimens and NT551 ceramic valves were made to ANL for NDE assessment. The cylindrical test specimens are part of the machining study (see machining study in this report) while the ceramic valves had completed 500 hours of cyclic impact tests.

Presentations

None

Future Work
Bench tests of the ceramic and TiAl prototype valves will begin in the next reporting period. Strength tests will be performed on the cylindrical test specimens to determine the viability of super-fine machining steps on silicon nitride. NDE results from ANL are anticipated in the next reporting period for the new ceramic valves and the cylindrical test specimens.

Table I. Bench test matrix for NT551 valves for completing 500 hours on valve rig.

Test Configuration	Valve contact angle (deg)	Seat insert contact angle (deg)	Valve guide
A	30	30	standard
B	45	45	standard
C	45	30	standard
D	30	30 – eccentric machined	standard
E*	30	30	nonstandard
F*	45	45	nonstandard
G*	45	30	nonstandard
H*	45	30 – eccentric machined	nonstandard

*note: items E-H were not completed due to excessive rubbing of the valve in the valve guide

Engineered Surfaces for Diesel Engine Components

M. Brad Beardsley and Jesus G. Chapa-Cabrera
Caterpillar Inc.

Objective/Scope

Engine testing of thermal sprayed coatings has demonstrated their use as thermal barriers and wear coatings can reduce fuel consumption, reduce wear and reduce component temperatures. The durability of thermal sprayed coatings, particularly thermal barrier coatings, remains as the major technical challenge to their implementation in new engine designs. New approaches to coating design and fabrication will be developed to aid in overcoming this technical hurdle. New laser technology of surface dimpling, cleaning and laser assisted spraying will be applied to enhance adherence and increase coating strength. Refinements of current seal coating technologies will be developed to further enhance the durability of the coating structure. New quasicrystalline materials will be evaluated as thermal barrier coatings as well as wear coatings for ring and liner applications and as low friction coatings for camshafts and crankshafts. Plasma spraying, D-Gun and HVOF processing will be used to develop these new coatings.

Technical Highlights

Laser Tacking - Laser tacked TBC specimens for tensile adhesion testing have been processed and will be tested to determine the effect of the laser tacking on adherence of the coatings. Two coatings, a 0.20 mm thick bond coating and a two-layer thick bond coating/ceramic, 0.50 mm total thickness were processed. Two areas of the specimens were "key-holed" tacked, with melting of the materials into the substrate. The beam width was ~20 microns in diameter in both areas.

Laser Assisted Thermal Spraying – Fraunhofer USA will provide assistance in determining the best process path for the thermal barrier coating materials. A visit to the Dresden Fraunhofer is planned for late April at which time they will be able to demonstrate the process and provided details on what is required. A YAG laser system will be installed in Caterpillar's thermal spray laboratory to continue the development for thermal barrier coating systems. Planned installation at Caterpillar is end of second quarter 2004.

Laser Dimpling for Adherence – Discussions with the IREPA and ISPE institutes in France were held in regard to their patent PROTAL process for creating clean, roughened surfaces for thermal spraying. This process has been shown to be quite successful in elimination of the need for grit blasting of aluminum and titanium substrates using Q-switched lasers. The Q-switched laser technology will be investigated for surface prep of steel and cast iron substrates by Caterpillar. A trip to France for further discussion with the inventors is planned for April, 2004.

Quasicrystals – Diffusion couples of the aluminum in the quasicrystal have been run at Iowa State University. The couples included a 4140 steel substrate, two NiCrAlY bond coatings with different chrome and aluminum contents and a FeCrAlY bond coating. Initial results of the diffusion experiments show a smaller diffusion zone with higher aluminum content of the bond coatings. Full microstructural and microprobe chemical analysis is underway.

Future Plans

Pull testing of the laser-tacked specimens will be done. Full microprobe analysis of the quasicrystal diffusion couple samples will be completed and oxidation test specimens will be sprayed. Planning for a trip to Fraunhofer in Dresden, Germany is underway.

Travel

None this quarter, no trips are planned for next quarter.

Status of FY 2003 Milestones

321. Determine the effect on TTBC bond strength due to laser micro-dimpling of the substrate surface prior to coating. (July 31, 2003)

Q-switched laser technology has been identified as a path to achieve surface topography required for bonding without the need for grit blasting. A visit to France to discuss collaboration to extend this technology to steel and cast iron is planned for April, 2004.

322. Determine the effect on TTBC coating strength and permeability due to laser shock peening after coating application. (July 31, 2003)

The Q-switched laser technology will be investigated for this effect. April 2004.

323. Determine the effect on the hardness and microstructure of the TTBC due to laser assisted plasma deposition. (July 1, 2003)

No progress to report.

324. Incorporate torsional fatigue testing results into life models. (Completed May 29, 2002)

The final report of this work has been received from the University of Illinois.

325. Develop FEA models to aid in the design of life prediction tools for the TTBC system. (December 1, 2003)

No progress to report.

325. Evaluate the microstructure of the ceramic TTBC material using varying laser power.

No progress to report.

Publications

None this period.

Cermet Composites for Wear Applications

T. M. Yonushonis, R. J. Stafford, M. Henrichsen, and D.J. Gust
Cummins Inc.

Objectives

- Follow-on work from DOE Cooperative Agreement DE-FC05-97OR22538 by Cummins Inc. and Oak Ridge National Laboratory.

- Continue process optimization for a cermet material comprised of hard titanium carbide (TiC) particles in a tough nickel aluminide (Ni_3Al) metallic matrix.

- Establish and document process requirements for a hard surface cast material, by casting the iron into a pre-form layer of tungsten carbide (WC) powder to form a hard composite wear-resistant surface.

- Develop potential applications in heavy-duty diesel engine fuel systems for these two previously identified unique wear-resistant materials.

Introduction

Early product and process development on the TiC/Ni_3Al cermet was done at Oak Ridge National Laboratory and was centered on various formulations varying the percentages of titanium carbide powder in the nickel aluminide metal matrix. Then extensive milling studies of the TiC were performed, which were made all the more difficult due to the need to perform the milling in an oxygen (O_2) devoid atmosphere. All this was followed by extensive bending strength, surface wear, and thermal expansion analysis.

The development of this TiC/Ni_3Al cermet material has moved to a potential production supplier, CoorsTek. Then with the identification of a Cummins Inc. Fuel System component to prototype out of this cermet, the process needed to be evaluated and optimized for near-net shape precision injection molded parts.

The move to production like lots of material from CoorsTek required the refurbishing of injection molding equipment to include a vacuum/Ar atmosphere. A multi-component binder formulation was developed next using several polymeric components which are compatible with solvent extraction, the primary method used to accomplish polymer de-binding in a defect free state after the molding operation. This binder system also provides for initial wetting of powders during mixing, provides a strong feedstock matrix for injection molding at a reasonably low temperature, and provides a broad working viscosity at very high solid loading while maintaining uniform filling of complex component molded shapes. Further, the mixing is being performed in a double planetary type closed heating mixing vessel. In order to minimized the opportunity for oxidation of the submicron TiC powder, a mixing cycle was developed by initially evacuating the mix chamber, followed by flowing argon (Ar) gas during heating of the cermet powders and binding system. Several test batches of material were used to purge/clean-out the injection molding machine screw and barrel.

Several injection molding test bar trials were run, with ultimately a very good narrow part weight distribution for a batch of over 100 test bars. Solvent debinding was used to extract about two-thirds of the binding system, leaving a strong component for handling. The residual binder is then removed during part sintering. The sintering, like the mixing, is done in a non-oxidizing environment. The initial sintering done at ORNL was done in an Ar overpressure furnace. These initial sintered microstructures were about 98% dense. For this cermet material the target density has been specified as >99%. Optimization of sintering cycle continues at both ORNL and CoorsTek. Injection molding tooling is in place and currently molding test bars at CoorsTek. Material property testing to verify material composition suitability, followed by prototype component manufacturing and rig evaluation at Cummins will complete the program.

Early work and all continuing work of the tungsten carbide (WC) pre-forms have been done with Advanced Powder Products, Inc. mixing, sintering, and pressing these pre-forms. There was some very early success, followed by several years of unsuccessful attempts by APP, and internally at Cummins Inc., to duplicate that early success. All attempts have been unsuccessful. A significant material/process re-evaluation and intense analysis of the early successful pre-forms has lead Cummins Inc. to believe that a bimodal pore distribution is a potential reason for the success. In addition to the lack of the larger pores, a second likely barrier to cast iron infiltration is a possible change to a higher sintering temperature (to add strength to these pre-forms) as a reason for the lack of success.

This work is currently progressing with a planned Taguchi experiment, to establish either the additional larger pores are needed like the early bimodal pre-form distribution, or the higher sintering temperature had a role in inhibiting the infiltration of the cast iron into the tungsten carbide pre-forms during the pouring. Once pre-forms are successfully infiltrated in casting, material property measurements and wear testing will be done on the composite material. This data will then be used to guide the recommendation for potential diesel engine applications.

Results

A production size material batch has been compounded and the design shrinkage for the TiC/Ni_3Al cermet material has been established by CoorsTek. Further work by CoorsTek is on-hold, until Cummins has completed Falex-6 pin-on-disk wear testing. This wear testing is scheduled to begin January 2004.

The Taguchi experiment tungsten carbide (WC/cast iron) samples were poured in late December 2003, but have not been received at Cummins for evaluation and analysis. Several diesel engine applications have been identified for this process, but the in-ability to duplicate the early success has been very frustrating. Success here will be a great motivator and could have significant dividends.

Nanoengineered Materials

J. Sankar, Z. Xu, and S. Yarmolenko
North Carolina A & T State University

Objective/Scope

Develop a liquid phase electrolyte deposition technique to process yttria stabilized zirconia (YSZ) thin films for solid oxide fuel cells.

Task

Develop a facility for the thin film processing through the liquid phase electrolytic deposition. Study the parameters that control the deposition processes.

Technical Highlights

Electrolytic deposition has been developed as a new technology in ceramic processing for processing of nanostructured thin films and powers. Cathodic electrolytic deposition is achieved via hydrolysis of metal ions or complexes by an electro-generated base to form oxide, hydroxide or peroxide deposits on cathodic substrates. Hydroxide and peroxide deposits can be converted to corresponding oxide by thermal treatment.

The interest in this technique stems from a variety of its advantages, such as low cost of equipment, rigid control of processing thickness and uniformity as well as the possibility of forming coatings on substrates of complex shape. The uniformity of ceramic coatings results from the insulating proprieties of deposits and the electric field dependence of the deposition rate.

In this report, the experimental studies of deposition YSZ complex ceramic coating on Ni substrates will be presented. The technique and process of crack filling in the deposited film were investigated experimentally.

Commercial high purity zirconium dichloride oxide hydrate, $ZrOCl_2 \cdot 8H_2O$, and yttrium nitrate hexahydrate, $Y(NO_3)_3 \cdot 6HO_2O$ were used as the source materials to form metal oxides and hydroxides. Hydrogen Peroxide, H_2O_2, and Poly(diallyldimethylammonium chloride) (PDDA) were used as additives. The mixture of methanol and deionized water with a volume ratio of 3:1 was used as solvent. The total metal concentration of Zr^+ and Y^+ in the solution was 1×10^{-3} M. The atomic ratio of Y^+ to Zr^+ was 16% with which to prepare an electrolyte materials close to the composition of $(Y_2O_3)_{0.8}(ZrO_2)_{0.98}$ for SOFCs. Concentration of 5×10^{-3} M for H_2O_2 and 0.5 g/l of PDDA were used, respectively. Cathodic deposits were obtained by the galvanostatic method on Ni at current densities ranging from 1~10 mA/cm^2. The electrochemical cell for deposition included a cathodic substrate centered between two parallel platinum counterelectrodes. After drying at room temperature, the electrolytic deposits were thermally annealed followed by characterizations and subsequent deposition, drying and annealing cycles in order to achieve a crack-free coating. Power scraped from some room temperature dried samples were used for thermogravimetric analysis (TGA). The thermoanalyzer was operated in air between room temperature and 850°C at a heating rate of 5°C/min. The morphologies of the coating were characterized with optical and scanning electron microscopes.

Results and Discussion

Thermogravimetric analysis of the room temperature dried deposits from solutions with different additives is shown in Fig.1. In the case of deposition with H_2O_2 as additive, the weight loss of the deposits continues monotonically to increase when it was heated, and most of the weight loss (~38%) occurs below 400°C after which there is no significant weight change. This weight loss is associated dehydration of the hydroxide. According to the X-ray diffraction study of the thermally treated deposited from 0.005 M $ZrOCl_2 \cdot 8H_2O$ with H_2O_2 as additive, small peaks which attributed to tetragonal phase of zirconia appeared at 400°C. The TG data of the deposits with 0.5g/l PDDA as additive appear in a very different way. Three sharp reductions of the sample weight can be noticed in the graph, with the first one below 200°C, the second below 400°C, and the third below 600°C. There is no significant weight loss was found when the temperature exceeded 600°C. The total weight loss was approximately 79%. The weight loss is believed to be associated with dehydration of the hydroxide and the burn out of the polymer.

Figure 2 shows the deposition weight gain versus deposition time with the prepared solutions. When the current density was maintained at 3 mA/cm^2, as shown by the curves Fig.2(c) and (d), the deposition weight gain in the PDDA added solution is lower than that with the H_2O_2 added solution within 8 min. The deposition weight gain in the solution with PDDA increases monotonically within the entire time duration in the experiment, while in the solution with H_2O_2, the deposition weight gain increases before 4 min, then start to decreases gradually thereafter. The decrease of the deposition weight gain in this case may be interpreted by the result of

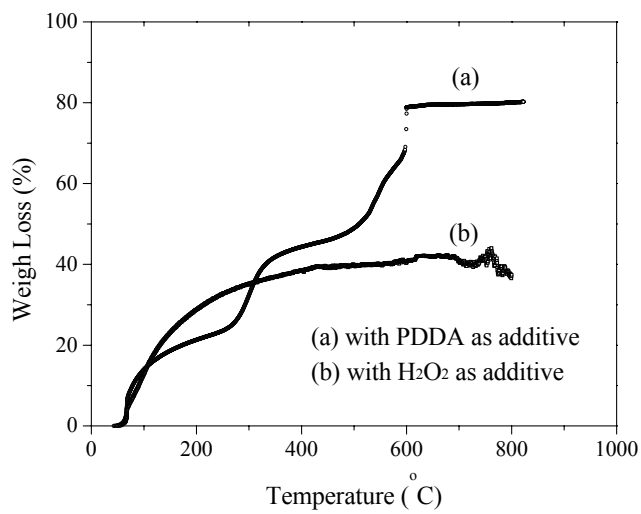

Figure 1. Thermogravimetric analysis data for deposits obtained from 0.001 M ($ZrOCl_2$ + $Y(NO_3)_3$) and additives a) PDDA , b) H_2O_2, respectively.

spallation. There is no spallation for the deposits from the solution with PDDA addition, because the binging effect of the polymeric electrolyte. When the current was held at 8 mA/cm^2, the deposition rates in the both solutions are higher than at the lower current. Unfortunately, the depositions were not able to be performed longer than 6 min, because the voltage limitations of the present power supply (maximum 60 V).

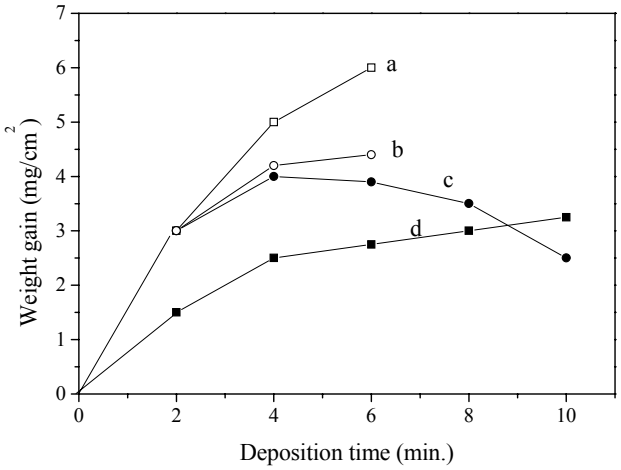

Figure 2. Deposition weight gain in the solution of 0.001M of $ZrOCl_2$ and $Y(NO_3)_3$ versus deposition time at 8 mA/cm^2 with a) 0.5 g/l PDDA, b) 0.005M H_2O_2 as additives, and at 3 mA/cm^2 with c) 0.005M H_2O_2 and d) 0.5 g/l PDDA as additives.

Figure 3 shows morphological evolution of the YSZ films coated on Ni substrates at a current destiny of 10 mA/cm^2. When the deposition duration was only 0.5 min, the film was very thin. The water in the film can easily reach the surface during drying under room temperature, therefore, the film is smooth and the cracks are less and smaller as shown in Fig. 3(a). When the deposition time was prolonged, the film became thicker, and the surface drying rate was higher than that in the film. This interprets the how the cracks were formed. In the light of this understanding, the time of each deposition was limited to 1 min in the later experiments.

Crack formation is an intrinsic problem with liquid phase deposition, especially when water is used as all or part of the solvent. According to the principle of the cathodic deposition, the cathode as a substrate must be conductive. The substrates used in this experiment are all conductive metal or oxides. The deposited zirconium and yttrium hydroxides are less conductive, and their oxides are non-conductive. Therefore, as the deposits build up, the resistance of the film increases and therefore, the deposition rate becomes lower. This deposition mechanism can be used to fill the cracks. The operation steps include the repetition of deposition, thermal annealing. The previous deposits need to be annealed to become nonconductive, and then the subsequent deposition will only take place in the conductive areas, i.e. the cracks. Fig. 4 shows an example of the crack filling accomplished by repetition of the deposition and thermal annealing. In the Fig.4(a), the film is cracked in to isolated flakes on the substrate after annealing.

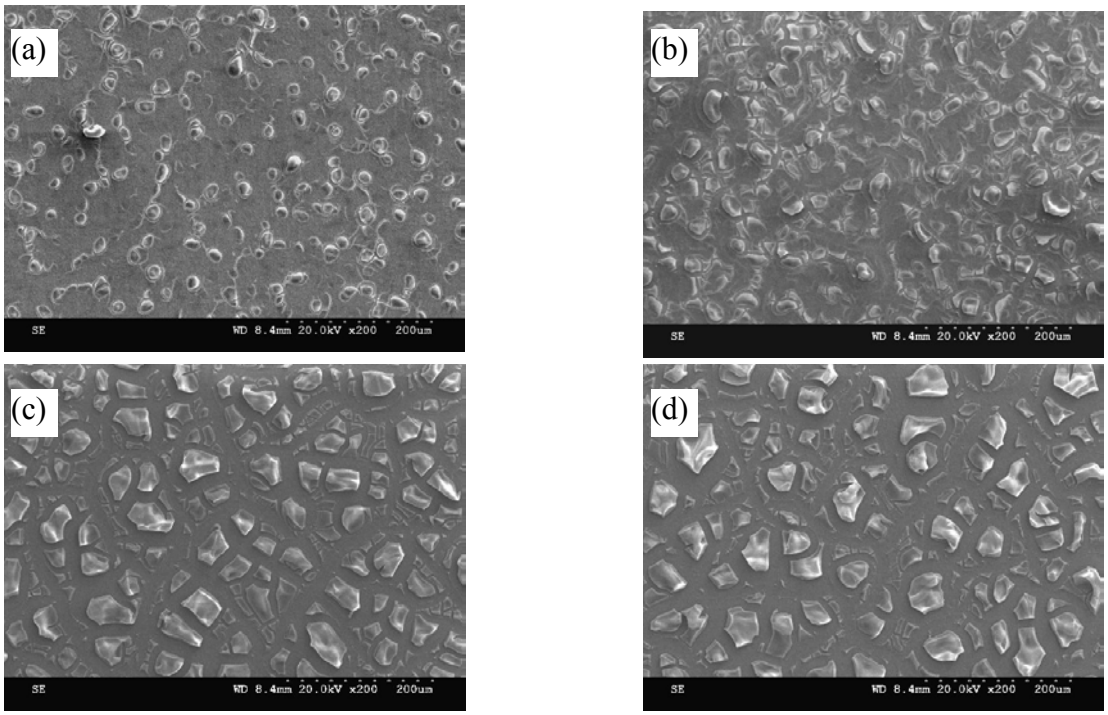

Figure 3. SEM images of the YSZ films coated on Ni substrates at current destiny of 10 mA/cm^2, total metal concentration:1×10^{-3} M, with 5×10^{-3} M of H_2O_2 as additive. The depostion temperature 1.5°C for the deposition time a) 0.5 min, b) 1.0 min, c) 1.5 min, and 2.0 min.

The subsequent 3 min deposition falls into the cracks as shown in Fig. 4(b). After a total deposition time of 15 min, the cracks were filled and the width of the small crack is lass than 0.5 μm on the surface. The coating in the solution with PDDA as binding phase had a very different appearance from those depositions in the solution without binder. On the surface of coating with PDDA binder, there are much less and smaller cracks. In majority of the coated area, cracks were hardly found even after thermal annealing at 650°C. Fig.4(f) was taken from a typical cracked area to demonstrate the crack filling for this instance.

Conclusions

Through the experimental studies, electrolytic deposition technique demonstrated its promise to prepare oxide coatings at very low cost and ease. Continuous films can be obtained by optimization of the time in each deposition combining with thermal treatment and proper number of processing repetitions. The cracks can be further suppressed by using polymeric electrolyte PDDA.

Status of Milestones

On Schedule

Communications/Visitors/Travel

None

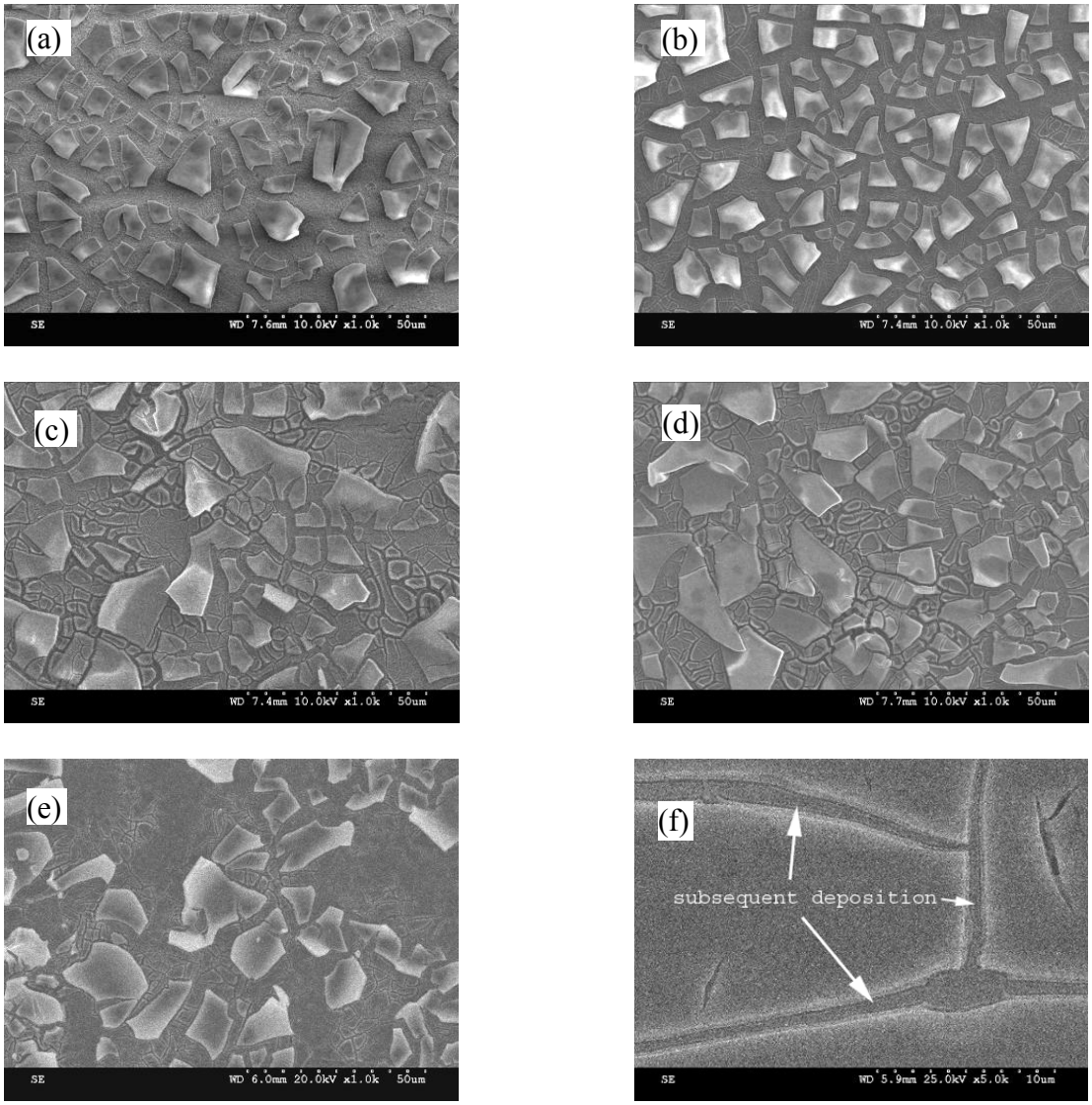

Figure 4. SEM images of the coatings on a Ni substrate deposited at a current density of 5 mA/cm^2 in the solution of 1×10^{-3} M $ZrOCl_2$ and $Y(NO_3)_3$, 5×10^{-3} M H_2O_2 for a) 3 min, b) 6 min, c) 9 min, d) 12 min, and e) 15 min, while d) 12 min deposition in solution with 0.5 g/l PDDA. Deposition was performed in a repetition manner. Each processing procedure consists of three 1 min depositions between which there was a 30 min drying at room temperature. An annealing at 650°C was then conducted for 30 min after a 48 h drying of the sample, which was followed by the subsequent processing procedure.

Problems Encountered

None

NDE of Diesel Engine Components

J. G. Sun and J. M. Zhang
Argonne National Laboratory
and M. J. Andrews
Caterpillar, Inc.

Objective/Scope

Emission reduction in diesel engines that are designated to burn several types of fuels has lead to assessing ceramic engine valves to mitigate valve corrosion and extend service lifetimes. The objective of this work is to evaluate several nondestructive evaluation (NDE) methods to detect defect/damage in structural ceramic valves for diesel engines. The primary NDE to be utilized is the elastic optical scattering or laser scattering method. The goal is to demonstrate that investigations using this method can identify defects/damage that can be used for predicting material microstructural and mechanical properties. There are two tasks to be completed: (1) Characterize surface/subsurface defects and machining damage and correlate NDE data with mechanical properties for rectangular and cylindrical flexure test specimens of candidate silicon nitrides selected for fabricating into prototype valves. Laser-scattering studies will be conducted at various wavelengths using a He-Ne laser and a tunable-wavelength solid-state laser to optimize detection sensitivity. NDE studies will be coupled with examination of surface and subsurface microstructure and fracture surface to determine defect/damage depth and fracture origin. NDE data will also be correlated with mechanical properties. (2) Assess and evaluate accumulated damage in full-size ceramic valves due to rig or engine tests. All prototype silicon nitride valves will be examined at ANL prior to bench tests, after accumulating a specified number of test hours, and at the end of the planned test runs.

Technical Highlights

Work during this period (October-December 2003) focused on acquiring and analyzing laser-scattering NDE data to determine processing- and operation-induced subsurface flaws in 100-hour and 500-hour bench-tested NT551 Si_3N_4 ceramic valves.

1. Elastic Optical Scattering NDE for Subsurface Defect/Damage

We spent limited effort in this period on laser-scattering examination of machining-induced damage in cylindrical SN235P Si_3N_4 specimens. NDE data will be analyzed and presented in the next quarterly report.

2. Laser-Scattering Characterization of Si_3N_4 Valves

During this period we continued acquiring and analyzing laser-scattering NDE data for processing- and operation-induced subsurface defects/damages in ten 100-hour and 500-hour bench-tested NT551 Si_3N_4 ceramic valves (shown in Fig. 1) that we received from Caterpillar Inc. in the last period. Two of the valves were tested for 100 hours using eccentric valve-seat insert, and the other eight valves were tested for 500 hours with either eccentric valve-seat inserts or combinations of matched or mismatched contact angles between valve and insert surfaces (either 30 or 45-degree angles). Laser-scattering scans were conducted for all valves and the NDE data were analyzed. Typical results of these analyses are presented below.

Fig. 1. Photograph of ten NT551 Si_3N_4 valves after 100- and 500-hour bench tests.

Two valves, identified previously as 273 and 277, have been analyzed by laser-scattering NDE after they were bench-tested for 100 hours (see our quarterly report for period Jan.-Mar. 2003). They were then bench-tested for additional 400 hours using eccentric valve-seat inserts and are now identified as CV-8 and CV-15, respectively. Figure 2 shows laser-scattering images of the valve-head section of valve CV-15. The scanned axial length was 30 mm (the top 4-mm region is the contact area) and is aligned in the vertical direction in the images. The scan resolution was 10 microns along the axial direction and 0.02 degree along the circumferential direction. In Fig. 2a, the horizontal size of each pixel corresponds to the surface circumferential length within a 0.02-degree angle, which is 11 microns at top and 2 microns at the bottom because of the change of valve radius. The horizontal pixel size in Fig. 2b is normalized to a constant dimension of 11 microns. Figure 2 indicates no significant damage from the 500-hour bench test, except the wear scars (two darker horizontal stripes) within the contact surface. The reduction of scattering intensity within the scared area is due to surface damage of increased roughness and contamination (embedded metal particles from the metal seat insert). A few darker lines are observed near the fillet-radius region (bottom of the images); those are scratch marks with contaminated material attached on the surface. Figure 3 shows the detailed laser-scattering image of the contact surface of valve CV-15. One subsurface flaw (high optical-scattering spots) near the top edge is indicated in the figure. Detailed laser-scattering image and photomicrograph of the edge flaw is shown in Fig. 4. The scatter image in Fig. 4a appears to be rough because the scan pixel size (~10 micron) is too large to resolve the detailed microstructure of the material. These laser-scattering NDE data in Figs. 2-4 are consistent with and similar to those obtained when the valve was bench-tested for 100 hours (as shown in Figs. 2 and 6 of our Jan.-Mar. 2003 quarterly report). Therefore, the additional 400-hour bench test did not generate significant subsurface damage.

Figures 5a-b show photomicrographs of the wear scars in the contact area for valves CV-15 after 100- and 500-hour bench tests, respectively. It is apparent that the wear scars (or surface damage) were mainly produced from the initial 100-hour test. However, surface wear is observed in most of other valves after 500-hour bench tests.

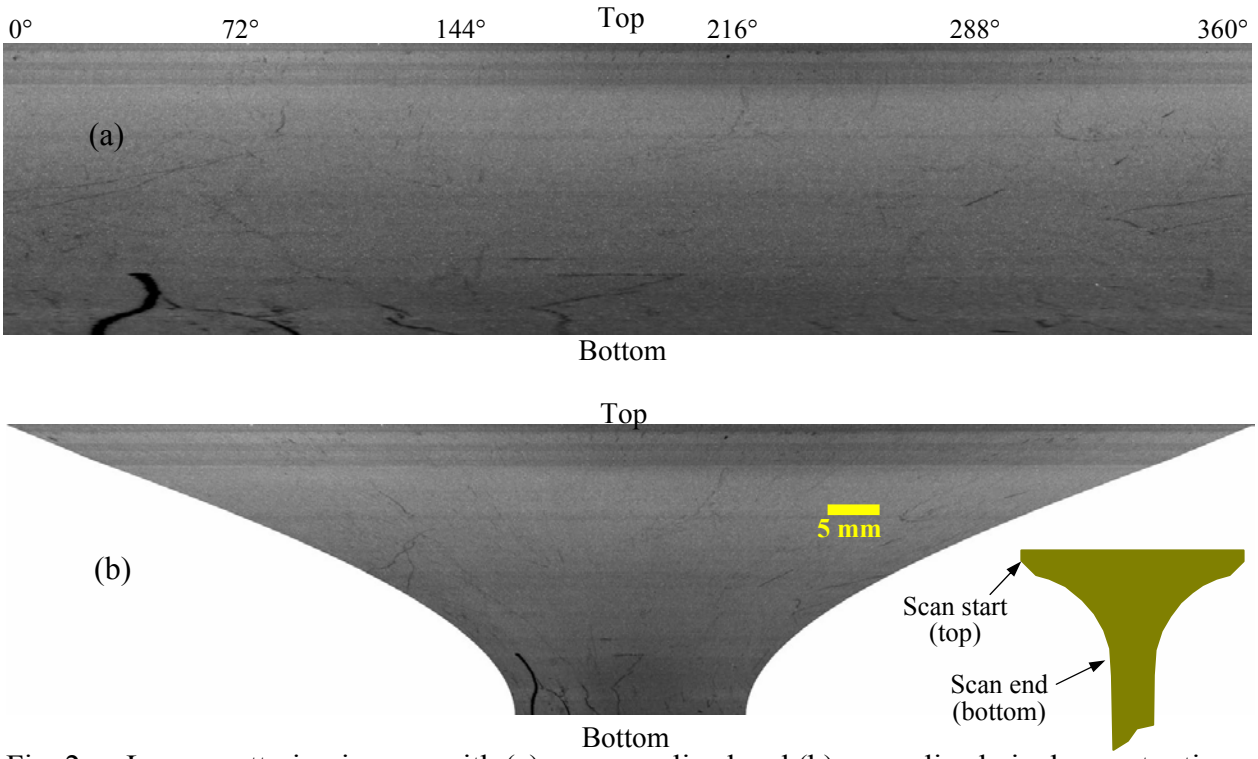

Fig. 2. Laser-scattering images with (a) un-normalized and (b) normalized pixel-aspect ratio for valve-head section of NT551 valve CV-15 after 500-hour bench test.

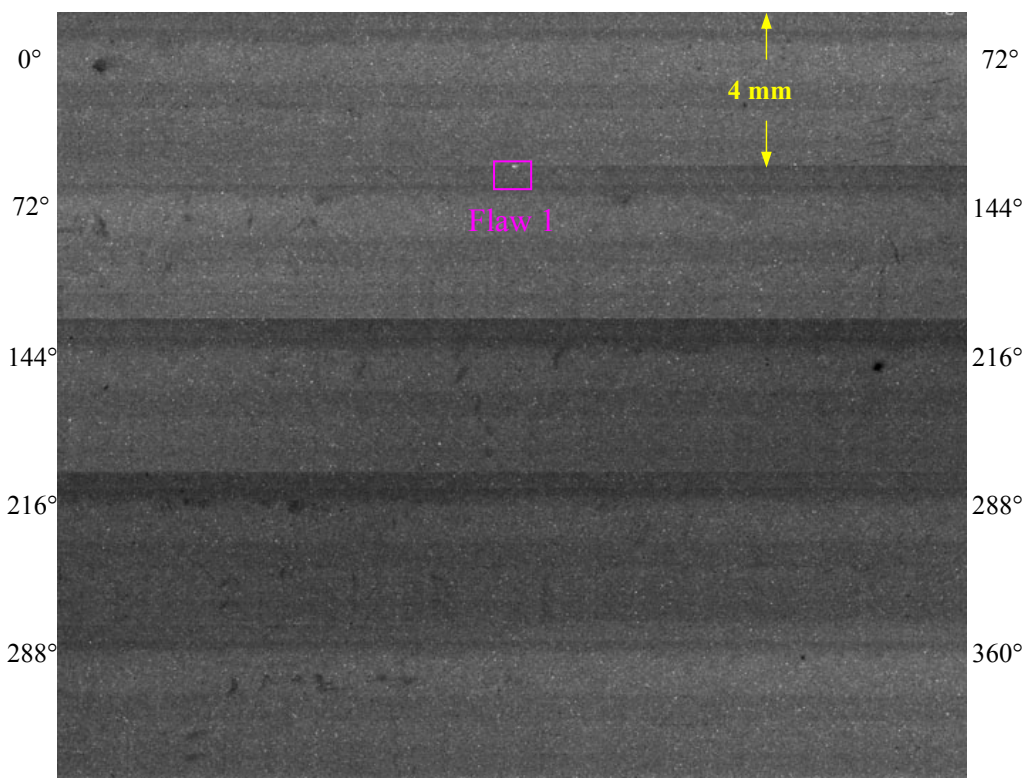

Fig. 3. Laser-scattering image of the contact surface of NT551 valve CV-15 after 500-hour bench test (one flaw near the top edge is indicated).

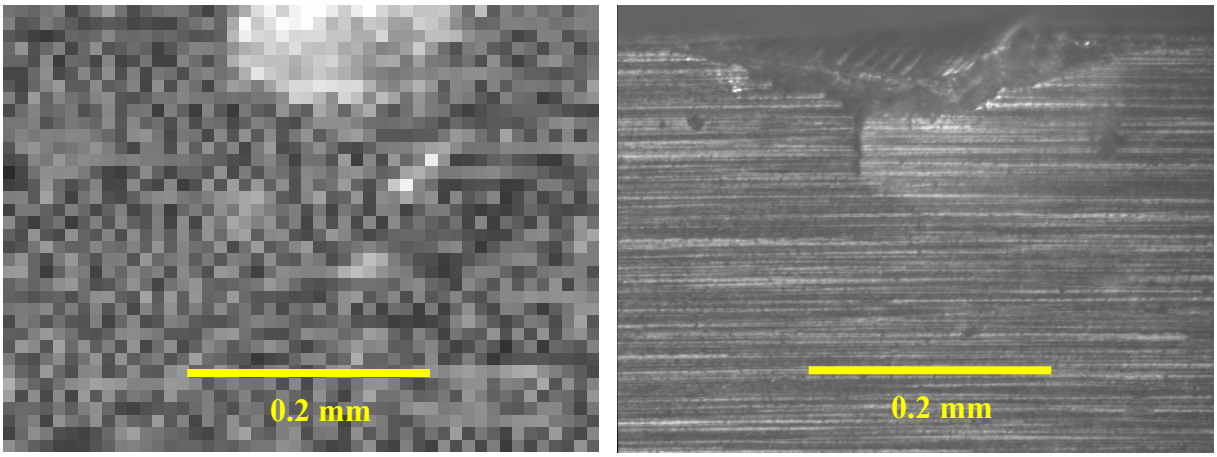

(a) (b)

Fig. 4. (a) Detailed laser-scattering image and (b) photomicrograph of a subsurface flaw (chip) at top edge of contact surface of NT551 valve CV-15 after 500-hour bench test.

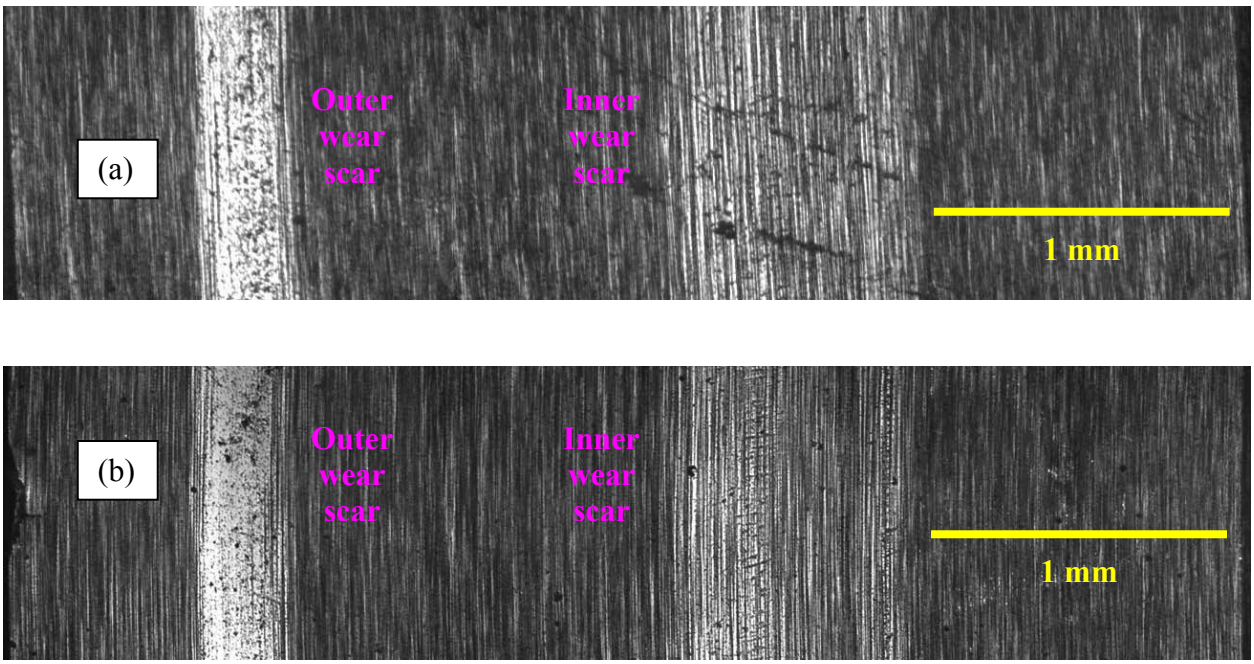

Fig. 5. Photomicrographs of wear scars on the contact surface of NT551 valve CV-15 after (a) 100-hour and (b) 500-hour bench tests.

Although most detected defects/damages in the ten valves are relatively small (< 0.2 mm), subsurface flaws of significant size and severity are found in valve CV-19. Figure 6 shows the laser-scattering image of the valve-head section of valve CV-19 after 500-hour bench test. Several long and strong optical-scattering lines are indicated in Fig. 6. A detailed scatter image and a photomicrograph of the valve surface in the radius region are shown in Fig. 7. The subsurface damages appear to be regularly spaces so they are likely introduced from the machining process.

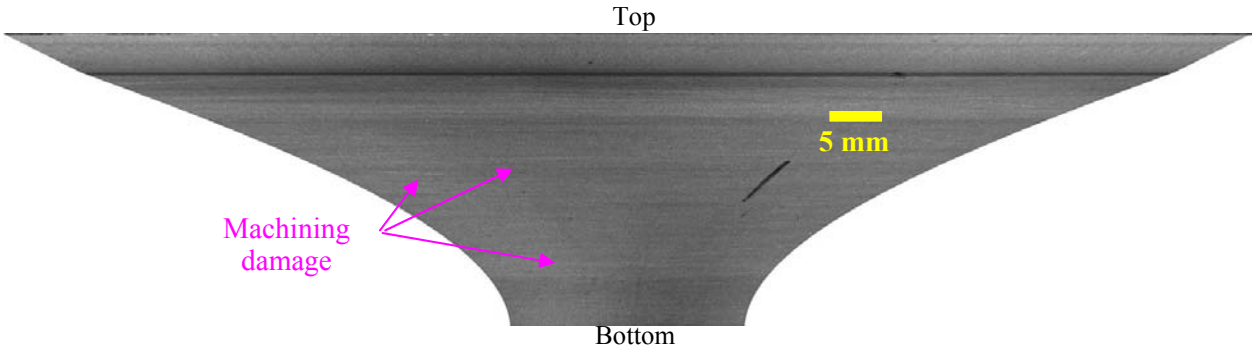

Fig. 6. Laser-scattering scan image for the valve-head section of NT551 valve CV-19 after 500-hour bench test.

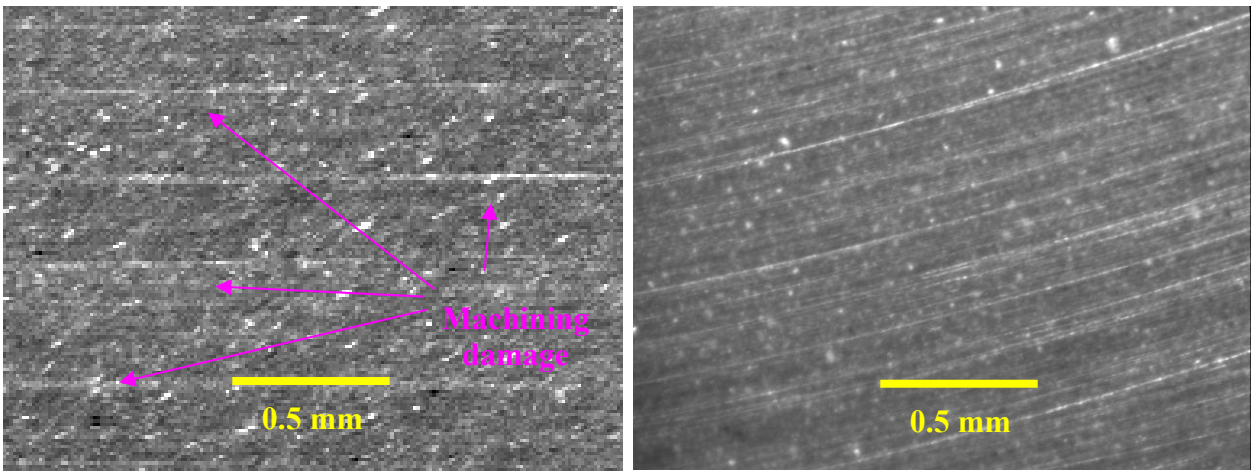

(a) (b)

Fig. 7. (a) Detailed laser-scattering image and (b) photomicrograph of subsurface damages (machining marks) on the surface of NT551 valve CV-19 after 500-hour bench test.

Status of Milestones

Current ANL milestones are on schedule.

Communications/Visits/Travel

Dr. M. J. Andrews and Dr. A. Ramesh of Caterpillar Inc. visited ANL on Oct. 8, 2003 to discuss project issues.

Problems Encountered

None in this period.

Publications

A paper entitled "Laser Scattering Characterization of Subsurface Defect/Damage in Silicon Nitride Ceramic Valves" by J. G. Sun, J. Zhang, and M. J. Andrews was submitted for publication in the Proceedings of the American Ceramic Society's annual Cocoa Beach Conference, Cocoa Beach, FL, Jan. 25-30, 2004.

Durability of Diesel Engine Component Materials

Peter J. Blau
Oak Ridge National Laboratory

John Truhan
University of Tennessee, Knoxville, TN

Jun Qu
ORISE Post-Doctoral Fellow

Objective/Scope

The objective of this effort is to enable the development of more durable, low-friction moving parts in diesel engines for heavy vehicle propulsion systems by conducting friction, lubrication, and wear analyses of advanced materials, surface treatments, and coatings. The scope of materials and coatings is broad and includes any metallic alloy, intermetallic compound, ceramic, or composite material which is likely to be best-suited for the given application. Parts of current interest include scuffing-critical components, like fuel injector plungers and EGR waste gate components. Bench-scale simulations of the rubbing conditions in diesel engine environments are used to study the accumulation of surface damage, and to correlate this behavior with the properties and compositions of the surface species. The effects of mechanical, thermal, and chemical factors on scuffing and reciprocating sliding wear are being determined. Results will be used to develop graphical methods for scuffing performance mapping and to select materials for durability-critical engine components.

Technical Highlights

In the previous quarterly report, the scuffing resistance of a variety of candidate materials for heavy duty fuel injector plungers was reported. Data were obtained using a fuel-lubricated, cylindrical 'pin-on-twin' cylinders test in which an upper cylinder oscillates on a pair of lower cylinders oriented perpendicularly to the axis of the upper cylinder. The onset of scuffing was determined by periodically comparing the friction force versus time wave form with the initial wave form recorded for the first stoke. This comparison allows for the determination not only of when scuffing initiates but also where it occurs along the wear scar and its rate of propagation. A wide variety of material types were tested, including: hardened AISI 52100 steel, zirconia ceramic, TiN-coated steel, and several composites consisting of different concentrations of TiC particles in a Ni_3Al matrix.

Results of the scuffing tests were presented to representatives of the Fuels Systems Business Unit of Cummins, Inc. on 11/10/03 at the Cummins Technical Center in Columbus, IN. It was found that the results generated by this 300 sec pin-on-twin test correlated reasonably well with Cummins long term field experience using some of these same materials, particularly for materials that either scuffed readily, such as 52100 steel, and materials that did not normally scuff in service, such as zirconia. Based on these discussions, a modification of the test geometry (described later in this report) will be made in an effort to better differentiate between low and medium scuff-resistant materials.

The recent acquisition of a loop abrasion tester for our laboratory enabled us to compare the abrasive wear resistance of the same materials with their scuffing resistance from the pin-on-twin test. Consisting of a slowly-moving strip of abrasive, this machine conforms to an ASTM standard test procedure ASTM G 174-03 [1]. The loop abrasion test is conducted without lubricant and involves rubbing a continuous loop of abrasive paper (30 μm-diameter alumina in this case) under load (200 gf) for one hour, after which either the mass loss or wear volume is determined. These results have been summarized in a paper submitted to the ASTM Journal of Testing and Evaluation (see Publications, item 3). In order to apply this test, which normally uses flat test specimens, to the cylindrical geometry of our pin-on-twin specimens, a new sample holder was designed and a geometric model to translate wear scar width into wear volume was developed. To enhance the usefulness of the standard, periodic measurements of the mass loss and scar width were made to track the time dependency of the wear process. The test apparatus and the modified sample holder, with a cylindrical sample installed, are shown in Fig. 1.

(a) 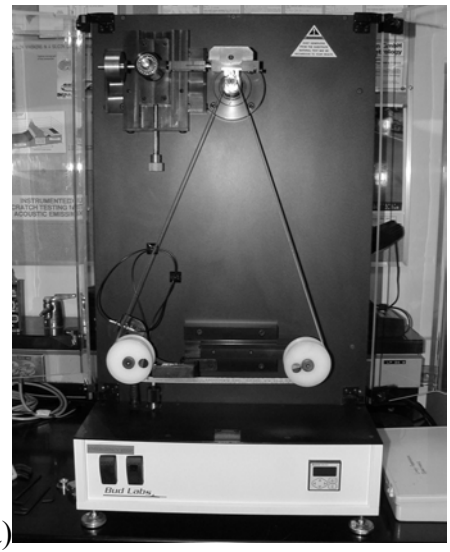 (b) 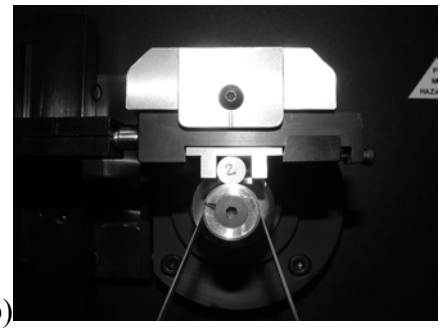

Figure 1. Loop abrasion test setup (a) overview and (b) close-view of the cylindrical specimen, specimen holder, and tape. Note that cylinder axes are parallel.

The loop abrasion test is simple to carry out and its results are quite repeatable compared with typical sliding wear test results. For example, the wear volume is plotted in Fig. 2 as a function of the sliding distance for the metal, ceramic, and cermet materials. As indicated by the range bars on the plot, very good repeatability was achieved. The cermet C10 had the lowest wear rates in both wear-in and steady-state. All test materials showed an initially high wear rate (during wear-in) followed by a relatively low steady-state wear rate thereafter. The tape abrasivity dominated the wear rate, but the contact stress change from a line contact to a widening scar had only a slight influence in the results shown here.

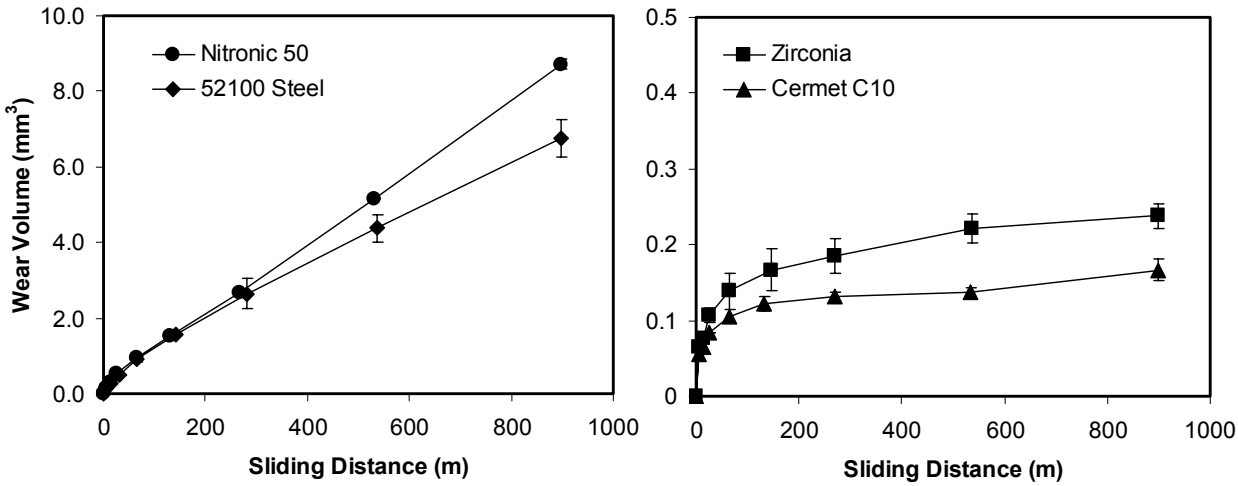

Figure 2. The wear volume as a function of the sliding distance.

Table 1 qualitatively summarizes the results from the pin-on-twin and loop abrasion tests compared to field experience in operating fuel injectors. Both laboratory tests show similar rankings of materials to the field experience. TiN coated specimens could not be adequately evaluated with the loop abrasion test because the thin coating is quickly worn away in the first several minutes. After wear-through, the abrasion resistance is more reflective of the substrate than the coating. The loop abrasion test can probably be adapted to coating evaluation if a finer grit abrasive and/or a lower load is used, but that remains to be explored.

Table 1.
Comparison of Material Performance in Laboratory tests to Field Experience

Material	Pin-on-Twin Test	Loop Abrasion Test	Field Experience
52100	Moderate scuffing	High abrasion	Moderate scuffing
Zirconia	No scuffing	Very low abrasion	No scuffing
TiN Coated Steel	Light scuffing	Not applicable	Very light scuffing
Composites	Very light scuffing	Very low abrasion	Almost no scuffing

The fuels systems engineers at Cummins expressed interest in being able to perform a rapid screening test with good predictability for field performance but they felt that the test, as configured, did not differentiate as well between materials that were intermediate performers. A proposal was thus made to alter the pin-on-twin configuration to slide the top pin in a direction parallel with the axes of the bottom pins instead of transverse to them. It was felt that this would better simulate service conditions while retaining the relatively high contact stresses needed to initiate scuffing. An additional advantage of that geometry is that elongated wear scars would be produced on both the top and bottom pins allowing for a better determination of the wear scar morphologies and mechanisms. New fixtures have already been fabricated and testing of the parallel pin-on-twin test will be started shortly.

Future Plans

1. Conduct scuffing tests using parallel pin-on-twin configuration, which is designed to better simulate the stresses and types of damage seen in actual plunger components.
2. Investigate the effects of surface finish, contact pressure, and reciprocating frequency on scuffing characteristics.
3. Determine suitable variables and construct scuffing maps of fuel injector materials.

Travel

From 11/09/2003 to 11/10/2003, J. Truhan and J. Qu visited the Cummins Technical Center in Columbus, IN to discuss research results, obtain field experience, and seek cooperation in future studies of diesel fuel injection systems and other critical diesel engine components.

Status of Milestones

1) Evaluate and report on the usefulness of scanning acoustic microscopy for characterizing the extent of subsurface damage arising from high-temperature scuffing. (March 31, 2003 – completed.)
2) Report on the effects of sulfur in the fuel on the scuffing behavior of current and future candidate fuel injection system materials (September 30, 2003 - completed).
3) Prepare transition diagrams for current and promising, new fuel system materials that exemplify the relationship between real contact pressure, surface finish, and the onset of scuffing in diesel fuel environments. (March 31, 2004)
4) Develop a model for selecting materials and their optimal surface finishes for scuffing applications in diesel engines. (September 30, 2004**)**

Publications

1. J. Qu, J. Truhan, and P.J. Blau, "Detecting the Onset of Localized Scuffing with the Pin-on-Twin Fuel-Lubricated Test for Heavy Duty Diesel Fuel Injectors," *Tribology International* (under journal peer review).
2. J. Qu, J. Truhan, and P.J. Blau, "Evaluating Candidate Materials for Heavy Duty Diesel Fuel Injectors Using a 'Pin-On-Twin' Scuffing Test," *Tribology International*, (under ORNL internal review).
3. J. Qu, J. Truhan, and P.J. Blau, "Application of the ASTM Loop Abrasion Test to Cylindrical Specimens," *J. of Testing and Evaluation* (submitted).

Numbered References

[1] ASTM Standard G 174-03, "Standard Test Method for Measuring Abrasion Resistance of Materials by Abrasive Loop Contact."

Life Prediction of Diesel Engine Components

H. T. Lin, T. P. Kirkland, A. A. Wereszczak, and M. K. Ferber
Oak Ridge National Laboratory
and M. J. Andrews
Caterpillar Inc.

Objective/Scope

The valid prediction of mechanical reliability and service life is a prerequisite for the successful implementation of structural ceramics and advanced intermetallic alloys as internal combustion engine components. There are three primary goals of this research project which contribute toward that implementation: the generation of mechanical engineering data from ambient to high temperatures of candidate structural ceramics and intermetallic alloys; the microstructural characterization of failure phenomena in these ceramics and alloys and components fabricated from them; and the application and verification of probabilistic life prediction methods using diesel engine components as test cases. For all three stages, results are provided to both the material suppliers and component end-users.

The systematic study of candidate structural ceramics (primarily silicon nitride) for internal combustion engine components is undertaken as a function of temperature (< 1200°C), environment, time, and machining conditions. Properties such as strength and fatigue will be characterized via flexure and rotary bend testing.

The second goal of the program is to characterize the evolution and role of damage mechanisms, and changes in microstructure linked to the ceramic's mechanical performance, at representative engine component service conditions. These will be examined using several analytical techniques including optical and scanning electron microscopy. Specifically, several microstructural aspects of failure will be characterized:

(1) strength-limiting flaw-type identification;
(2) edge, surface, and volume effects on strength and fatigue size-scaling
(3) changes in failure mechanism as a function of temperature;
(4) the nature of slow crack growth; and
(5) what role residual stresses may have in these processes.

Lastly, numerical probabilistic models (i.e., life prediction codes) will be used in conjunction with the generated strength and fatigue data to predict the failure probability and reliability of complex-shaped components subjected to mechanical loading, such as a silicon nitride diesel engine valve. The predicted results will then be compared to actual component performance measured experimentally or from field service data. As a consequence of these efforts, the data generated in this program will not only provide a critically needed base for component utilization in internal combustion engines, but will also facilitate the maturation of candidate ceramic materials and a design algorithm for ceramic components subjected to mechanical loading in general.

Technical Highlights

Studies of dynamic fatigue behavior in four-point bending for Kyocera SN235P silicon nitride after 1000h exposure to an oil ash environment at 850°C in air were completed during this reporting period. The SN235P silicon nitride billets were fabricated with the same powder batch used to process the SN235P exhaust valve blanks. The SN235P exhaust valves will be employed for bench rig as well as engine tests at Caterpillar after the completion of valve machining and NDE. This study was carried out to verify the mechanical reliability of co-processed valve materials after long-term exposure to a simulated diesel engine environment. The co-processed SN235P silicon nitride bend bars were longitudinally machined based per the revised ASTM C116 standard with 600 grit surface finish. The test silicon nitride samples were place in platinum crucibles and covered with commercial grade 10W30 engine oil. The crucibles with oil-covered silicon nitride bend bars were heated in a furnace at 600°C for approximately 30 minutes to ash the oil. After completion of oil-ash conversion, the samples covered with 1-2 mm oil ash powder were then heat-treated at 850°C for 1000h in an ambient air. The results previously generated for the as-machined SN235P samples, co-processed with the exhaust valve blanks, showed a very high fatigue exponent (N ~ 93) at 850°C, indicative of no susceptibility to SCG process (Fig. 2 and 3). Therefore, the dynamic fatigue tests for exposed SN235P samples were only carried out at 850°C and 0.003 MPa/s in air per ASTM C1465 due to the limited number of specimens.

Results of dynamic fatigue tests at 850°C and 0.003 MPa/s showed that the exposed SN235P silicon nitride exhibited a very comparable inert characteristic strength to those obtained from the as-machined samples tested under the same condition (Table 1, and Fig. 1-3). Also, the exposed SN235P samples showed a higher Weibull modulus than the as-machined samples. The higher Weibull modulus of exposed samples may arise from the surface sealing effect due to the formation of oxide scale after exposure. A detailed analysis of fractography and SEM examination will be carried out to identify the critical strength limiting flaws as well as the extent of oxidation/corrosion zone in selected test samples. The dynamic fatigue results suggest that the SN235P-CP exhibits excellent corrosion resistance to diesel engine environment and would meet the application criteria for exhaust valve components of diesel engines.

Studies of dynamic fatigue properties of a commercial grade silicon nitride, i.e., SN147-31E, manufactured by Ceradyne Advanced Ceramic, Inc., CA, have also been initiated during this reporting period. The SN147-31E was processed with similar sintering additives to those employed for SN147-31N evaluated previously. However, the SN147-31E contains a crystalline secondary phase achieved by a post heat treatment. Thus, it is anticipated that SN147-31E would exhibit a higher temperature mechanical reliability than SN147-31N due to the presence of crystalline secondary phase.

Dynamic fatigue results showed that the longitudinally machined SN147-13E exhibited a characteristic strength that is 20% lower than that obtained from the SN147-31N machined and tested under the same conditions (Table 2 and Fig. 4 and 5). The lower strength of SN147-31E could be due to the change in internal residual stress resulting from the crystallization process of secondary phase(s) by post heat treatment. On the other hand, the transversely machined SN147-31E showed a minor decrease (~8%) in characteristic strength as compared with the SN147-31N. The minor difference in strength between SN147-31E and –31N, which were transversely machined, could be due to the similarly dominant strength limiting flaws, i.e.,

surface machining flaws. However, the SN147-31E exhibited a lower Weibull modulus than that obtained for SN147-31N.

Status of Milestones

Milestone: "Complete testing and analysis of prototype silicon nitride valves after bench rig testing" was on schedule.

Communications / Visitors / Travel

Communication with M. J. Andrews at Caterpillar on the update of the dynamic fatigue test results of Kyocera SN235P silicon nitride after 10000h oil immersion test.

Communication with M. J. Andrews at Caterpillar on the on the update of the dynamic fatigue test results of Ceradyne SN147-31E silicon nitride

Communication with M. J. Andrews at Caterpillar on the machining status of the MOR bend bars from SN235P valve blanks.

Communication with Edgar Lara-Cuzio at ORNL on the update status for the CRADA with Cummins to evaluate the candidate diesel particulate filter materials.

Problems Encountered

None.

Publications

None.

References

[1] H. T. Lin, T. P. Kirkland, M. K. Ferber, and M. J. Andrews, "Life Prediction of Diesel Engine Components," Heavy Vehicle Propulsion System Materials Program Quarterly Technical Progress Report to DOE Office of Transportation Technologies, Oct. – Dec. 2002.
[2] H. T. Lin, T. P. Kirkland, M. K. Ferber, and M. J. Andrews, "Life Prediction of Diesel Engine Components," Heavy Vehicle Propulsion System Materials Program Quarterly Technical Progress Report to DOE Office of Transportation Technologies, Jan. – March 2003.
[3] H. T. Lin, T. P. Kirkland, M. K. Ferber, and M. J. Andrews, "Life Prediction of Diesel Engine Components," Heavy Vehicle Propulsion System Materials Program Quarterly Technical Progress Report to DOE Office of Transportation Technologies, Apr. – June 2003.

Table 1. Summary of uncensored Weibull and strength distributions for Kyocera SN235P silicon nitride specimens longitudinally machined per ASTM C1161. Data of Kyocera SN235/SN235P, also machined longitudinally, generated previously are used for comparison.

Material	# of Spmns. Tested	Stressing Rate (MPa/s)	Temp. (°C)	Uncens. Weibull Modulus	± 95% Uncens. Weibull Modulus	Uncens. Chrctstic Strength (MPa)	± 95% Uncens. Chrctstic Strength (MPa)
SN235P-CP*	30	30	20	11.94	8.58. 15.94	820	794, 847
SN235P-CP*	30	0.003	20	14.56	10.93, 18.64	741	721, 761
SN235P-CP*	30	30	850	20.56	15.16, 26.87	684	671, 697
SN235P-CP*	30	0.003	850	19.44	14.49, 25.01	621	608, 633
SN235P-CP**	15	0.003	850	30.40	19.47, 44.19	660	647, 672

* Specimens were machined from co-processed billets of exhaust valve blanks.
** Specimens were exposed to an oil ash environment at 850°C for 1000h in air.

Table 2. Summary of uncensored Weibull and strength distributions for Ceradyne SN147-31E silicon nitride specimens transversely machined per ASTM C1161. Data of SN147-31N machined longitudinally as well as transversely is used for reference.

Material	# of Spmns. Tested	Stressing Rate (MPa/s)	Temp. (°C)	Uncens. Weibull Modulus	± 95% Uncens. Weibull Modulus	Uncens. Chrctstic Strength (MPa)	± 95% Uncens. Chrctstic Strength (MPa)
SN147-31N*	15	30	20	21.73	14.07. 31.09	836	814, 858
SN147-31N**	15	30	20	13.76	8.96, 19.59	677	649, 705
SN147-31E*	15	30	20	17.30	10.86, 25.58	668	645, 690
SN147-31E**	15	30	20	7.44	4.89, 10.58	623	575, 671

* Specimens were longitudinally machined.
** Specimens were transversely machined.

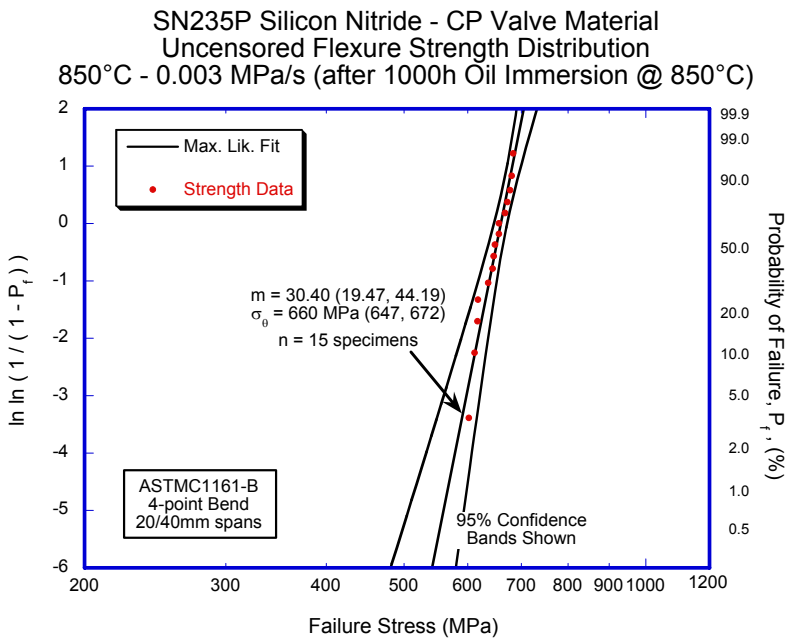

Figure 1. Strength distribution of Kyocera SN235P-CP longitudinally machined and tested at 850°C and at 30 MPa/s after 1000h exposure in oil ash environment at 850°C in air.

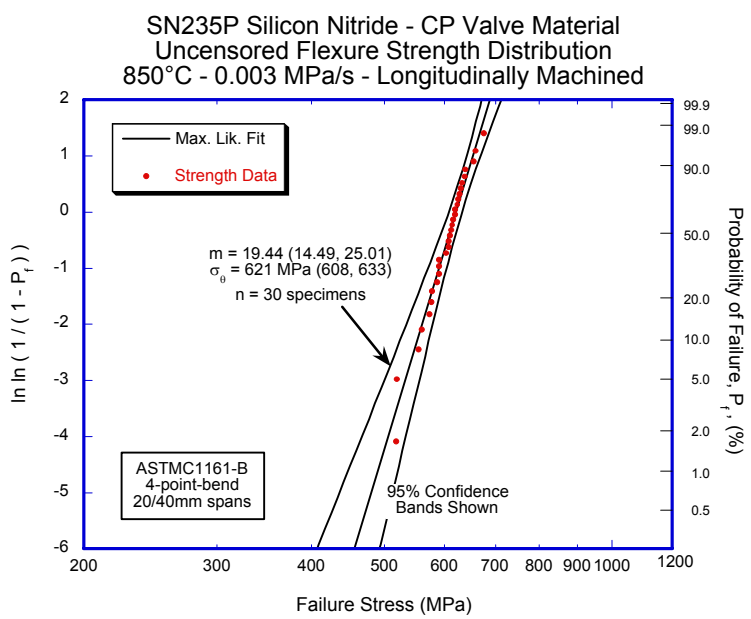

Figure 2. Strength distribution of Kyocera SN235P-CP longitudinally machined and tested at 850°C and at 30 MPa/s.

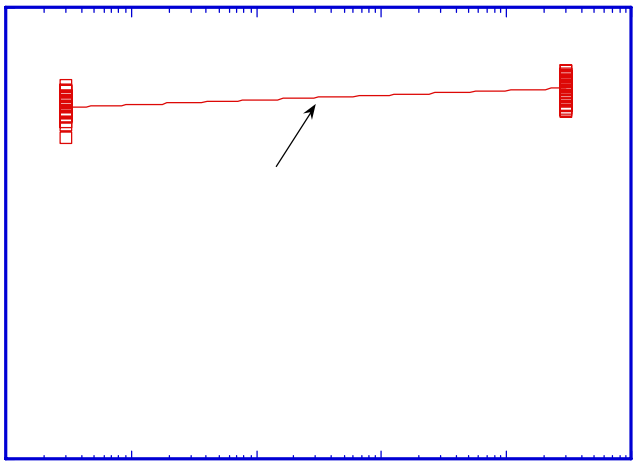

Figure 3. Failure stress versus stressing rate curve of SN235P-CP silicon nitride longitudinally machined and tested at 850°C in air.

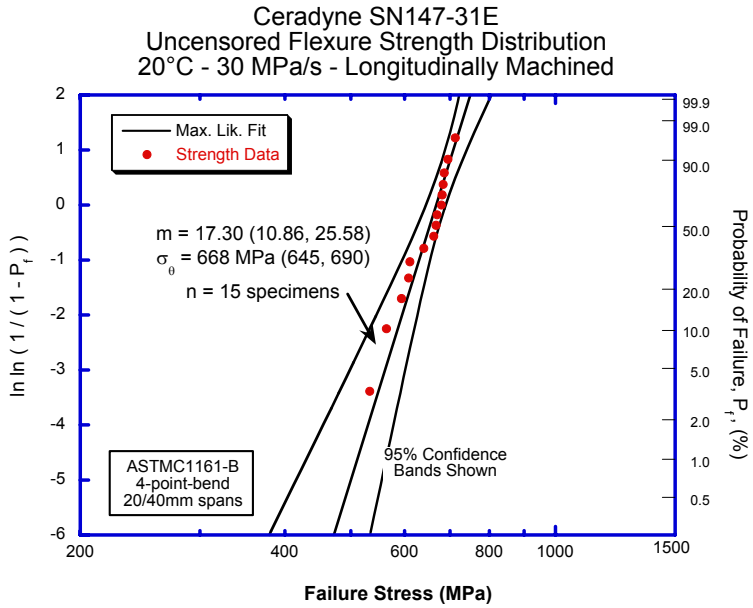

Figure 4. Strength distribution of Ceradyne SN147-31E longitudinally machined and tested at 20°C and at 30 MPa/s.

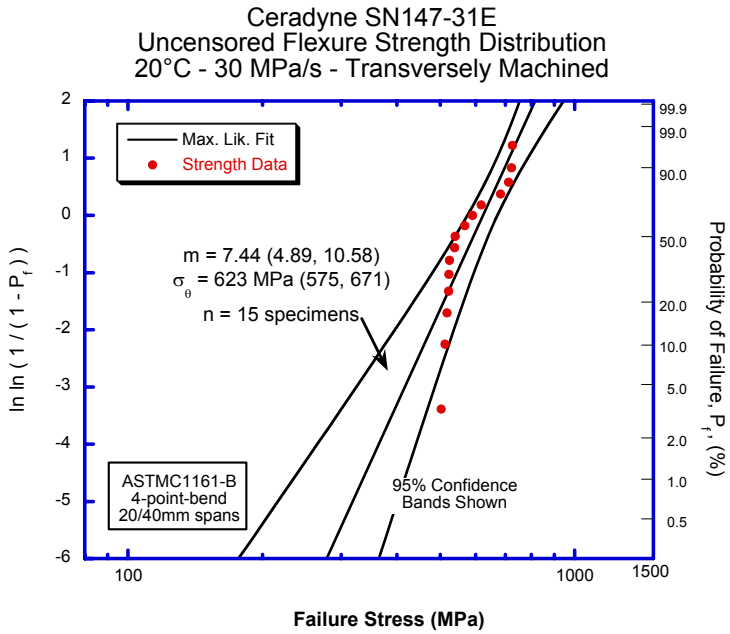

Figure 5. Strength distribution of Ceradyne SN147-31E transversely machined and tested at 20°C and at 30 MPa/s.

Advanced Machining and Sensor Concepts

Albert Shih
University of Michigan

Objective/Scope

The objective of this research is to investigate new technologies for cost-effective machining of Ti alloys. New tool materials and comprehensive finite element modeling of the machining process are applied to gain better understanding of effects of machining process parameters and the deformation, stress and temperature in the tool and titanium workpiece.

Technical Highlights

This quarter marks the beginning of this project. Ti alloys have great promise as the light-weight material for future sustainable transportation. Due to the advancement of new titanium raw-material production technologies, the material cost of titanium is expected to be significantly reduced in the future. However, the manufacturing cost of components made of Ti alloys, particularly the machining and joining processes, is still high. For the aerospace industry, which is leading the use of Ti alloys, the high cost of machining and joining of Ti alloys due to rapid tool wear have been a major technical challenge. This research is aimed to establish collaborations with the Thirdwave Systems on finite element based software for machining process modeling and the Kennametal on the cutting tool material and coating development. Thirdwave Systems is currently leading a DoD and industry sponsored consortium on developing advanced modeling tools for titanium machining. This consortium is emphasizing on end milling, a process used extensively to manufacture aircraft structural parts. Complementing the existing consortium activities, this research targets on titanium turning and drilling, which are two critical processes for the heavy-duty engine component manufacturing.

1. Titanium machining

The Ti alloys has low thermal conductivity, about 6 to 7 W/m-K (vs. 45 W/m-K of 4340 steel and 167 W/m-K of aluminum alloys). The low thermal conductivity results the high temperature in both the chip and tool. The high temperature softens the tool material and promotes the tool diffusion wear. In the machined Ti chip, the serrated chip with adiabatic shear band due to thermal instability can be observed. The low thermal conductivity of Ti alloys makes the heat difficult to transfer outside the deformation zone during the chip formation. The high temperature is confined in the deformation zone, softens the work-material, generates even larger deformation and heat, and further increases the temperature in a narrow band of deformation zone. An adiabatic shear band is therefore created. The adiabatic shear band formation also creates the oscillatory cutting forces, activates the tool chatter and vibration, and deteriorates the surface roughness. The tool vibration causes the chipping of the tool edge during the machining of Ti alloys. In summary, the diffusion wear and tool cutting edge chipping are the two dominate wear mechanisms for machining of Ti alloys. To enable the cost-effective machining of Ti alloys, research efforts are aimed to overcome these two technical challenges. The state-of-the-art in machining of Ti alloys has been summarized in two review papers [1,2].

2. Finite element modeling of titanium machining process

Finite element modeling of machining processes has advanced rapidly in the past two decades. It has evolved from research in the laboratory to a necessary production tool in industry. Inputs for machining process modeling software are the properties of work- and tool-materials, friction between the tool-chip interface, thermal conduction and convection properties surrounding the tool and working in the cutting area, geometry of the tool, and process parameters (feed, speed, etc.). The software can predict the cutting forces, stresses and strains in the tool and workpiece, heat generation and temperature distributions, the required power of the machine, and tool and chip contact stress. The AdvantEdge software developed by ThirdWave is used in this study for finite element modeling of the machining of Ti-6Al-4V. The basic 2D orthogonal cutting modeling is first studied.

Two sets of modeling were conducted. The first set uses uncoated WC-Co cutting tool. The rake angle was 5 deg, depth of cut was 1 mm, and tool edge radius was 0.02 mm. The initial temperature of tool and workpiece was 20 deg C. Two variables are the cutting speed (30, 50, 70, and 100 m/min) and feed (0.05 and 0.1 mm per revolution). The feed is uncut chip thickness in orthogonal cutting. The second set use TiN coated WC-Co cutting tool with different coating thickness.

3. Results and Discussion

Table 1 summarizes the results from finite element modeling of the machining using uncoated WC-Co tool. The direction of cutting force (F_c) and feed force (F_f), which can be measured using a dynamometer, is parallel and perpendicular to the relative velocity of the tool and workpiece, respectively. The F_c and F_f are transformed to the normal force and friction force on the tool rake face, denoted as F and N, respectively.

$$F = F_c \sin\alpha + F_f \cos\alpha \tag{1}$$

$$N = F_c \cos\alpha - F_f \sin\alpha \tag{2}$$

The coefficient of friction on the rake face $\mu = F/N$.

The specific cutting energy, u_s, which represents the energy required to remove a unit volume of work-material, is calculated from the cutting force (F_c), feed (t), and depth of cut (w).

$$u_s = \frac{F_c}{wt} \tag{3}$$

At 0.05 mm feed, high cutting speed increases the cutting and feed forces, specific cutting energy, and peak tool temperature. The cutting speed does not significantly change the coefficient of friction. The peak temperature of 670°C is high and can promote the chemical reaction or diffusion wear of the tool material. At 0.1 mm feed, the cutting forces are much higher. The higher cutting speed does not generate the high cutting forces as in 0.05 mm feed. This can be due to the balance of strain-rate hardening and thermal softening effect. Higher tool and workpiece temperatures exist at 0.1 mm feed. The peak temperature of the tool reaches 760°C, higher than that with 0.05 mm feed.

The finite element modeling can provide detailed results of the stress, strain, and temperature distributions. Two example contour plots of the temperature in the tool, chip, and workpiece at 30 and 100 m/min cutting speed and 0.1 mm feed are shown in Fig. 1. Different patterns of chip curling and different levels of chip and tool temperature can be recognized. High tool and chip temperatures at high cutting speed can be seen in the temperature contours.

The effect of tool coating and type of tool coating on machining of Ti-6Al-4V can also be analyzed using the finite element modeling. An example of using the same WC-Co tool with TiN coating of 1, 2.5, and 5 μm thickness is analyzed. The cutting speed was 30 m/min, feed was 0.05 mm, rake angle was 5°, tool edge radius was 0.02 mm, and initial temperature was 20°C. The coating, as a thermal barrier, can reduce the peak temperature of the tool. It is unclear why the cutting and feed forces increase significantly at thicker tool coating setup. More study is underway to understand the modeling of coating in finite element analysis.

Table 1. Results of orthogonal cutting of Ti-6Al-4V with uncoated WC-Co tool.

Feed (mm)		Cutting Speed (m/min)			
		30	50	70	100
0.05	Cutting Force (N)	60-63	55-66	84-103	95-117
	Feed Force (N)	32-52	33-46	64-86	72-88
	Friction Force (N)	37-57	38-52	71-94	80-98
	Normal Force (N)	57-58	52-62	78-95	88-109
	Coefficient of Friction	0.65-0.98	0.73-0.84	0.91-1.00	0.9-0.91
	Specific Cutting Energy ($x10^6$ J/m^3)	1200-1260	1100-1320	1680-2060	1900-2340
	Peak Tool Temperature (°C)	446	502	600	674
0.1	Cutting Force (N)	206-260	226-235	215-246	213-240
	Feed Force (N)	135-185	135-162	132-187	144-167
	Friction Force (N)	152-207	154-182	150-208	162-187
	Normal Force (N)	193-243	213-220	203-229	200-225
	Coefficient of Friction	0.79-0.85	0.72-0.83	0.74-0.91	0.81-0.83
	Specific Cutting Energy ($x10^6$ J/m^3)	2060-2600	2260-2350	2150-2460	2130-2400
	Peak Tool Temperature (°C)	488	558	677	758

Table 2. Results of TiN coating thickness on machining of Ti-6Al-4V.

Coating Thickness	No Coating	1 μm	2.5 μm	5 μm
Cutting Force (N)	60-63	69-92	74-106	115-152
Feed Force (N)	32-52	52-78	58-88	113-160
Friction Force (N)	37-57	58-86	64-97	123-173
Normal Force (N)	57-58	64-85	69-98	105-137
Coefficient of Friction	0.65-0.98	0.90-1.01	0.94-0.99	1.17-1.26
Specific Cutting Energy ($x10^6$ J/m^3)	1200-1260	1380-1840	1480-2120	2300-3040
Peak Tool Temperature (°C)	446	381-388	397-399	369-399

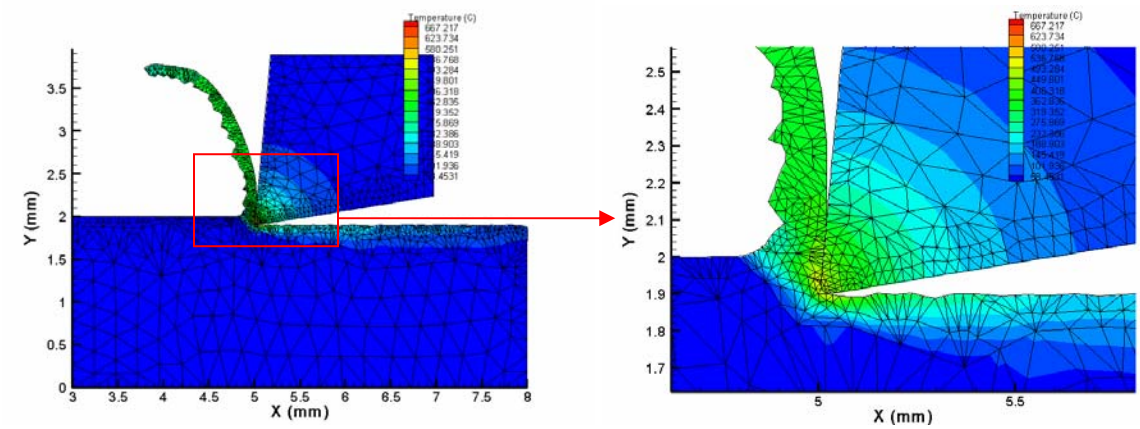

(a) 30 m/min cutting speed

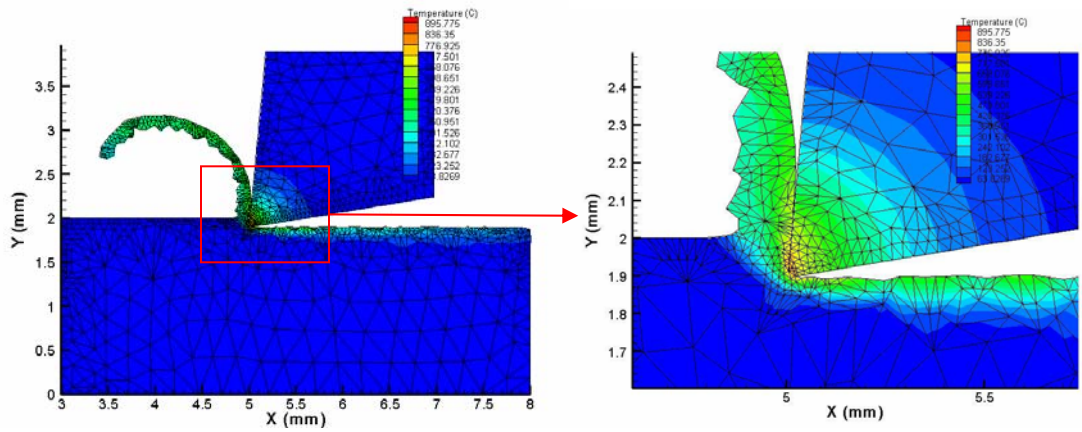

(b) 100 m/min cutting speed

Figure 1. Contour plots of the tool, chip, and workpiece temperature (0.1 mm feed).

4. Future Work

This research is continuing in both modeling and experiment. More comprehensive modeling with different type of coating and multi-layer coating has been completed in 2D orthogonal cutting of Ti alloys. We are studying the Thirdwave's 3D cutting model. We are also setting up the lathe turning experiment with the dynamometer for force measurement at University of Michigan. The workpiece is the Ti rod and tube. Rui Li, the graduate student working on this project, is expected to work at HTML ORNL, starting in mid-Jan 2004.

Status of Milestones

Milestone 1: 2D finite element modeling of titanium machining process.

Status: Extensive study of cutting speed, feed, and coating effects has been conducted using the Thirdwave AdvantEdge software to analyze the machining of Ti-6Al-4V.

Milestone 2: 3D finite element modeling of titanium machining process.

Status: Preparation is on-going to acquire the license from Thirdwave on the 3D finite element machining model. A new PC workstation has been purchased.

Milestone 3: Investigation of TiC-based cutting tool material.
Status: In the discussion stage to select the tool material.

Milestone 4: Titanium turning tests.
Status: Experiments are setting up at Univ. of Michigan for lathe turning of Ti alloys. The same experiment is expected to be set up at ORNL in Jan. 2004.

Milestone 5: Titanium drilling tests
Status: Nothing to report.

Communications/Visit/Travel

Albert Shih visited ORNL on Nov. 13th and Cummins on Nov 14th.

Publications

J. Kong, A.J. Shih, "Infrared Thermometry for Diesel Exhaust Aftertreatment Filter Temperature Measurement," *SAE Transactions,* (accepted).

References

[1] J.X. Yang and C.R. Liu, 1999, "Machining Titanium And Its Alloys," Machining Science and Technology (3) 107-139.
[2] E.O. Ezugwu, Z.M. Wang, 1997, "Titanium alloys and their machinability-a review," Journal of Materials Processing Technology (68) 262-274.

Advanced Cast Austenitic Stainless Steels For High Temperature Exhaust Components

P. J. Maziasz, John P. Shingledecker, and N. D. Evans
Oak Ridge National Laboratory
and M. J Pollard
Caterpillar, Inc.

Objective/Scope

The objective of this new CRADA project is commercial scale up of the new modified cast austenitic stainless steels developed by Caterpillar and ORNL as cost-effective high-performance alternatives to the standard SiMo ductile cast iron used for most diesel engine exhaust manifold and turbocharger housing components. Cast austenitic stainless steels can withstand prolonged exposure at temperatures of 750°C or above, and are much stronger than SiMo cast iron above 550-600°C. The new modified stainless steels (CF8C Plus and CN12 Plus) have better aging resistance and ductility after creep than standard commercial grades of the same steels. These data would indicate better fatigue and thermal fatigue resistance than commercial cast stainless steels, and much better than SiMo cast iron. Resistance to cracking during the severe thermal cycling is necessary for exhaust components. This project provides the more comprehensive properties data needed by designers to qualify these new alloys for component applications and optimize component designs. This new advanced diesel engine CRADA (Cooperative Research and Development Agreement) project (ORNL02-0658) began on July 21, 2002, and will last at least three years. More detailed information on this project must be requested directly from Caterpillar, Inc.

Technical Highlights

Background

Advanced large diesel engines must have higher fuel efficiency as well as reduced exhaust emissions, without sacrificing component durability and reliability. They require exhaust manifolds and turbocharger housings made from materials that can withstand temperatures ranging from 70 to 750°C or higher in a normal duty cycle. Such materials must withstand both prolonged, steady high-temperature exposure as well as more rapid and severe thermal cycling. New technology to reduce emissions and heavier duty cycles will push temperatures in these critical components even higher.

Current diesel exhaust components are made from SiMo ductile cast iron, and higher engine temperatures push such materials well beyond their current strength and corrosion limits. The previous CRADA produced systematic data comparing cast CN12 stainless steel and SiMo cast iron for such diesel exhaust component applications. That data demonstrated a clear tensile strength advantage of standard CN12 steel above 550-600°C, and even larger advantages in creep strength and fatigue life above 700°C. The previous CRADA project also developed new CN12-Plus and CF8C-Plus modified cast austenitic stainless steels with better creep strength, and significantly better aging resistance and thermal fatigue resistance than standard CN12. The purpose of this follow-on CRADA project is commercial scale up of these new modified cast stainless steel heats. This project will develop the systematic and thorough data base required by designers to optimize component design, and to qualify them for trial component production.

Approach

Prior work on lab-scale (15 lb induction melts with argon cover gas) heats of CN12 - Plus and CF8C – Plus and screening tests (aging, tensile, creep) at 800-850°C at ORNL provided a best composition of each alloy for commercial scale up. High-temperature fatigue testing at Caterpillar Technical Center has identified a significant advantage of the CN12-Plus steel. Two commercial stainless steel foundaries have produced 500 lb heats of the new CN12-Plus and CF8C-Plus stainless steels for testing and evaluation. One of those commercial foundaries has been chosen to produce an addition static cast and a new centrifugally-cast heat of the CF8C-Plus steel. ORNL is also producing another set of laboratory heats to verify establish the effects of other minor additions on the high temperature strength of the new modified CF8C steel.

Technical Progress

Tensile and fatigue testing were completed previously, and thermal fatigue testing of as-cast material was completed last quarter at Caterpillar. Tensile data on the new commercial scale-up heats of the standard and modified cast stainless steels show that the CF8C Plus is about as strong as the standard and modified CN12 steels, but still has the same high ductility as the standard CF8C steel. This combination of good strength and ductility gives the CF8C-Plus excellent fatigue and thermal fatigue resistance at high temperatures, as shown for isothermal fatigue at 800°C in Fig. 1.

An "engineered microstructure" alloy design approach gave the new CF8C -Plus steel a very stable austenite parent matrix phase that is free of the δ-ferrite typically found in standard CF8C steel in the as-cast condition. Creep strength of CF8C-Plus at high temperatures comes from nano-scale dispersions of NbC precipitates that form and remain stable, and are much finer than found in standard CF8C steel. Because CF8C-Plus has no δ-ferrite, it is also free of σ-phase after long term aging at 650-700°C and above relative to standard CF8C.

CF8C-Plus was deliberately designed to have a combination of good strength and ductility at both higher and lower temperatures in order to achieve its best thermal fatigue resistance. Aging of tensile/fatigue specimens for 10, 000 h at 700-850°C continued at ORNL this quarter. Aging to 1000 h was completed last quarter, and specimen tensile testing began at Caterpillar this quarter. Aging to 10,000 h continues this quarter. Microstructural analysis of previously aged or creep-tested specimens of lab-scale heats of CF8C-Plus and CN12-Plus steels was completed last quarter, and microcharacterization of tested specimens of the new commercial heats began this quarter.

Additional lab-heats of CF8C-Plus were cast at ORNL last quart to define the effects of other minor alloying additions and establish their limits for commercial heats, and creep testing began this quarter. Initial creep testing at 850ºC and 75 MPa shows good strength of the base alloys and alloys with W and Cu additions, but poorer strength in alloys with B or Al added. Finally, one of the commercial foundaries was chosen by Caterpillar to produce another static sand cast heat and a centrifugally-cast heat of CF8C-Plus, and material was received at ORNL and specimens for creep, tensile and fatigue testing were made this quarter.

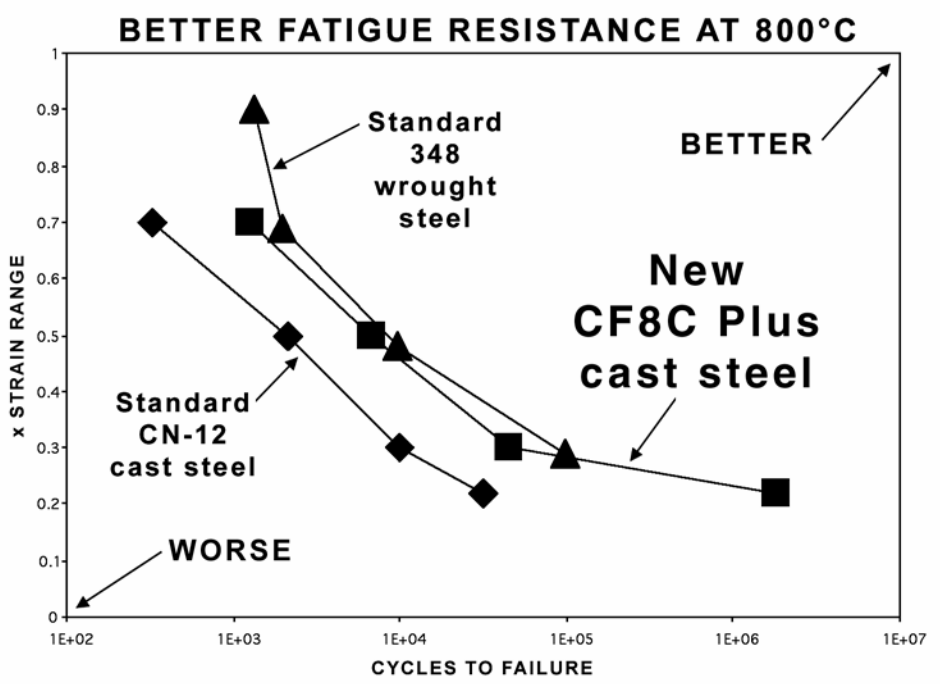

Figure 1 – Isothermal fatigue properties measured for various strain ranges by Caterpillar for the commercial scale-up heats of standard CN12 and the new CF8C-Plus stainless steels at 800°C in air.

Communications/Visits/Travel

Detailed team communications between ORNL and Caterpillar occur regularly, at least once or twice a week. The new 3 year CRADA began on July 21, 2002, when the previous CRADA ended.

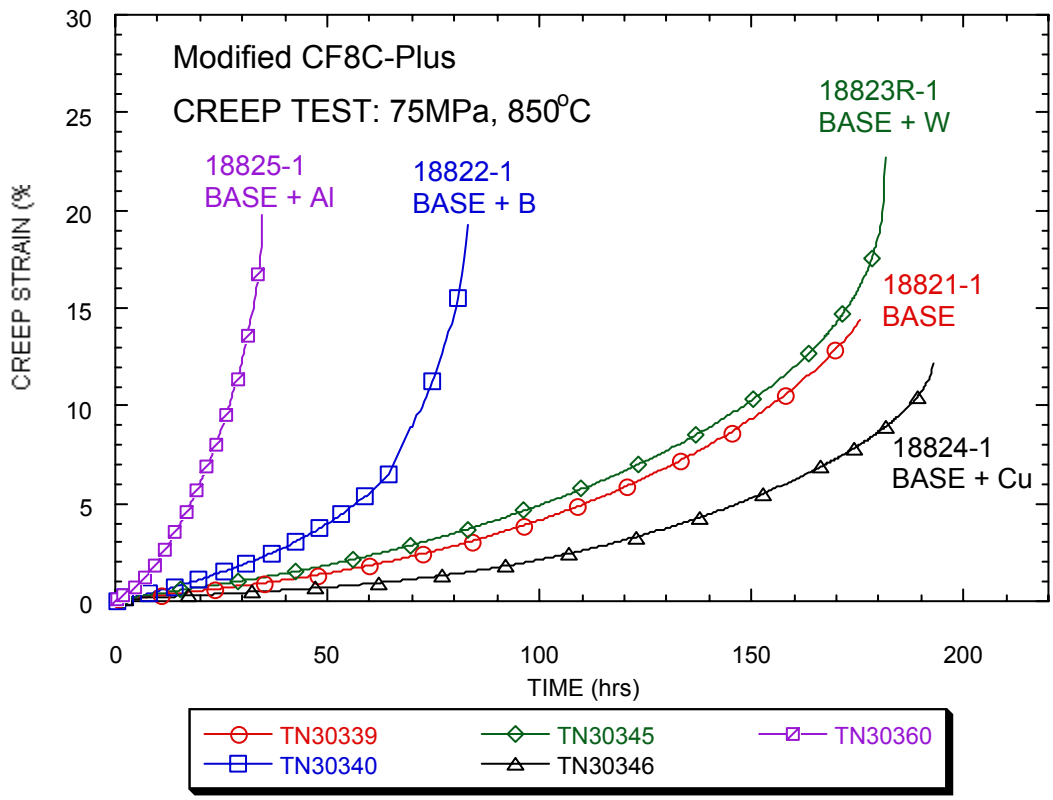

Figure 2 – Creep-rupture testing (at ORNL) of new lab-scale heats varying minor alloying additions to CF8C-Plus cast stainless steel at the conditions indicated.

An invention disclosure and patent application on cast austenitic stainless alloys with improved performance were completed by Caterpillar and filed with the U.S. Patent Office in December, 2000. It is entitled "Heat and Corrosion Resistant Cast Stainless Steels with Improved High Temperature Strength and Ductility," by P.J. Maziasz (ORNL), T. McGreevy (U. of Bradley/CAT), M.J. Pollard (CAT), C.W. Siebenaler (CAT), and R.W. Swindeman (ORNL). Several quarters earlier, two separate new patent applications were developed and submitted to the U.S. Patent Office, one on the CF8C Plus steel and the other on the CN12 Plus steel.

Status of Milestones

Formal milestones were imbedded in the previous CRADA and in the new CRADA, which is part of the DOE/OFCVT Heavy Vehicle Propulsion Materials Program, but a task in the ORNL FWP. As before, all milestones have been successfully achieved on or significantly ahead of schedule.

Publications/Presentations/Awards

The new CF8C-Plus Cast Stainless Steel was awarded a 2003 R&D 100 Award at the 41st Annual R&D 100 Award banquet held in Chicago, IL on October 16, 2003.

A Tech Spotlight article “High Temperature Cast Stainless Steel” by Phil Maziasz and Mike Pollard appeared in the October, 2003 (vol. 161, no. 10, pp. 57-59) issue of Advanced Materials and Processes, published by ASM-International, Materials Park, OH, and a C15 Caterpillar truck diesel engine and highlight appeared on the cover.

Laser Surface Texturing of Lubricated Ceramics

Peter J. Blau
Oak Ridge National Laboratory

Objective/Scope

The objective of this effort is to evaluate the frictional benefits of laser dimple patterns on the lubrication of ceramic surfaces. This project is part of a joint Argonne National Laboratory/ ORNL analysis of the benefits of a laser surface texturing (LST) process developed by Prof. Itzhak Etsion, Surface Technologies, Ltd., Israel. That process uses a computer-controlled laser to produce a pattern of shallow, rounded dimples on bearing surfaces. Based on calculations, preliminary tests, and limited field trials, the developer claims that LST enhances the ability of a lubricated surface to establish a load-bearing hydrodynamic film that decreases friction relative to a non-dimpled surface. The ORNL portion of this joint effort is focused on two aspects of LST: (1) conducting reciprocating tests on LST ceramic surfaces using lubricants with various viscosities, and (2) determining the microstructural changes associated with the LST process. These results will be placed into context with other methods for surface engineering.

Technical Highlights

Examination of Shock-Peened Ceramics. Laser shock peening (LSP) is a promising, new way to modify the surface properties of materials. It can harden metals but its effects on ceramics are less well known. Since LSP might improve friction and wear, it was felt to be of interest to compare the tribological properties of LST ceramics with LSP ceramics. In August 2003, M. Ferber and A. Wereszczak, ORNL, visited Laser Shock Peening Technologies, Inc. of Dublin Ohio, to conduct initial tests of LSP on various materials, including SiC, a material of interest in the present work. Results of these initial tests on SiC were not encouraging, as shown in Fig. 1.

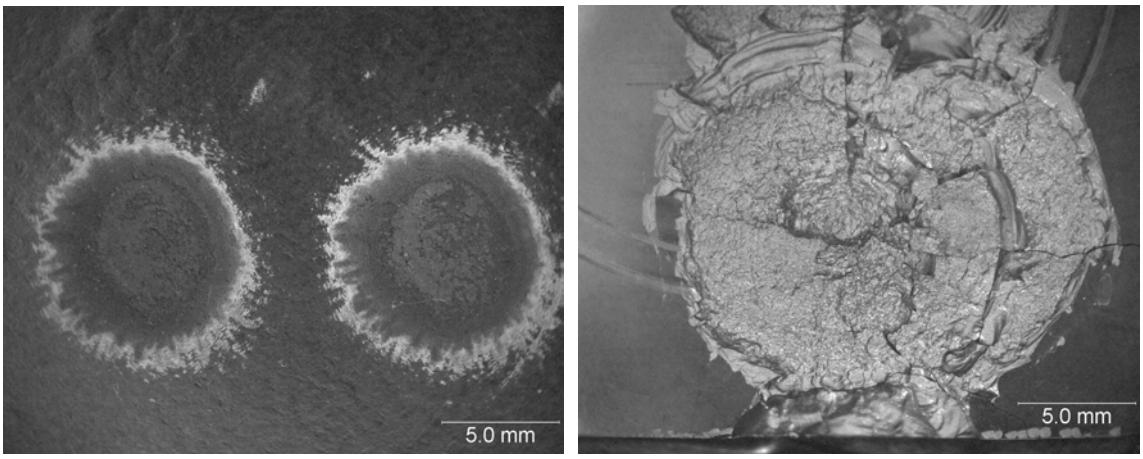

(a) (b)

Figure 1. (a) Front side of the LSP SiC tile, (b) rear side of the LSP SiC tile.

Figure 1(a) shows two laser shock peening sites on the front surface of a polished 6.4 mm thick tile of Hexaloy SA (SiC). Figure 1 (b) shows the back side of the same piece. Massive spallation on the back of the tile raises concerns about the applicability of this technique to brittle materials, but initial tests were not optimized and there may be other LSP conditions that

produce less damage in ceramics. Further studies of the tribology of LSP ceramics will be delayed until the analysis of the other LSP materials is more complete.

Testing Strategy. Results and progress of this project to-date were discussed privately with Prof. I. Etsion of Surface Technologies, Ltd. The difficulties of achieving the excellent alignment needed for observing the advantages of lubricated, dimpled surfaces were discussed. Options include redesigning the testing system or conducting longer running-in procedures to fit the surfaces better. Another option is to switch from an oscillating testing mode to a unidirectional sliding mode. It was also suggested by Etsion to use starved lubrication conditions rather than fully-flooded conditions, as was done in the work thus far. These recommendations will be evaluated during the coming quarter and changes made to the testing conditions for LST TTZ and SiC materials.

Future Plans

(1) Continue microstructural analysis of the LST TTZ and SiC.
(2) Redesign tests of LST TTZ and SiC to use unidirectional sliding rather than reciprocating motion, and conduct a new series of tests under starved lubricating conditions.

Travel

P. Blau attended the International ASME/STLE Tribology Conference in Ponte Vedra, Florida, on October 26-29, and presented an invited paper in the session on surface engineering (see below). During the conference, Blau discussed future testing strategies with Prof. I. Etsion.

FY 2004 Milestones

1) Prepare a literature review of techniques uses to achieve changes in friction by surface patterning and compare these with laser dimpling. (January 2004 – in progress)
2) Complete characterization of the effects of laser dimpling on the micro-mechanical properties and fine structure of TTZ and SiC ceramics (September 2004).

Presentation

P. J. Blau, "Challenges for the Application of Engineered Surfaces to Tribosystems Subjected to Multiple Contact Modes," International ASME/STLE Tribology Conference, October 26-29, 2003, surface engineering session organized by S. M. Hsu.

High Density Infrared Surface Treatment of Materials for Heavy-Duty Vehicles

T. N. Tiegs, D. C. Harper, F. C. Montgomery, and C. A. Blue
Oak Ridge National Laboratory

Objective/Scope

High Density Infrared (HDI) technology is relatively new to the materials processing area and is gradually being exploited in materials processing. For many applications in heavy-duty vehicles, superior properties, such as corrosion and wear resistance, are only required at the material surface. The project using HDI technology will be exploratory and will examine (1) application of wear-resistant coatings, and (2) modification of plasma-sprayed coatings.

Technical Highlights

Earlier work had shown that adherent coatings of hardmetal compositions could be applied to a variety of metal substrates. Cross-sections of the coatings and base alloys revealed some large porosity within the coatings and also at the interface with the underlying alloy. These bubbles are believed to be porosity that is trapped during the melting of the coating. To minimize the presence of the bubbles, the IR treatment procedure was modified to give a double exposure of the coating to produce a remelting of the coating. This would allow the bubbles to escape during the second melting. A similar technique has been used before with silica refractories to reduce trapped porosity. The effects of the double exposure on the properties of the coating and underlying base metal will be determined. Several samples have been treated and are currently being examined.

To determine the performance of the coatings, wear testing is being planned. The testing will be done in conjunction with the University of Tennessee, which currently has facilities to do the testing.

Status of Milestones

On schedule.

Communications/Visits/Travel

None.

Problems Encountered

None.

Publications

None.

Titanium Alloys for Heavy-Duty Vehicles

Paul C. Becker
Oak Ridge National Laboratory

Objective/Scope

There are a large number of programs focused on reducing the cost of Ti powder and ingot by 50%. If any of these programs reaches this target, the cost of Ti might be become attractive enough for use in heavy duty diesel engines for certain applications where weight reduction is critical. In addition, there is a desire on the part of the military to not only reduce the weight of transportation but to reduce the magnetic signature as well. This project explores the feasibility of replacing the cast iron (C.I.) in diesel engine heads and blocks with Ti. Ti is close to 40% lighter than cast iron and is non-magnetic. By using a Ti-6Al-4V casting alloy in place of grey cast iron in just these two components, hundreds of pounds of weight can be saved depending on the size of the engine. In addition, due the superior strength and fatigue properties of Ti compared to C.I., Ti affords the opportunity to upgrade the power of the engine without extensive design changes.

This project will employ finite element analysis (FEA) to model a Cummins 5.9L, B-Series diesel engine running at 305hp. The temperatures and stresses will be computed at various locations on the two castings for both the currently used cast iron and for the Ti-6-4 alloy. Based on the modeling and a comparison of the two materials, a determination of the feasibility of using Ti-6-4 will be made. The modeling work will be contracted out to Ricardo, Inc. who has in-house, the model for this engine, and the experience to perform the necessary computer operations, and to interpret the results.

Depending on the results of the initial modeling, additional modeling iterations may be needed to obtain the optimum combination of materials for the head and block. For example, this may mean that a cast iron head or an Al head may be coupled with a Ti block.

Technical Highlights

The first set of modeling iterations consisted of modeling the engine block and head without any design modifications. Cast iron was compared to Ti-6-4. However, since it was expected that if an actual engine block were to be made of Ti, a Fe cylinder liner would have to be used in order to have good piston ring to liner compatibility. Thus, the FEA model was modified to accommodate this liner for future iterations.

Head

From a mechanical fatigue strength point of view, both the cast iron and the Ti alloy were acceptable. No serious issues were uncovered. However, when the temperatures were computed at various locations on the head, serious issues arose with the Ti. Ti has a much lower thermal conductivity than cast iron and this produced unacceptably high temperatures in the valve bridge area of the flame face. Temperatures as high as 700°C were computed. This means that there will be a serious problem of thermal fatigue failure in that region along with problems of valve and valve seat distortion and failure. Finally, lubrication at these temperatures will be

impossible. Unless there are some radical design changes to the head, it appears that Ti is not a good material for this component.

Block

The modeling of the engine block was a different matter. No stress and temperatures problems were computed. As a matter of fact, the Ti looked much better than the currently used cast iron, especially in fatigue. The modeling of the block was in a "worst-case" situation, since no Fe liner was incorporated into the model. Since the Fe has a very high thermal conductivity, it is expected that a block with Fe liners will behave even better than what was modeled. The very high strength of the Ti compared to the cast iron should allow for some design modifications that can further reduce the weight of the block casting.

Status of Milestones

Milestone: "Complete the modeling of the head and block castings in both cast iron and Ti-6-4. Provide an analysis of the feasibility of using Ti for these castings." The milestone was met on time.

Communication/Visitors/Travel

The results of the first milestone were communicated to Sid Diamond at the DOE. Also, Cathy Wong of the Naval Surface Warfare Center was sent a copy of the results. Ernie Schwarz of TARDEC was made aware of the program goals and its results.

Problems Encountered

None

Future Work

Three more FEA modeling iterations will be performed in order to fully determine the best combination of materials for this engine's head and block. These are:

1) Ti head combined with a Ti block having Fe liners.
2) Cast iron head combined with a Ti block having Fe liners.
3) Aluminum head combined with a Ti block having Fe liners.

Publications

None

Mechanical Behavior of Ceramic Materials for Heavy Duty Diesel Engines

A. A. Wereszczak and M. K. Ferber
Ceramic Science and Technology (CerSAT) Group
Oak Ridge National Laboratory

Objective/Scope

The application of more ceramic components in engines and transportation systems would be enabled if they could be confidently manufactured and machined faster (i.e., more cost-effectively) and if mechanisms that limit their mechanical performance were understood, predictable, and controlled. This project quantifies "quasi-plasticity/fracture thresholds" in ceramics (e.g., cubic oxides and non-oxides, nanoceramics and nanocermets, piezoelectric ceramics, micaceous ceramics, and traditional structural ceramics) and examines the competing mechanisms that dictate when and how quasi-plasticity or fracture dominates the other during controlled and instrumented static and dynamic indentation and scratch testings. The thorough understanding of the competition of fracture and quasi-plasticity in ceramics will enable improved and faster means of ceramic component manufacturing and surface engineering (e.g., ductile regime machining) and maximize mechanical performance when surface condition (e.g., bending) or when surface-located events (e.g., wear, impact) are service-life-limiters in engine and transportation system components.

Technical Highlights

Two primary efforts occurred during the present reporting period - assemblage of the indentation and scratch testing facility, and the creation of new software that will be used in the modeling of indentation behavior of material microstructures.

Indentation and Scratch Testing Facility

Instrumented Hertzian indentation of ceramics is an elegant method to assess and quantify the competition between quasi-plasticity and fracture processes [1]. The onsets of quasi-plasticity and fracture (σ_y and σ_c in Fig. 1, respectively) can be repeatably determined for a given material by interpreting the load/unload history of a Hertzian indent. A "static" Hertzian indentation system was constructed during the present reporting period. An acoustic emission system will be used with the indentation systems to monitor acoustic events throughout each indentation tests. A "dynamic" Hertzian indentation system was procured (Fig. 2) at the end of FY03 and its use will enable the study of the effect of rate (a third axis of Fig. 1) on quasi-plasticity and fracture onsets.

An instrumented (pendulum) scratch tester was ordered and its arrival is anticipated in early Q2. A schematic of it is shown in Fig. 3. The system will be used to characterize and interpret quasi-plasticity and fracture processes in ceramics. Linkages between its generated results and grindability and other machining parameters are being sought.

A Tukon 2100 Microhardness Tester having load capability between 10 and 50,000 grams was purchased and was set up in the indentation laboratory. Microhardness (Knoop or Vickers or

both) of all materials that are Hertzian indented or scratch tested is being measured and documented with this new system.

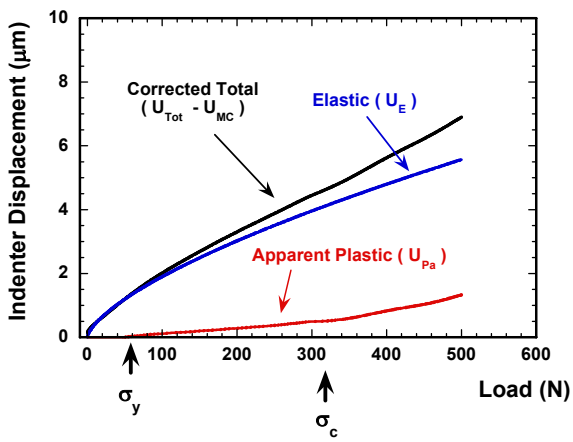

Figure 1. Indenter displacement (i.e., depth of penetration) as a function of indentation load. These results are from a 2.25mm diameter diamond indenter used to indent a hot-pressed SiC. Quasi-plasticity (σ_y) and fracture (σ_c) onsets shown - the former is associated with "dimple" initiation and the latter with the initiation of ring/cone cracking.

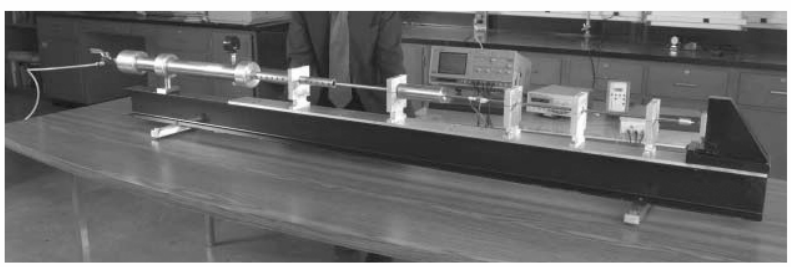

Figure 2. Dynamic hardness/indentation system used to determine the sensitivity of σ_y and σ_c on rate. Image supplied by G. Subhash.

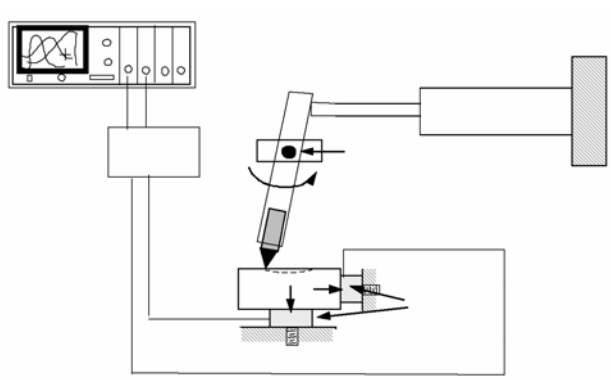

Figure 3. Schematic of pendulum scratch tester that will be used to characterize quasi-plasticity and fracture processes in ceramics. Image supplied by G. Subhash.

Indentation Modeling and Development of μ-FEA Software

An axisymmetric ANSYS model was constructed to analyze stresses due to Hertzian indentation (loading and unloading). It was written so that the properties and diameter of the indenter and the properties of the indented material are readily inputted and changed. CerSAT's Resonant Ultrasound Spectroscopy system will be used to determine the elastic properties needed for that modeling. The effect of friction and plasticity can be considered as well. An example of a model and resulting stresses at maximum load and after unloading are shown in Fig. 4.

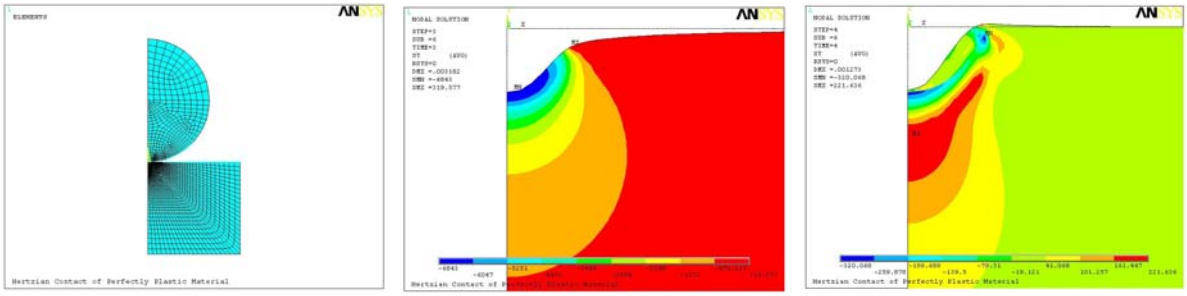

Figure 4. Mesh (left) of Hertzian indentation model. Axial stresses (middle) and displacements due to Hertzian loading at maximum load in a SiC indented by a diamond ball (ball not shown), and residual axial stresses (right) and displacements after complete unloading. Yield stress of the material was exceeded in this example, so indentation "pile-up" is portrayed in the right-hand image.

A need was identified to be able to model indentation-induced deformation processes (i.e., quasi-plasticity and fracture processes) of real microstructures rather than idealized and homogeneous ones. Consequently, the PIs developed "μ-FEA" which is a LabVIEW executable program that serves as a pre- and post-processor to ANSYS Finite Element Software and enables stress analyses of simulated or real microstructures. An example of its execution is shown in Fig. 5. A scanning electron microscope (SEM) was used to take digital picture (Fig. 5-left) of a complicated microstructure of an environmental barrier coating system. μ-FEA then facilitated the reconstruction of that microstructure in ANSYS (Fig. 5-middle). Once that model is in ANSYS, stress analyses can readily proceed and be interpreted. The analyses shown in Fig. 5-right illustrates residual stresses that are due to thermal expansion mismatches of all the constituents shown in Fig. 5-left. Instead of determining residual stresses, μ-FEA will be used to model indentation stresses that cause quasi-plasticity and fracture processes in real microstructures.

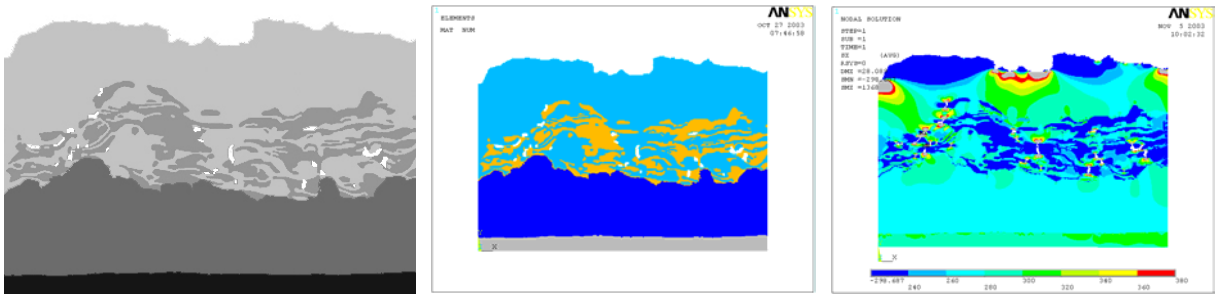

Figure 5. SEM-generated digital image of a coating system (left). μ-FEA reconstructed image in ANSYS (middle). Residual stress field due to CTE mismatches of constituents (right).

Status of FY 2004 Milestones
On schedule.

Communications/Visits/Travel
Numerous communications occurred with Prof. Ghatu Subhash of Michigan Technological University about instrumented dynamic indentation and instrumented scratch testing of ceramics. Formal interactions are planned between the PIs and Subhash.

Wereszczak met with Ron Chand on Nov. 5 to discuss linkages between instrumented scratch results and ChandKare's Grindability parameter and potential interactions.

Wereszczak and Ferber visited the Naval Research Laboratory, Washington DC, on Dec. 8 to meet with Mark Bashkansky and discuss Optical Coherence Tomography characterization and future interactions.

Hong Wang (Johns Hopkins University) visited Dec. 10 to give a seminar on dynamic tested of materials and to discuss mutual research with CerSAT staff. A post-doctoral research opportunity is being pursued.

Publications
A Contractor's Request to Assert Copyright form for *μ-FEA* software was submitted to ORNL management for their consideration an authorization.

References
1. A. A. Wereszczak and R. H. Kraft, "Instrumented Hertzian Indentation of Armor Ceramics," *Ceramic Science and Engineering Proceedings*, **23** 53-64 (2002).

Deformation Processes for the Next Generation Ceramics

Paul F. Becher and Chun-Hway Hsueh
Oak Ridge National Laboratory

Objective/Scope

This project seeks to determine how to exploit the deformation response of ceramics to enhance mechanical properties and develop novel shape forming with particular emphasis on the impact of nano-scale microstructures.

Technical Highlights

A literature search was conducted on the mechanical properties of nanocrystalline materials with emphasis on ceramic systems. Past studies have attempted to look at the deformation behavior in nanocrystalline oxides but have generally used materials that densities of < 90% of theoretical [1]. These should be considered compaction studies and not deformation studies. Even in studies of metallic alloys where nearly fully dense nanocrystalline samples are made by very high-pressure compaction, one has to question if "cold-welded" grain boundaries behave the same as those exposed to some thermal treatment where relaxation/restructuring can occur. In ceramics, high-pressure compaction, which has been used extensively, neither produces sufficiently dense bodies (i.e., > 95% of theoretical density) nor real grain boundaries.

In the past, many studies on the plastic deformation response of nanocrystalline oxides relied heavily on TiO_2, presumably because it was the focus of the early research on the synthesis of nanometer sized oxide powders [2]. There was also evidence that, as compared to TiO_2 with micrometer grain size, the ionic transport was greatly increased in nanocrystalline TiO_2 [3], which suggested that creep deformation might be substantially promoted. However, recent studies of nanocrystalline cubic ZrO_2 [4] reveal that the ionic conductivity, hence transport, is several orders greater than that of nanocrystalline TiO_2 even at modest temperatures (i.e., 500°C). These findings recommend nanocrystalline ZrO_2 as the most promising oxide for exploring and exploiting the plastic deformation at temperatures at low temperatures.

Our plans call for evaluating the deformation of nanocrystalline ceramic films, which we have facilities and expertise to fabricate; however, it is clear that the potential benefits will require access to dense, bulk nanocrystalline ceramics. To this end, a subcontract is being placed at Pennsylvania State University with Prof. J. H. Adair, who has demonstrated capability for producing dense, bulk nanocrystalline oxides of sufficient sizes [5] to permit mechanical properties to be evaluated at ORNL by rigorous test methods.

In addition, applied electrical fields have been shown to enhance deformation in conventional microcrystalline oxides having sufficient ionic bonding character [6]. Nanocrystalline ZrO_2, which is an excellent solid electrolyte, offers an excellent material to explore the additional effects of electrical fields on low temperature deformation.

References

1. M. J. Mayo, R. W. Siegel, A. Narayanasamy, and W. D. Nix, "Mechanical Properties of Nanophase TiO2 as Determined by Nanoindentation," J. Mater. Res., 5(5) 1073-82 (1990).
2. (a) R. Birringer, U. Herr and H. Gleiter, "Nanocrystalline Materials – A First Report," Supplement Trans. Jpn. Inst. Met. 27:4352 (1986). (b) J. Karch, R. Birringer and H. Gleiter, "Ceramics Ductile to Low Temperature," Nature Lttrs. 330(10) 556-8 (1987).
3. H. L. Tuller, "Ionic Conduction in Nanocrystalline Materials," Solid State Ionics, 131: 143-57 (2000).
4. I. Kosacki, T. Suzuki, V. Petrovsky and H. U. Anderson, "Electrical Conductivity of Nanocrystalline Ceria and Zirconia Thin Films," Solid State Ionics 136-7: 1225-33 (2000).
5. K. Kimel and J.H. Adair, "Aqueous Synthesis of Well-Dispersed Less than 10 nm Yttria Tetragonally Stabilized Zirconia at 200°C by Precipitation from Homogeneous Solution Using Complexation Chemistry," J. Am. Ceram. Soc., accepted for publication.
6. D. Yang and H. Conrad, "Influence of an Electric Field on the Superplastic Deformation of 3Y-TZP," Scripta. Mater. 36(12) 1431-5 (1997).

Status of Milestones

New project

Communication/Visits/Travel

Subcontract is currently being processed to fund the optimization of the processing of nanocrystalline oxides at Pennsylvania State University under the direction of Dr. J. H. Adair.

Publications

New project

Development of Titanium Components for a Heavy-Duty Diesel Engine Turbocharger

Mark J. Andrews
Caterpillar Inc.

Introduction

The present cost of producing titanium has significantly decreased, and the future forecast is for the decreasing trend to continue, making titanium alloys an attractive alternative to other strong, lightweight materials. Turbochargers on diesel engines play an integral role in meeting emission regulations and controlling fuel economy. Caterpillar Inc. has introduced the use of two turbocharger systems on some on-highway diesel engines in order to meet current and future emission regulations. The presence of two turbocharger systems challenges the already limited under the hood space for on-highway truck applications and so the development of an alternative turbocharger system that is smaller and lightweight is of great interest.

Project Objectives

The purpose of this program is to develop one or more heavy-duty diesel engine components using titanium alloys. The chosen engine components must demonstrate an improvement in fuel efficiency while reducing emissions. Caterpillar has selected the turbocharger wheel as an engine component to be fabricated from titanium aluminide (TiAl). In addition, Caterpillar has patented a new compact design for the turbocharger known as the HEAT™ (High Efficiency Air Turbo) that will utilize the TiAl turbo wheel. The HEAT™ consists of two compressor wheels and one turbocharger wheel attached to the same driveshaft. One compressor wheel is made from an aluminum alloy while the second compressor wheel is made of Ti-6V-4Al.

In order for the HEAT™ to meet the performance specifications of two turbocharger systems, a high strength, lightweight turbo wheel must be developed, which is the primary objective of this project. Thus lightweight titanium materials (e.g., TiAl) are the *enabling* technologies for the successful development of this new turbocharger design that will meet transient emission regulations while improving the engine's fuel efficiency.

Approach

An interdisciplinary team has been organized at Caterpillar to develop the TiAl turbowheel. Staff members from the Advanced Materials Technology (AMT) will lead and manage the project development efforts. Experts from the Large Engine Center (LEC) Air Systems division will work with Engine Research to design and bench test the turbo wheel. Manufacturing and Process engineers from the Mossville Engine Center (MEC) will work with machining experts at the Advanced Production Technologies to develop a cost competitive manufacturing implementation plan.

Summary

Two of the three subcontractors that were initially identified for the project have completed contract agreements with Caterpillar. The third subcontract is in the negotiation phase; alternative vendors have been preselected in the event that a contract is not completed with the third vendor.

A prototype HEAT™ has been built and tested on an internally designed Caterpillar gas stand. The purpose of this prototype was to validate the compression capacity of the HEAT™ design. Since the turbo wheel was made from Inconel 713, no measurements regarding the transient response of the prototype were planned. The test results indicate that the HEAT™ likely has the potential to meet the air requirements of the engine. It should be noted that the gas stand has limitations in that the test speeds available are one-third of normal operating speeds, and the test uses ambient air conditions.

Finite element modeling of the existing HEAT™ design has been completed using TiAl material properties. This modeling serves as the baseline for future designs and was anticipated and included in the project plan. The results from the modeling indicate that the existing wheel configuration will likely be loaded beyond the yield strength of TiAl, and so the anticipated redesign plan for the wheel was confirmed. The vibration frequencies were estimated through the same modeling and were found to be several orders of magnitude greater than the wheel's natural frequency.

The LEC Air Systems group has ordered and received 14 TiAl turbo wheels from a vendor that has interest in supplying TiAl wheels to Caterpillar. The wheels were essentially the result of casting trials and contained porous regions visible to the naked eye. Since the wheels did not meet print specifications, they were sold to Caterpillar at a significantly reduced price and are planned for use only in upcoming friction weld trials.

A purchase order has been placed for 30 TiAl wheels from a second casting vendor using the preferred TiAl, and shipment of this order is anticipated in the next reporting period. The material property database test matrix has been completed and quotes for obtaining the test material and for performing the tests are in circulation.

Future Plans

A redesign of the turbo wheel will commence once Engine Research completes the aero analysis. Welding trials with scrap TiAl wheels will commence in the next reporting period. A purchase order for the test samples is anticipated for completion in the next reporting period.

Surface Modification of Engineering Materials for Heavy Vehicle Applications

Stephen Hsu, Xaiolei Wang, Yhun Chae, and Lewis K. Ives
National Institute of Standards and Technology

Objectives

- Organize an international cooperative research program on an integrated surface modification technology under the auspice of the International Energy Agency (IEA)
- Design and identify surface features and patterns that can achieve friction reduction and enhanced durability for heavy duty diesel engine components.
- Develop understanding and appropriate models to explain the texturing effects on frictional characteristics. Develop appropriate thin films and coatings to achieve synergistic and complementary relationship with texturing to enhance performance.
- Discover and develop surface chemistry for protecting the films and coatings which work in synergy with the textures.

Approach

- Review literature on the current practices on surface texturing, thin films, and lubricant chemistry.
- Design various surface textures and measure their effects on friction and wear.
- Explore economical ways to fabricate these surface textures on appropriate materials surfaces.
- Develop test methodology to measure the effects of these textures on friction and wear reduction.
- Develop mapping techniques to define the limits of applicability in terms of operating parameters such as load and speed for a given materials pair.
- Conduct research to develop an integrated system approach to combine the best practices in thin films, coating, and surface chemistry for performances unrealizable by individual approach alone.
- Concurrently, organize an international cooperative research program under the auspice of the International Energy Agency (IEA) to pool resources and share this energy conservation technology worldwide.
- Under IEA annex IV, seek approval from the IEA executive committee and organize a US national working group centered at NIST to provide industrial inputs and exchange information with other national groups.

Technical Highlights

- Organized a special symposium on an integrated surface modifications technology during the ASME Joint Tribology Conference on Oct. 27-29, 2003. Speakers from Finland, Sweden, UK, and Israel described activities in their countries and DOE, NIST, ANL, ORNL, NSF describe various research activities in the US. Caterpillar and others provide an industrial perspective and need. The symposium was well attended and the international participants agreed to join the IEA program when approved.
- Developed a detailed proposal on forming an annex IV on integrated surface modification technology. Attended the IEA executive committee meeting held in Oakland on Oct. 22,

2003, and presented the detailed plan to the executive committee. Awaiting formal approval from the executive committee.

- The effect of geometry of the surface features were successfully compared on an equal area of coverage basis. Surface features of circles, triangles, narrow ellipses were fabricated using photolithographic techniques on carbon steel and stainless steel. Different geometries gave different levels of friction reduction. Orientation of surface features was also found to influence the friction reduction significantly.

The basic concept of this project is to use surface texturing features to artificially generate fluid lift force (hydrodynamic forces) to lower friction. Historically, such techniques work in high speed low load situations such as seals, journal bearings, and conformal contacts. In heavily loaded contacts, wear of the surface features makes such effects short-lived. The approach we have taken is to integrate wear resistant thin films, surface reactive chemistry to protect the surface features and to provide a low surface energy interface. Such integrated surface technology may lead to substantial energy savings in power transmission components in engines.

Last report detailed the effects of different surface texture geometries in the same pattern on an equal area coverage basis. A pin-on-disk wear tester was used for testing. Load and sliding speed were varied to control the contact conditions. Tests were conducted using mineral oil without additives having a viscosity of 2.73×10^{-5} m^2/s @ 40 ºC. Pin and disk specimens were fabricated from cold rolled 1017/1018 steel and 304 stainless steel. Friction force was monitored and recorded during the test. A photolithography method employing a mask fabricated with features of the size, shape, and spacing for the desired texture pattern used to produce surface textures on specimens. A photoresist was applied to the polished ($R_a \approx 0.01$ μm) test surface and exposed to light through the mask. After development the specimen was electrolytically etched to produce texture features of the desired depth. Geometries compared included circular and elliptical dimples. Experiments were also run on directions parallel to the shape and perpendicular to the shape. Elliptical dimples perpendicular to the sliding direction showed most friction reduction.

This quarter we continue our work by examining the effect of triangular dimples. Table 1 gives the characteristics of two different patterns, circular and triangular dimples on the pin specimens by the photolithography method. The feature area-density and feature depth were the same for both patterns. To assess the effect of orientation, two sliding directions, indicated by arrows in Table 1, were investigated for the triangles. Test results for the patterns are shown in Fig. 1 and compared to a polished pin without texture. The pin and disk materials in this example were cold rolled 1017/1018 steel. To control lubricant film thickness, sliding speed and applied load were varied in the range, 0.023 m/s-0.23 m/s and 1 N-35 N, respectively.

The concept for the triangles was based on compressing the oil within a narrower and narrower channel, therefore generating higher and higher fluid pressure. May be the ellipses are only "poor" triangles. Since the orientation of the features with respect to the sliding direction showed significant difference, the triangles were oriented up TV (sliding towards the apex of the triangle) and down TA (sliding towards the base of the triangle).

In Fig. 1 shows the friction for all features. Since all the area density is the same, the depth of the features is identical, and the lubricant used is a purified paraffinic oil of the same viscosity

without any additives, the observed effect should be only due to the shape of the features. If the friction reduction is mainly due to continuum fluid mechanics, then the shape of the features should not make that much difference. And orientation of the shape with respect to the sliding direction should not affect the friction reduction as well.

To facilitate comparison of all the features including orientation effects, the coefficient of friction is plotted as a function of the Sommerfeld number (viscosity x speed/load). This is the classical Stricbeck curve showing the friction transition from boundary lubrication to mixed lubrication regime and to the hydrodynamic lubrication regime. The baseline of no texture is shown for comparison. The triangle showed dramatic orientation effects. Sliding towards the base of the triangle showed friction reduction only slightly worse than ellipse (sliding perpendicular to the ellipse). This is surprising. Triangle sliding towards the apex actually showed instability and higher friction than the baseline case in most of the speed and load conditions.

Many experiments were conducted on these features and we are beginning to define the critical velocity (velocity below which no friction reduction was found), critical load (maximum load beyond which the surface features do not show any effects). A three dimension plot will be used to highlight the effective ranges of speed and load for each of the surface features.

High load experiments

Circular dimples were used to conducted high load experiments using stainless steel specimens. The load was raised up to 93 N on a smaller sample pin so the apparent contact pressure was approximately 15-20 MPa. To prevent wear of the dimples, a fully formulated synthetic lubricant was used. Baseline without dimples and dimpled specimens were compared. In each case, the dimples caused high friction.

Discussions

We have confirmed that under high speed, low load conditions, surface texturing can reduce friction of metal-to-metal contacts. The fact that geometric shape and orientation direction made a different suggests that common fluid mechanics explanation (dimples increase hydrodynamic pressure) maybe insufficient to explain the results. Contact mechanics, edge stresses (sealing the features), leakage rates around the edges, and turbulence inside and around the features may provide additional insights. Under boundary lubrication conditions, the fluid flow is not continuous inside the contact, so a different model will need to be developed to guide the continual advances needed to develop this technology.

IEA Organization

A special technical symposium on Integrated Engineered Surfaces was organized at the ASME/STLE Joint Conference in Oct. 28, 2003, at Sawgrass Marriott Resort and Beach Club, Ponte Vedra Beach, Florida. The symposium was well attended and speakers from six countries came and reported on their approaches and results.

INTEGRATED ENGINEERED SURFACES
SESSION 1
Session Chair and Organizer: Dr. Stephen Hsu, NIST, Gaithersburg, MD

Engineered surfaces involve surface texturing, thin film modifications, and lubrication chemistry. We intend to explore this emerging field with many invited speakers around the world to assess the current knowledge, identify future potentials, and establish a community network. This symposium will seek to bridge academic research with industrial applications.

8:30 AM – "An integrated approach S. M. Hsu, NIST, USA
9:00 AM - "Tribology opportunities from surfaces engineered at the nanoscale," Jorn Larson Basse, NSF, USA
9:30 AM - "State of the art in laser surface Texturing," Izhak Etsion, Technion, Israel
10:30 AM - "The effect of surface texture on stiction, friction, and wear," Koji Kato, Tohoku University, Japan
11:00 AM - "Tribological mechanisms of textures in dry and boundary lubricated sliding" Prof. Staffan Jacobson, Uppsala University, Sweden
11:30 AM - "Challenges for the application of engineered surfaces to tribosystems subjected to multiple contact modes" Peter Blau, Oak Ridge National Laboratory, USA
2:30 PM - "Effect of Laser texturing on lubrication regime transitions" L. Ajayi, Argonne National Lab.
3:00 PM - "Measurement of materials properties at the nanoscale: Directions and limitations," David Mendel, National Physical Laboratory, UK
3:30 PM – Break
4:00 PM "Surface distress modeling fro engineered surfaces in low lambda regime," Diann Hua, Caterpillar, USA
4:30 PM – "Tribological Optimization of thin coatings – a modeling approach," Kenneth Holmberg, Technical Research Center of Finland, Finland.
5:00 PM - "Nanoscale engineering of surface coatings for improved boundary lubrication," Ali Erdemir, Argonne National labs, USA
5:30 PM - "Surface texturing to produce specific size and shape of UHMWPE particles for biomaterial application," H. W. Fang, S. M. Hsu, NIST, USA

As can be seen from the program, representatives from Sweden, UK, Israel, Japan, Finland, US national labs, University, US industry all spoke in this symposium. Afterwards, we have a short meeting among the representatives of the countries involved and all agreed to participate in the IEA activity and made the ASME/STLE joint Tribology meeting an annual event to meet and discuss progress in each country.

Travel

1) Attended the IEA Executive Committee held on Oct. 22, 2003 in Oakland, CA and presented a detailed proposal on an integrated surface technology to the executive committee. 2) Attended ASME/STLE Joint Conference in Oct. 28, 2003 at Sawgrass Marriott Resort and Beach Club, Ponte Vedra Beach, Florida.

Status of FY 2003 Milestones

1.) Organize a symposium on contact reliability to compare testing procedures used in different countries (Oct. 2002).

–Done-- Completed a symposium among the participating countries on IEA activities on Oct. 29, 2002 during the ASME Tribology Conference in Cancun, Mexico.

2.) Propose to the IEA Executive Committee the formation of a new Subtask related to performance testing of nanostructured coatings for friction reduction (Jan. 2003).

Proposed a new subtask to the DOE program managers on an integrated surface technology. A workshop was held at NIST on March 11, 2003 in which ORNL, ANL, BNW and DOE headquarters were represented. A general agreement was reached to embark on this technology.

3.) Initiated a new technical activity on an integrated surface technology and organized an international research program per interagency agreement in May 2003.

Completed.

Table 1. Characteristics of two surface textures prepared by photolithography method.

	Pattern & Sliding dir.	Dimension (μm)	Depth (μm)	Pitch (μm)	Area of a dimple (μm^2)	Area density (%)
Circle	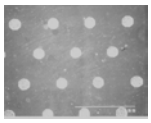	150	8	500	17671	7
Triangle	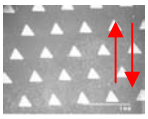	187	8, 10	500	17671	7

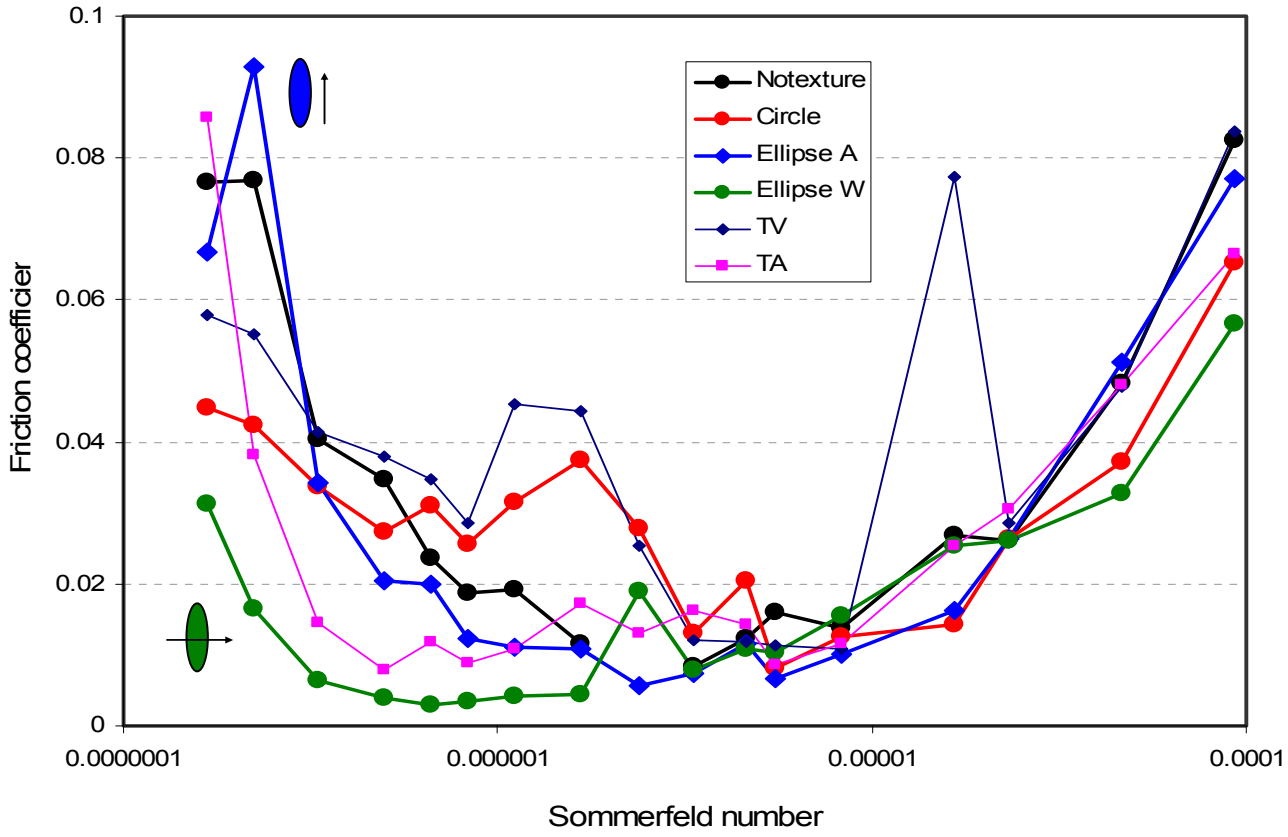

Figure 1. Pin-on-disk test results for different surface textures produced on pin surface by photolithography method compared with results for pin surface without texture.

Implementing Agreement for a Programme of Research and Development on Advanced Materials for Transportation Applications

M. K. Ferber
Oak Ridge National Laboratory

Objective/Scope

The International Energy Agency (IEA) was formed via an international treaty of oil consuming countries in response to the energy crisis of the 1970s. A major objective of the IEA is to promote secure energy supplies on reasonable and equitable terms. The governing board of the IEA, which is composed of energy officials from each member country, regularly reviews the world energy situation. To facilitate this activity, each member country provides energy experts who serve temporary staff assignments at IEA headquarters. These staff or secretariat support the governing board by collecting and analyzing energy data, making projections in energy usage, and undertaking studies on specialized energy topics. The governing board is also assisted by several standing groups; one being the committee on energy research and technology (CERT), which encourages international cooperation on energy technology. Implementing agreements (IAs) are the legal instruments used to define the general scope of the collaborative projects. There are currently 40 active implementing agreements covering research topics such as advanced fuel cells, coal combustion science, district heating and cooling, enhanced oil recovery, fluidised bed conversion, fusion materials, solar heating and cooling, pulp and paper, hydropower, heat pumping technologies, hybrid and electric vehicles, high temperature super conductivity, wind turbines, and high temperature materials. A complete listing can be found at the IEA website, www.iea.org.

This progress report summarizes recent activities in the implementing agreement entitled, "Implementing Agreement For A Programme Of Research And Development On Advanced Materials For Transportation Applications" (IA-AMT). This implementing agreement currently consists of two active annexes: "Annex II: Co-Operative Program on Ceramics for Advanced Engines and Other Conservation Applications" and "Annex III: Co-operative Program on Contact Reliability of Advanced Engine Materials." The motivation for this IA is the development of new and improved ceramic materials, brittle material design methods, and life prediction methodology. The objective of Annex II is coordinated R&D on advanced ceramics leading to standardized methods for testing and characterization.

The Executive Committee for the IA on Advanced Materials is also exploring the possibility of adding a new effort focusing on light weighting of materials.

Technical Highlights

The Executive Committee Meeting was held on Wednesday, October 22, 2003, at the Oakland Marriott City Center, 1001 Broadway, Oakland, CA 94607. The meeting, which was held in conjunction with the 55th Pacific Coast Regional & Basic Science Division Fall Meeting, began at 13:30 hours and was adjourned at 18:00 hours. The executive committee members in attendance were:

- Sidney Diamond - Department of Energy (DOE) Office of Transportation Technologies (United States Executive Committee Chairman),
- Matt Ferber - Oak Ridge National Laboratory (ORNL) (Operating Agent Technical Representative, United States Alternate Committee Member, and Working Group Coordinator of Subtasks 11 and 13),
- Rolf Wäsche - Bundesanstalt für Materialforschung und-Prüfung (BAM) (German Executive Committee Member),
- Katsuji Otsubo - New Energy and Industrial Technology Development Organization (Japanese Executive Committee Member)

The major objectives of this meeting were to (1) conduct a technical information exchange between the participating countries, (2) review the status of the active subtasks in Annex II (11 and 13), (3) discuss current progress of Annex III, which focuses on contact damage assessment, and (4) consider new activities.

A preliminary web site was created for the IA-AMT. The purpose of the site is to (1) describe the scope and motivation for the implementing agreement and (2) provide users with access to reports and databases generated by the implementing agreement. Once the site is approved by the executive committee members it will be made available on a public server.

Status of Milestones

All milestones are on track.

Communications/Visits/Travel

The author attended and chaired the aforementioned Executive Committee Meeting.

Publications

None.

References

None.

Testing Standards

George Quinn
Ceramics Division
NIST
Gaithersburg, MD 20899

Objective/Scope

This task is to develop mechanical test method standards in support of the Propulsion Systems Materials Program. Test method development should meet the needs of the DOE engine community but should also consider the general USA structural ceramics community as well as foreign laboratories and companies. Draft recommendations for practices or procedures shall be developed based upon the needs identified above and circulated within the DOE engine community for review and modification. Round robins will be conducted as necessary. Procedures will be standardized by ASTM and/or ISO.

Technical Highlights.

1. General

Minor issues regarding several standards (ASTM hardness C 1326 and C 1327, fracture toughness C 1421, ISO 17565 flexural strength at high temperature were cleared up this quarter. We resumed the error analysis of flexural rods, which is a final step needed before a draft standard is crafted. A Guide to Practice for Fractography has been started.

2. Fracture Toughness

Preliminary discussions about revising the ASTM standard were held with Mike Jenkins at University of Detroit. A list of possible ballot item revisions was prepared and sent to Mike for review and possible blending with other input. The definitions of the terms for "B" and "W" were reviewed. These are the specimen cross-section dimensions, but there's considerable variability in how the terms are used in ASTM standards. Six kits of Standard Reference Material 2100 were sold in November 2003.

The University of Konstanz in Germany sent word that they had tested a SRM 2100 bend bar fragment by the Vickers indentation crack length method. In response to this inquiry and several other like it that periodically come in, we prepared a set of informational notes on why the Vickers crack length method is not reliable for measuring fracture toughness.

3. Flexural Strength of Advanced Ceramics – Rectangular Specimens

Nearly all work on updating the ASTM standards and finishing the ISO standards is now complete. We believe that ASTM C-1161-02c is the definitive ASTM version and no further changes will be necessary in the foreseeable future. The ISO 15765 for high temperature flexural strength was finally finished and printed. We are glad these are done once and for all.

4. Fractography

Work continued on a NIST user-friendly "Guide to Best Practice" for fractographic analysis. An outline of the whole Guide and the chapter on fracture mirrors were finished. An appendix has a set of guidelines for how to measure fracture mirror sizes and how to estimate the fracture mirror constants. This set of guidelines constitutes a first attempt at a standard method for fracture mirror measurements. Although the ASTM standard practice for fractography of ceramics, C 1322 has recommendations to measure mirror sizes, no specific guidance was included on precisely how to go about making the measurements. A detailed correspondence was exchanged with Scott Glaesemann at Corning about their experiences and recommendations for measuring fracture mirrors in glass optical fibers.

Two manuscripts on machining damage cracks in silicon nitride rods and bars were revised and sent back to the Machining Science and Technology Journal.

5. Flexural Strength Testing of Cylindrical Ceramic Specimens

We resumed the error analysis of flexural strength testing of cylindrical rods. Now that we have considerable experience with this methodology, specimen preparation issues, and fractographic analysis of broken rods, the error analysis is the last necessary step before crafting the draft standard.

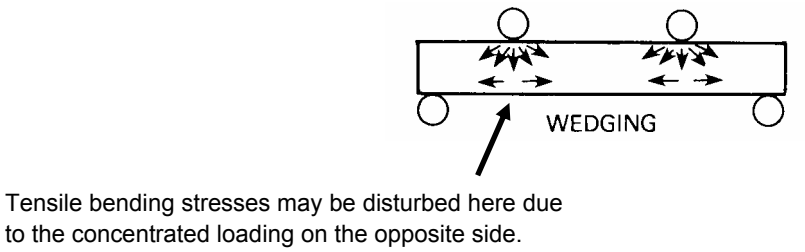

Figure 1 Wedging stresses from concentrated loads.

A detailed literature search was done on the concentrated load problem. The concentrated load where the loading point applies force to the bend specimen or rod creates not only high contact

stresses where the fixtures touches the specimen, but also wedging stresses that disturb the tensile stress field on the opposite side. Depending upon the size of the specimen and the fixtures, and the force necessary to break the specimens, the error can be several percent or more. This can lead to excessive breakages under the load points. The specimen and loading roller sizes must be chosen to minimize this error. An error analysis for the rectangular beam was derived twenty years ago, but an analogous analysis for rod specimen has apparently never been done. Finite element analysis may have to be applied, but first we are searching for a closed-form solution in the literature. We have a practical remedy for the problem, in the form of cradles inserts for fixtures which can distribute a concentrated load, but it would still be helpful to determine what are the bounds for utility of normal bend fixtures with round rods without the need for the special cradles. Over the summer we contacted Professor Phillip Koshy of McMaster University in Canada for some help, but he was unable to follow through with an analysis. We contacted Professors Hutchinson at Harvard University and William Sharpe at Johns Hopkins University, both mechanical engineers with a good background in solid mechanics, but neither were aware of a closed form solution.

6. Hardness

Most of our conventional hardness activities are complete after years of work. Minor revisions to the two ASTM standards (C 1326 for Knoop and C 1327 for Vickers) were approved in the fall of 2003. Only 4 changes were made to the Vickers standard and 3 to the Knoop standard. One involved relaxing the numerical aperture of the objective lens of the microscope used to measure the indentations slightly to make the ASTM version compatible with the ISO 14705 standard that was adopted two years ago. A specification for the allowable asymmetry of a Vickers indentation, also taken from the ISO standard, was added to C 1327. Statements encouraging measurement of the Indentation Size Effect (ISE) were also added. The ISE is a phenomenon whereby hardness varies with the indentation load. Usually hardness standards require hardness be measured at one indentation load, but much more information can be obtained by measuring the whole hardens curve. These standards are now designated C 1326-03 and C 1327, where the "03" denotes the edition year (2003). The proof of the revised Knoop hardness standard C 1326-03 was reviewed in November and that for the Vickers standard C 1327 in December. ASTM published both as separates.

7. New Applications Subcommittee for ASTM Committee C-28 Advanced Ceramics

The new ASTM Subcommittee C 28.04 Applications is now up and running under the leadership of Dave Caruthers. Prior relevant activities and background information on ASTM Committee C-28 were sent to Dave and to Steven Gonczy, the incoming chairman of Committee C-28.

8. Other

Kristin Breder's draft static fatigue standard was reviewed and comments sent to her for consideration. Kristin was unable to attend the November Committee C-28 meeting in Tampa, so Mr. Quinn acted on her behalf on this standard. Several negatives had been received the last time this item was formally balloted. In particular, there were unresolved issues about the language on whether the slow crack growth parameters had to be evaluated by the power law equation ($V = AK_I^N$), and whether this was preferred, or whether alternative logarithmic expressions were acceptable. At the Tampa meeting, a consensus was tentatively reached that the alternatives are equally acceptable but that they should be given the same treatment and detail as devoted to the power law expression.

Status of Milestones

412149	Prepare ballot-ready first ASTM draft of cylindrical rod flexure strength test	April 2002 **Overdue**
412151	Prepare review paper on flexural testing of cylindrical rods.	October 2002 **Overdue,Ongoing work on error analysis**

Communications/Visits/Travel

Tiny glass spheres were sent to Edgar Lara-Curcio for him to try some crushing experiments. NIST will be investigating this procedure in the future. It can be considered a variant of the diametric compression strength test.

Mr. Quinn had discussions with Steve Gonczy and Dave Carruthers about applications standards in ASTM Committee C28.

A set of drawings of bend fixtures was sent to D. Shellman at Penn State.

Andy Wereczszack of ORNL visited NIST for discussions about Hexoloy SP and coating fractures in Si/Si_3N_4.

A letter about machining damage in silicon nitride was sent to Daimler Benz in Stuttgart.

Bob McClung was contacted about the status of ASTM nondestructive standard C 1212 and C 1175 and their renewal.

Correspondence was exchanged with Scott Glaesemann at Corning about measuring fracture mirrors in glass optical fibers.

Publications and Presentations

1. G. D. Quinn, L. K, Ives, and S. Jahanmir, "Machining Damage Cracks: How to Find and Characterize Them by Fractography," Ceram. Eng. Sci Proc., 24 [4] (2003) pp. 383-394.

Rolling Contact Fatigue

A. A. Wereszczak
Ceramic Science and Technology (CerSAT)
Oak Ridge National Laboratory

Objective/Scope

The understanding and control of contact damage behavior of ceramics under rolling and sliding conditions are enablers to more widespread utilization of ceramics as cam followers, valves, valve seats, and other important transportation-related components. International interest exists to understand the fundamentals of rolling contact fatigue (RCF) of ceramics because greater control (or minimization) of RCF will result in longer life of such components. Rolling contact fatigue is internationally studied through a variety of test methods and analytical approaches; interest exists in the present project to link their measured performances. Toward that, RCF studies (primarily of Si_3N_4) involving both international and domestic interactions are being pursued as Annex III of the International Energy Agency (IEA) agreement.

Technical Highlights

The NTN three-ball-on-rod RCF tester arrived from NIST and it was installed in the laboratory during the present reporting period.

A technical plan developed by NIST's Bill Luecke to determine what role grinding damage (i.e., sub-surface damage) has on rolling contact fatigue performance of Ceradyne's Ceralloy 147-31N Si_3N_4 will proceed at ORNL but with some extra planned characterization. A matrix of rods were rough-ground to differing levels of severity and they were all then identically finish ground - the goal was to produce a variation of subsurface damage among them. Many of the finished cylinders from those sets were cut in half axially - 4-pt flexure testing was planned for them with the intent to explore how that (controlled) subsurface damage affects flexure strength. Conventional microhardness and Hertzian indentation testing will be performed to determine if/how existing subsurface damage affects hardness.

In addition to the tests described in the preceding paragraph, CerSAT's rotary bend fatigue (RBF) tester is being modified so that "rotating flexure strength" (RFS) tests can be performed. The intent is to rotate a cylindrical specimen in the RBF at some controlled frequency (e.g., 20 Hz) while an applied load on the free end of the spinning specimen is monotonically increased until fracture is produced. The advantage of this test over conventional 4-pt-bend testing is the whole surface of the cylinder is being subjected to tensile stresses (from bending) whereas that is not the case with 4-pt-bending of a cylinder. It is felt that such a test, when conducted in parallel to RCF testing, will provide results that will aid in the interpretation of how subsurface damage affects RCF performance. Rod stock of Ceralloy 147-31N was ordered, and machined cylinders of it will be used as the model material for the development of RFS testing.

Various diameter balls of Saint-Gobain/Cerbec's NBD200 and SN101C Si_3N_4 compositions were acquired, sectioned, and polished in preparation for microhardness and Hertzian indentation testing. These balls are used in the RCF testing, so their properties will be measured and documented in parallel to those of the test rods.

Though Ceralloy 147-31N has been the focus of previous RCF studies at NIST, and continues to be a primary Si_3N_4 of interest in the present ORNL project, additional commercial Si_3N_4 and α-SiAlON compositions are being sought for inclusion in the testing matrix.

Each of the participating countries (Germany, Japan, UK, and the USA) have been tasked with writing a review report describing RCF test techniques and analysis methods used in their country. The US will be responsible for compiling all those reports and publishing the document as a DOE/IEA report.

Status of FY 2004 Milestones
On schedule.

Communications/Visits/Travel
Numerous communications occurred with Prof. Mark Hadfield of Bournemouth University (UK) to initiate a formal collaboration in FY04.

The PI visited NIST on Oct. 28 and met with Bill Luecke and George Quinn to talk about the present project and future test plans.

Numerous communications with Wataru Kanematsu (Japan), Mathias Woydt (Germany), and Roger Morrell (UK) occurred regarding RCF test plans and the arrangement of a January 27 meeting at Cocoa Beach, FL.

Publications
None.

References
None.